NASA CONTRACTOR REPORT

NASA CR-79

NASA CR-791

GROUND-BASED PHOTOMETRIC SURVEILLANCE OF THE PASSIVE GEODETIC SATELLITE

by R. L. Hostetler, R. H. Emmons, R. J. Preski, C. L. Rogers, and D. C. Romick

Prepared by
GOODYEAR AEROSPACE CORPORATION
Akron, Ohio
for Langley Research Center

NATIONAL AERONAUTICS AND SPACE ADMINISTRATION • WASHINGTON, D. C. • JUNE 1967

NASA CR-791

GROUND-BASED PHOTOMETRIC SURVEILLANCE OF THE PASSIVE GEODETIC SATELLITE

By R. L. Hostetler, R. H. Emmons, R. J. Preski,
C. L. Rogers, and D. C. Romick

Prepared under Contract No. NAS 1-6189 by
GOODYEAR AEROSPACE CORPORATION
Akron, Ohio

for Langley Research Center

NATIONAL AERONAUTICS AND SPACE ADMINISTRATION

For sale by the Clearinghouse for Federal Scientific and Technical Information
Springfield, Virginia 22151 – CFSTI price $3.00

CONTENTS

	Page
SUMMARY	1
INTRODUCTION	3
SYMBOLS	3
THEORY	6
Calibration	6
Satellite Observation	9
Statistical Evaluation	15
DESCRIPTION OF EQUIPMENT	18
Truck	18
Instrumentation Room	18
Observation Deck	19
Data Reduction and Transmission Equipment	23
PREPARATION AND FIELD START UP	24
Site Selection	24
Preliminary Orbit Geometry Analysis	25
OPERATIONAL DESCRIPTION	25
Orbital Analysis and Satellite Predictions	25
Observation Procedures	25
Data Conversion	27
Key Punching and Closed Loop Check	27
Computational Center Data Reduction	27
Data Analysis	28
RESULTS	29
Calibration	29
Statistical Error Analysis	31
Satellite Characteristics	32
Observation of the PAGEOS I Satellite	33
Trends	56
Computer Printouts	56
Satellite Scintillation	56
Goodness-of-Fit Program	60
CONCLUSIONS	64
General	64
Evaluation of Photometric Technique	64
Value of continuous V Band	65
Evaluation of Mobile Photometric Observatory	66
Appendix	
A Albedo Corrections of Ground-Based Photometric Observations of Satellite	67

Appendix | Page

B Sample Size Requirements for PAGEOS I Surveillance 73

C Filling Out Control Card I and the Data Point Information Card 81

D Description of Computer Program Printout for PAGEOS I Ground-Based Photometric Surveillance 87

REFERENCES 99

ILLUSTRATIONS

Figure | Page

1 Satellite phase angles (ψ) 10

2 Slant range and elevation angle as functions of height and subsatellite distance 10

3 Earth-reflected stellar magnitude increments 11

4 Absolute reflectance values of PAGEOS I aluminized Mylar material 14

5 NASA Mobile Photometric Observatory 19

6 Interior street-side wall of forward compartment 20

7 Interior curb-side wall of forward compartment 21

8 Mobile Photometric Observatory in deployed position 22

9 Telescope complex 23

10 Theoretical extinction versus altitude above mean sea level 24

11 PAGEOS I UBV stellar magnitudes, sigma magnitudes and radii of curvature, and reflectances 46

12 PAGEOS I UBV radii of curvature 49

13 PAGEOS I UBV specularity 52

14 Photometric data measurement in continuous V band - 13 July 1966. Satellite shows regular periodic peaks of intensity of reflected light 58

15 Photometric data measurement in continuous V band - 11 August 1966. Satellite exhibits relatively steady reflected light intensity 59

TABLES

Table		Page
I	PAGEOS I Characteristics for Combined Observation Periods	2
II	Calibration Constants for PAGEOS I	30
III	Pre-Shadow Error Analysis (24 June to 12 July)	31
IV	Post-Shadow Error Analysis	31
V	Weighted Average PAGEOS I Specularity Determinations	32
VI	PAGEOS I Observation Data - Ultraviolet (U) Band	34
VII	PAGEOS I Observation Data - Blue (B) Band	38
VIII	PAGEOS I Observation Data - Visual (V) Band	42
IX	Summary of Data for Continuous-Color Observations	57
X	Comparison of Tabular and Measured Values of Standard Stars	61
XI	Comparison of Tabular and Measured Values of Standard Stars Used in PAGEOS I Calibration	61

GROUND-BASED PHOTOMETRIC SURVEILLANCE OF THE PASSIVE GEODETIC SATELLITE

By R. L. Hostetler, R. H. Emmons, R. J. Preski,
C.L. Rogers, and D.C. Romick
Goodyear Aerospace Corporation

SUMMARY

The PAGEOS I satellite was observed during the first 60 days of its orbital life, and data on its characteristics obtained through photometric observation was reduced and analyzed. To obtain measurements, a truck-mounted mobile observatory was utilized. Observing equipment consisted of a 24-inch telescope and photometric instrumentation capable of measurements in the U, B, and V bands.

Palomar Mountain was selected for optimum viewing conditions. The fourth orbit (the first available from Palomar) was successfully observed on 24 June 1966 and at every orbital pass thereafter through 22 August 1966, except for a few nights when the sky was obscured by clouds or when instrumentation difficulties prevented operations. A total of 52 PAGEOS I passes were observed, 45 in three-color photometry and seven in single-color photometry. Over 5000 data points were recorded, with 50 percent in the U band, 25 percent in the B band, and 25 percent in the V band.

The raw data was reduced to obtain the PAGEOS I stellar magnitude, solar reflectance (assuming 50-foot radius of curvature), specular component of the reflected light, radius of curvature, and local variations of the radius of curvature.

The data on all these characteristics except the last has been reduced to mean and/or average values for each observed pass and for selected time periods (table I). Specularity, which is defined as the specular component of reflected light, is expressed as a percentage of the total reflected light. Table I also shows the standard deviation (σ) of magnitudes, the standard deviation of local radii of curvature, and a figure of merit for specularity values. The standard deviations for the period 17 July to 27 July increase as compared with other periods. On the raw data analog charts, this is exhibited as an increase in satellite scintillation. The start of this period correlates with the first PAGEOS I shadow entry.

For the pre-shadow period (24 June to 12 July) and the post-shadow period (17 July to 22 August), error analysis indicates the following maximum measurement error levels at a confidence level of 96 percent:

	Pre-Shadow	Post-Shadow
Radius of curvature	1.30%	0.92%
Specularity	0.55%	0.17%
Reflectance	2.81%	1.99%
Stellar magnitude	0.027%	0.02%

The indicated weighted average diameter of PAGEOS I in the V band (most dependable) is 100.1 feet, and the indicated weighted average specularity, considering all bands, is 98.4 percent.

It appears that the combined environmental factors at PAGEOS I's orbital height caused no measurable degradation in the first two months following deployment.

TABLE I. - PAGEOS I CHARACTERISTICS FOR COMBINED OBSERVATION PERIODS

Parameter	Total Pre-Shadow Run 24 Jun to 12 Jul 66			Post-Shadow Run 17 Jul to 27 Jul 66			Post-Shadow Run 5 Aug to 14 Aug 66			Post-Shadow Run 15 Aug to 22 Aug 66			Total Post-Shadow Run 17 Jul to 22 Aug 66		
	U	B	V	U	B	V	U	B	V	U	B	V	U	B	V
Number of data points	534	269	268	708	354	354	684	342	342	639	320	320	2031	1016	1016
Mean normalized magnitude	3.00	2.84	2.18	3.01	2.83	2.19	2.91	2.77	2.11	2.94	2.77	2.11	2.95	2.79	2.14
Standard deviation (σ) of magnitudes	0.21	0.22	0.21	0.33	0.37	0.34	0.23	0.22	0.23	0.23	0.23	0.20	0.28	0.28	0.27
Specularity, %	103.40	99.33	98.53	91.28	89.66	100.45	98.38	99.82	97.58	101.50	100.12	98.54	98.16	95.85	98.98
Figure of merit for specularity	43.48	29.50	28.76	33.96	21.04	26.19	52.78	38.76	37.39	47.86	34.02	37.45	71.92	48.35	53.67
Average radius of curvature, ft	47.15	49.05	49.52	45.92	48.04	49.51	48.78	50.45	50.45	48.48	50.34	50.70	47.64	49.54	50.21
Standard deviation (σ) radii of curvature, ft	4.55	4.94	5.11	8.47	10.13	8.37	5.20	5.18	5.37	4.98	5.13	4.71	6.47	7.08	6.46
Reflectance for 50-foot radius of curvature	0.779	0.854	0.870	0.720	0.794	0.856	0.832	0.903	0.902	0.822	0.899	0.914	0.789	0.863	0.890
Phase range, deg	86	86	86	108	108	108	100	100	100	87	87	87	108	108	108
B-V magnitude increment	0.66			0.64			0.66			0.66			0.65		
U-V magnitude increment	0.82			0.82			0.80			0.83			0.81		

INTRODUCTION

During the first 60 days after launch of the PAGEOS I satellite, a ground-based photometric surveillance was performed on the satellite using a 24-inch telescope mounted in a mobile observatory. The surveillance was conducted on Palomar Mountain, California.

The PAGEOS I surveillance was conducted to obtain satellite stellar magnitude, solar reflectance of the sphere's surface, specular component of the reflected light, satellite diameter, and local variations (if any) in the sphere's radius of curvature. Measurements of the satellite intensity were made using a time-shared, three-color filtering system, which conforms to the UBV Photometric System. Palomar Mountain was selected as an observation site to maximize the number of possible measurements within a 60-day observation period, and to permit measurements to be made during the satellite's first few orbits.

The theory behind satellite photometric surveillance includes calibration of sky and instrumentation by observation of standard stars, and equations to determine the various optical and physical characteristics of the satellite being observed. The method of calibration is based on a series of equations presented by Dr. R. H. Hardie (ref. 1) to (1) convert galvanometer deflections to the natural system's stellar magnitude and color indices; (2) correct these magnitudes and color indices for atmospheric extinction; and (3) transform them to their standard system values. Data reduction includes digitizing the analog data of satellite or star intensity and time that result from an observation; and use of computerized equations to obtain the satellite characteristics.

From 15 June to 22 August 1966, the mobile observatory and computer facilities were used to perform on-site observatory shakedown and attain operating proficiency, to conduct the actual observations or measurements, and to perform data reduction, data processing, and data analysis of the observed passes of the PAGEOS I satellite.

This report discusses first the theory of photometric observations of a satellite. A brief description of the observatory is included, and pre-operation preparations are described. Operating procedures from pass acquisition through data analysis, determinations of the analysis, and conclusions are then presented.

SYMBOLS

Å	angstrom unit, 10^{-10} meters
A_{sp}	weighting coefficient for specular reflection
a	albedo of earth
a_b	albedo of earth in a given band
antilog	antilogarithm operator: the number corresponding to the base 10 logarithm term which follows
B	blue band-pass filter stellar magnitude, standard system*
B_d	weighting coefficient for diffuse reflection

*Always extra-atmospheric; values for standard stars are obtainable from references 2 and 3.

B-V	B-V standard system color index, stellar magnitudes*
b	blue band-pass filter stellar magnitude, natural system
b-v	b-v natural system color index, stellar magnitudes
C	confidence level
C_s	solar constant, Btu/hr-ft^2
C_v	coefficient of variation
c	correction factor for albedo in a given band
c'	correction factor for albedo for terrain
D	slant range, distance from satellite to observer, ft
d	galvanometer deflection, inches (target + sky + dark) - (sky + dark)
E_0	illuminance value at zero stellar magnitude
E_d	diffuse component of illuminance
E_e	earth albedo illuminance
E_s	solar illuminance on the satellite
E_{sp}	specular component of illuminance
F	function; also, generalized albedo term
$f(\psi)$	Russell phase function
G_x	the function $(1 - k''_{u-b} X)$
h	orbital altitude, statute miles
J_x	the function $(1 - k''_{b-v} X)$
K	constant; also, factor of standard deviation
K_n	term relating incident illuminance to observed brightness (includes distance variations)
k'	primary atmospheric extinction coefficients
k''	second-order atmospheric extinction coefficients
M	mean value
m	stellar magnitude
m_K	constant in stellar magnitude equation
N	sample size
P_r	probability
R	satellite radius, feet
R_c	radius of curvature, feet
S	photometer gain, stellar magnitude units $S = 2.5 \log_{10}$ (photometer gain factor); also, specularity
U	ultraviolet band-pass filter stellar magnitude, standard system*
U-B	U-B standard system color index, stellar magnitudes*
u	ultraviolet band-pass filter stellar magnitude, natural system
u-b	u-b natural system color index, stellar magnitudes
V	visual band-pass filter stellar magnitude, standard system*
v	visual band-pass filter stellar magnitude, natural system

*Always extra-atmospheric; values for standard stars are obtainable from references 2 and 3.

X	atmospheric thickness, ($\cong$ secant z)
x	sample estimator; also, random variable
y	variable
z	angular distance from zenith
α	geocentric angle between earth-sun and earth-satellite vectors, radians
γ	reflectance, the ratio of the rate of reflection of radiant energy to its rate of incidence
Δ	increment, second minus first value
Δm_a	value of Δm computed using a for albedo
Δm_b	value of Δm computed using a_b for albedo
ϵ	system transformation scale factor, V determination
ζ	calibration zero-point term, stellar magnitude units
μ	system transformation scale factor, B-V determination; also, true parameter; also, micron unit (10^{-6} meters)
ρ	proportion of true parameter
σ	standard deviation
π	the constant 3.14159
ψ	system transformation scale factor, U-B determination; also, phase angle between satellite-sun vector and satellite-observer vector, radians

Note: a bar above a symbol denotes mean value

Subscripts

B	denotes blue band data, standard system
b	denotes blue band data, natural system
b-v	denotes b-v color index data
d	denotes diffuse values
f	denotes a function
m	denotes stellar magnitudes
o	denotes extra-atmosphere value (i.e., extrapolated to X = 0)
$\odot$	denotes solar magnitude
R_c	denotes radius of curvature
S	denotes specularity value
s	denotes solar value
sp	denotes specular value
t	denotes true value
U	denotes ultraviolet band data, standard system
u	denotes ultraviolet band data, natural system
u-b	denotes u-b color index data
V	denotes visual band data, standard system
v	denotes visual band data, natural system

THEORY

The theory behind satellite photometric surveillance includes: (1) calibration by standard stars to obtain the various second-order and primary extinction coefficients and transformation scale factors, and (2) equations to determine the various optical and physical characteristics of the satellite being observed.

Calibration

Considerations. - The method of calibration is based on equations and descriptions of procedures which were presented in their literal form by Dr. R. H. Hardie (ref. 1). These procedures were modified slightly to make them applicable to photometry of artificial satellites. The basic working equations are as follows (refer to list of symbols):

$$v = S_V - 2.5 \log_{10} (d_v) \quad (1)$$

where $S_V = 2.5 \log_{10}$ (photometer gain factor);

$$b\text{-}v = (S_b - S_v) - 2.5 \log_{10} (d_b/d_v); \text{ and} \quad (2)$$

$$u\text{-}b = (S_u - S_b) - 2.5 \log_{10} (d_u/d_b). \quad (3)$$

$$V = v - k_v' X + \epsilon(B\text{-}V) + \zeta_v; \quad (4)$$

$$B\text{-}V = \mu J_X (b\text{-}v) - \mu k'_{b-v} X + \zeta_{b-v} \quad (5)$$

where $J_X = 1 - k''_{b-v} X$; and

$$U\text{-}B = \psi G_X (u\text{-}b) - \psi k'_{u-b} X + \zeta_{u-b} \quad (6)$$

where $G_X = 1 - k''_{u-b} X$.

By substituting equations (1), (2), and (3) into equations (4), (5), and (6) we obtain:

$$V = \left[S_v - 2.5 \log_{10} (d_v)\right] - k_v' X + \epsilon(B\text{-}V) + \zeta_v \quad (7)$$

$$B\text{-}V = \mu J_X \left[(S_b - S_v) - 2.5 \log_{10} (d_b/d_v)\right] - \mu k'_{b-v} X + \zeta_{b-v} \quad (8)$$

$$U\text{-}B = \psi G_X \left[(S_u - S_b) - 2.5 \log_{10} (d_u/d_b)\right] - \psi k'_{u-b} X + \zeta_{u-b} \quad (9)$$

Note that equations (1) through (3) convert galvanometer deflections to the natural system's visual-band stellar magnitude and color indices, while equations (4) through (6) correct these magnitudes and color indices for atmospheric extinction (i.e., for X = 0) and also transform them to their standard system values. Equations (4) through (6) contain 11 "constants" (of various rigidities), the determination of which is the principal subject of the calibration procedure. The method of determination of the 11 calibration constants will be described in some detail in the following subsections.

Light suffers loss as it travels through the earth's atmosphere due to absorption, scattering, etc. In magnitude form, we may write the equation

$$m_o = m - kX, \qquad (10)$$

where X is the path length in units of air mass at the zenith of the observer and k is the extinction coefficient, which is the measure of light loss (expressed in magnitudes) for a celestial body at the zenith. The relative air mass, X, in units of the thickness at the zenith is given to a high degree of accuracy by the secant of the zenith distance, z. A more accurate equation for X is

$$X = \sec z - 0.0018167 (\sec z - 1) - 0.002875 (\sec z - 1)^2 - 0.0008083 (\sec z - 1)^3. \qquad (11)$$

Determination of second-order extinction coefficients. - To determine the second-order extinction coefficients k''_{b-v} and k''_{u-b} in equations (5) and (6), the following procedure is observed. The second-order terms are best determined separately by a differential technique by following close pairs of stars of widely differing colors through a wide range of X. The best results are obtained when the stars are at a zenith angle of 45° or greater. Following reference 1, the slopes of Δ (b-v) versus X Δ (b-v) and of Δ (u-b) versus X Δ (u-b), found either by graphical or least-squares methods, determine k''_{b-v} and k''_{u-b} respectively. The average of the slopes for the various pairs of stars determine the final results of the second-order coefficients. The second-order coefficient is negligibly small or indeterminate for bands located in the yellow or red. In the blue region, it commonly has a value of -0.02 to -0.04, depending on the bandwidth, while in the ultraviolet it is commonly defined as being zero.

Determination of scale factors for system transformation. - The quite rigid scale factors ϵ, μ, and ψ (eqs. 4, 5, and 6) can next be determined, making use of the previously determined second-order extinction coefficients. For this purpose it is desirable to observe a number of standard stars, ranging widely in color, but through substantially the same air mass - preferably all near the zenith. These differential observations should be accomplished in a short period of time to minimize the possibility of significant changes in the atmospheric extinction. The Pleiades, Hyades, and Praesepe star clusters are commonly observed for the purpose of scale factor determinations, but there are times, as on summer evenings, when none of these clusters is at a suitably small zenith distance. For these times, a sufficient number of suitable stars near zenith can generally be found by consulting the Arizona-Tonantzintla Catalog (ref. 3).

Since values of k_v', k'_{b-v} and k'_{u-b} are required for calculations of the scale factors, it introduces very little error into the results to assume approximate values for the three principal extinction coefficients (ref. 1, p. 201). For this calculation we assumed $k_v' = 0.15$, $k'_{b-v} = 0.15$, and $k'_{u-b} = 0.30$.

We proceed to determine the extra-atmosphere magnitudes and color indices in the natural system by making use of the following equations (ref. 1, p. 198):

$$v_o = S_v - 2.5 \log_{10} d_v - k_v' X \quad (12)$$

$$(b-v)_o = \left[(S_b - S_v) - 2.5 \log_{10} (d_b/d_v)\right] J_x - k'_{b-v} X \quad (13)$$

$$(u-b)_o = \left[(S_u - S_b) - 2.5 \log_{10} (d_u/d_b)\right] G_x - k'_{u-b} X \quad (14)$$

The next step is to collect the needed parameters and compute the following for each star:

$(V - v_o)$

$[(B-V) - (b-v)_o]$

$[(U-B) - (u-b)_o]$

The linear regression of the first two parameters versus B-V provides, either by least-squares solution or by faired plots, slopes which are ϵ and $(1-1/\mu)$, respectively. Similarly, the linear regression of $(U-B) - (u-b)_o$ versus U-B provides a slope which is $(1-1/\psi)$.

The scale factor ϵ will be close to zero, while μ and ψ will be near unity if the response of the natural system closely matches that of the standard system. This is desirable for the most reliable remaining determinations (for each satellite pass) of the three changeable primary extinction coefficients, k_v', k'_{b-v}, and k'_{u-b}, and finally of the three somewhat flexible zero-point terms ζ_v, ζ_{b-v}, and ζ_{u-b}, as required for the most accurate photometric data reduction. (See ref. 1, pp. 199-202.)

Primary extinction coefficients and zero-point terms. - For determination of the three primary extinction coefficients (k_v', k'_{b-v}, k'_{u-b}) and the three zero-point terms (ζ_v, ζ_{b-v}, and ζ_{u-b}), several standard stars (five or more) are observed along the satellite path both before and after the observation. From equations (4), (5), and (6), one performs a linear regression on each of the quantities $[v + \epsilon (B-V) - V]$, $[u\,(b-v)\, J_x - (B-V)]$, and $[\psi (u-b)\, G_x - (U-B)]$ versus X, which then provides slopes which are respectively k_v' and the modified coefficients $\mu k'_{b-v}$ and $\psi k'_{u-b}$. Having determined k''_{b-v}, k''_{u-b}, ϵ, μ, ψ, k_v', k'_{b-v}, and k'_{u-b}, we may use any standard star observations (including those made for the purpose of determining the primary extinction coefficients) to determine the semi-rigid zero-point terms.

$$\zeta_v = V - v - \epsilon (B-V) + k_v' X$$

$$\zeta_{b-v} = (B-V) - \mu J_x (b-v) + \mu k'_{b-v} X$$

$$\zeta_{u-b} = (U-B) - \psi G_x (u-b) + \psi k'_{u-b} X$$

From reference 1, we learn that good average values obtained at observatories such as Mount Wilson, which has an altitude and climate similar to that of Palomar Mountain, are $k_v' = 0.15$, $k'_{b-v} = 0.15$, and $k'_{u-b} = 0.30$. These are average values only for one observatory and values of the extinction coefficients for a single observation may vary considerably from these numbers.

Satellite Observation

General. - From careful observations of the intensity of sunlight reflected from a spherical artificial satellite, various inferences can be drawn concerning the present condition of its surface. For instance, the extent to which the initially specular reflecting surface has been degraded can be determined, as well as values of the mean and local effective radii of curvature of the satellite. In general, the following parameters may be obtained through the use of a ground-based photometric system: (1) stellar magnitude (normalized); (2) specularity and diffusivity of the surface of a satellite; (3) mean and local radii of curvature; and (4) reflectance, if radius of curvature is assumed. In this report the specular component of reflected light is called specularity. It is expressed as a percentage of the total reflected light.

Stellar magnitude. - Having previously determined the 11 extinction-calibration-transformation constants from the various stars used in the previously described programs, we turn our attention to the determination of the extra-atmospheric stellar magnitude of the PAGEOS I satellite. The equations used to determine the stellar magnitude of the satellite at any position along its orbit are identical to those of the standard stars. These equations (7, 8, and 9) reduce the satellite photometric observations from their raw data galvanometer deflections and the separately determined zenith distances to the standard system U-B-V magnitudes and color indices. The computer program (E-1213) that reduces the satellite stellar magnitude is described in a later subsection. This particular program computes not only the stellar magnitude and phase angle of the satellite (see fig. 1), but also prints out such coordinates as slant range, height, altitude, azimuth, right ascension, declination, etc. for each time. In addition, the computer incorporates such correction factors as normalization of each observed intensity to a uniform slant range, e.g., 2640 statute miles for PAGEOS I; and allowance for the contribution of earth albedo.

Normalized slant range: Normalization of the photometric data to a uniform range is accomplished by applying the inverse square law of illumination to the illuminances, first having determined the satellite's slant range at observation time. Figure 2 (from ref. 4) shows slant range and elevation angles as functions of height and subsatellite distance. Satellite photometric data must be normalized for the instantaneous slant range from the observer before a meaningful analysis can be made. The instantaneous slant range is computed for the times at which photometric data was taken from an accurate ephemeris of the satellite. It should be noted that a one percent error in slant range will propagate an error of 0.02 in the normalized stellar magnitude.

Contribution of earth albedo: The correction for the contribution of the earth's albedo (earthshine) for a specular spherical satellite is a function of the satellite's orbital height and geocentric angle α (elongation) from the sun. Figure 3 presents the nominal stellar magnitude increments based on a 0.36 earth-atmosphere albedo and a specular spherical satellite. The adjusted increment (see appendix A) must then be applied as a correction to the reduced stellar magnitude of a near-specular spherical satellite before proceeding to determinations of effective radii of curvature and reflectance, and to the degree of specularity of the surface.

Satellite stellar magnitude at various effective wave lengths: The satellite stellar magnitudes may be determined in the U or near-ultraviolet band (3600 Å), B or blue band (4200 Å), and V or visual band (5500 Å). The specular illuminance (E_{sp}) of the radiation received in the U, B, or V spectral regions (depending on which spectral region is switched in at a given time) is given by:

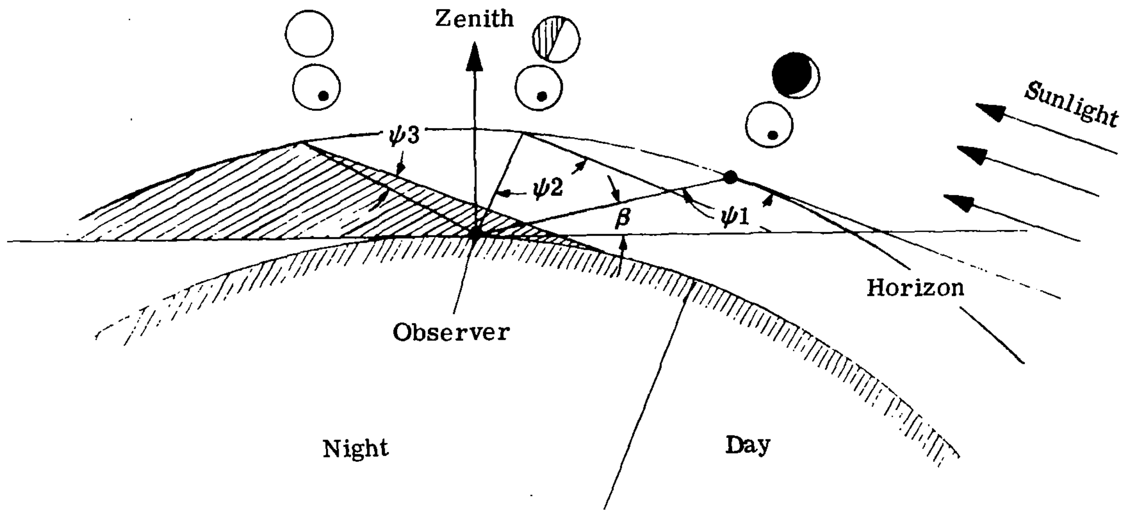

Figure 1. - Satellite phase angles (ψ).

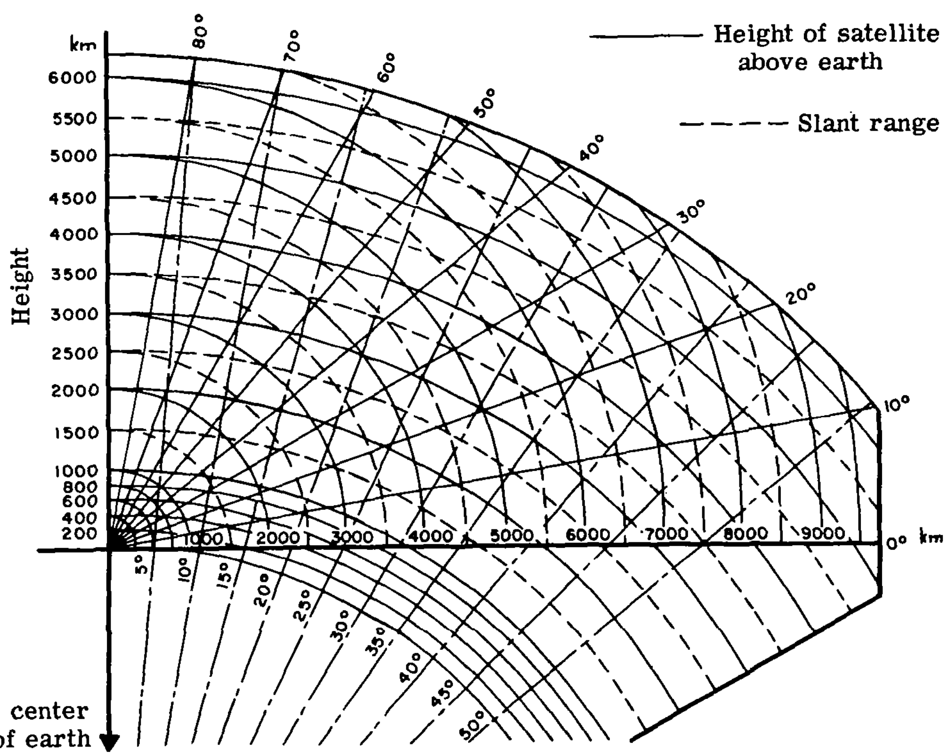

Figure 2. - Slant range and elevation angle as functions of height and subsatellite distance.

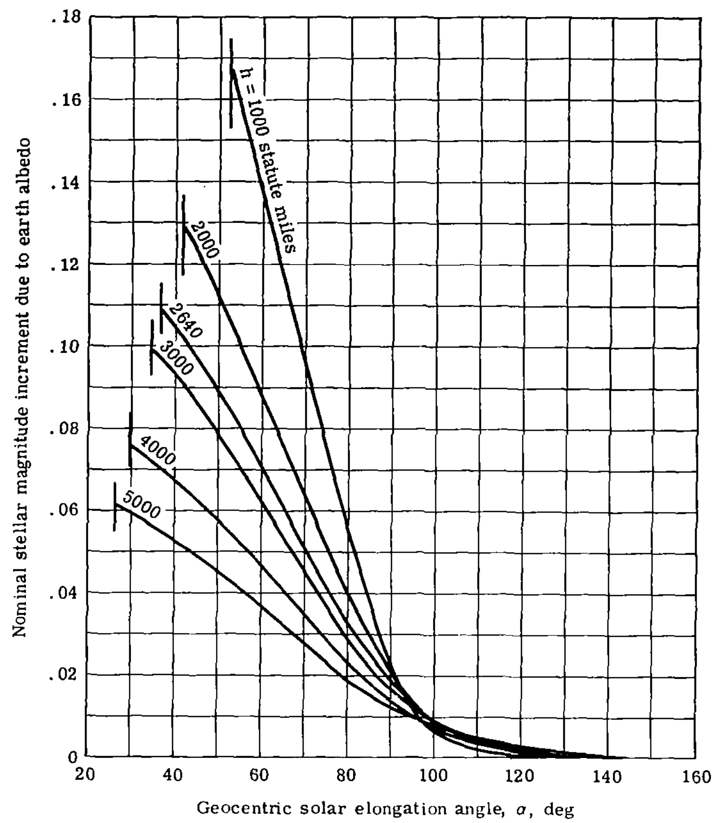

Figure 3. - Nominal stellar magnitude increments due to earth albedo for a specular spherical satellite.

$$\frac{E_{sp}}{E_0} = \text{antilog}\,(-0.4\ m_{sp}) \approx \frac{1}{4}\ \frac{E_s}{E_0}\left(\frac{R}{D}\right)^2 \tag{15}$$

Using this equation, the extra-atmospheric stellar magnitude, m_{sp}, for the specular component of a satellite can be determined. The stellar magnitudes for the diffuse spherical satellite are given by:

$$\frac{E_d}{E_0} = \text{antilog}\,(-0.4\ m_d) = \frac{2}{3}\ \frac{E_s}{E_0}\left(\frac{R}{D}\right)^2 f(\psi) \tag{16}$$

where $f(\psi) = \frac{1}{\pi}\ [\sin\psi + (\pi - \psi)\cos\psi]$.

<u>Determination of specular component of light reflected from a sphere's surface.</u> - The specular spherical satellite has a convex mirror surface that provides a small image reflection of the sun, equal in brightness regardless of the viewing angle. Conversely, a diffuse

sphere in sunlight exhibits phases like the moon or Venus. The integrated light from the diffuse sphere is a function of the phase angle ψ, which is the angle formed at the satellite between lines to the sun and the observer. As indicated in figure 1, the phase angle is zero when the phase is full. The illuminance of the diffuse sphere increases as the phase angle decreases to the limit at the eclipse.

To determine the specularity of a satellite, photometric measurements are made over a wide range of phase angles. For moderate orbit inclinations these phase angles can be measured during single passes, when the satellite orbit has reached approximately the coplanar condition shown in figure 1. For a polar-orbiting satellite, the range in phase angle during a single pass is limited, requiring the combination of carefully calibrated data from various passes to achieve the desired span of phase range.

The essential background and theory for the specularity determination is shown in equations (15) and (16) (from R. Tousey, refs. 5 and 6). These equations make possible the prediction of the extra-atmospheric stellar magnitudes, m, of specular and diffuse spherical satellites. The Russell phase function, $f(\psi)$, (ref. 7) gives the dependence of illuminance upon phase angle for a perfectly diffuse sphere that obeys Lambert's cosine law of reflection. (This law states that the reflection from a small area is proportional to the product of the cosine of the angle of incidence and the cosine of the angle between the normal and the direction to the observer.) These equations provide for photometric discrimination between specular and diffuse spherical reflecting surfaces. How closely the photometric data conforms to one or the other must be determined.

Equation (17) (from ref. 8) is the regression equation that permits this determination, where A_{sp} and B_d are the weighting factors for the specular and diffuse components, respectively, of the reflected light. They are determined by a least-squares best fit to the normalized photometric data. Finally, equation (18) (also from ref. 8) provides the fractional specularity.

The regression equation for determining specularity is:

$$\text{Antilog}\,(-0.4\ m) = 1/4\ A_{sp} + 2/3\ B_d\, f(\psi) \qquad (17)$$

$$\text{Specularity, } S = \frac{A_{sp}}{A_{sp} + B_d} \qquad (18)$$

where $f(\psi) = \frac{1}{\pi}\left[\sin\psi + (\pi - \psi)\cos\psi\right]$.

Before the analysis can proceed, the photometric data must be carefully calibrated and normalized. Observations of nonvariable stars of known illuminance are generally performed both before and after the satellite pass. The photometric data is then processed and the atmospheric extinction coefficients are determined. Simultaneously with the tracking of the satellite, the following information is time-correlated with the photometric data:

(1) Elevation (atmospheric thickness)

(2) Slant range

(3) Earthshine (effect of earth albedo)

(4) Phase angle

The calibrated photometric data is then processed for extra-atmospheric illuminance, normalized to zero earthshine and to a uniform slant range (2640 statute miles) by the inverse square law. A least-squares solution of the linear regression equation (17) yields best-fit values for the intercept A_{sp} and the slope B_d, which are then employed in equation (18) to determine specularity.

Mean and local radii of curvature. - While the satellite's specularity is a microtexture characteristic, the mean and local radii of curvature of a nearly spherical satellite describe its size and macrotexture.

Having previously determined the diffuse-reflecting weighting coefficient, B_d, it is possible to remove from the normalized magnitudes the contribution of diffuse reflection in each, $-2.5 \log 2/3 \, B_d f(\psi)$, to obtain purely specular magnitudes, m_{sp}. If a reasonable or previously measured value for the reflectance, γ, is adopted, the radius of curvature can next be determined in any optical band from the relation:

$$R_c(\text{ft}) = S^{-1/2} \text{ antilog} \left[\frac{m_\odot - m_{sp}}{5} - 0.5 \log \gamma + \log D + 0.30103 \right] \tag{19}$$

where $m_\odot$ is the U, B, or V magnitude of the sun for the date; D is the slant range in feet; R_c is the radius of curvature in feet; m_{sp} is the extra-atmospheric stellar magnitude contributed solely by the specular components of sunlight reflected from the satellite; and γ is reflectance. Since the observed illuminances depend on both γ and R_c in equation (19), one may be obtained only if the other is known.

From equation (19) the mean radius of curvature may be obtained from a large number of observations of the local radii of curvature. The range and variability of the local radius of curvature may be examined in light of the original design and available material for gross implications for a possible new mean radius of curvature.

Determination of reflectance if a radius of curvature is assumed. - By solving equation (19) for γ, one may obtain the reflectance for an assumed radius of curvature. The equation for this value is

$$\gamma = S^{-1} \text{ antilog} \left[\frac{m_\odot - m_{sp}}{2.5} - 2 \log R_c + 2 \log D + 0.60206 \right] \tag{20}$$

As before, this refers to all three colors (U-B-V) when the values of m_{sp} are known.

Correction of solar distances: The sun's visible radiation is constant in output to within one percent, but owing to the eccentricity of the earth's orbit, the sun's illuminance upon an earth satellite varies. For example, the sun's visual and stellar magnitude varies from -26.70 in early July to -26.78 in January. The corresponding distances are approximately 94.5×10^6 miles in July and 91.5×10^6 in January. These minor variations in magnitudes with the distance of the sun will be reflected in corresponding variations in the magnitudes for sunlit satellites, and for subsequent determinations of the satellite's effective radius of curvature, or U, B, or V reflectance, the instantaneous U, B, or V solar magnitude is required.

Reflectance: Previously measured absolute monochromatic reflectance values for a specimen of PAGEOS I surface material (see fig. 4) were processed to obtain nominal U-B-V band reflectances, as follows:

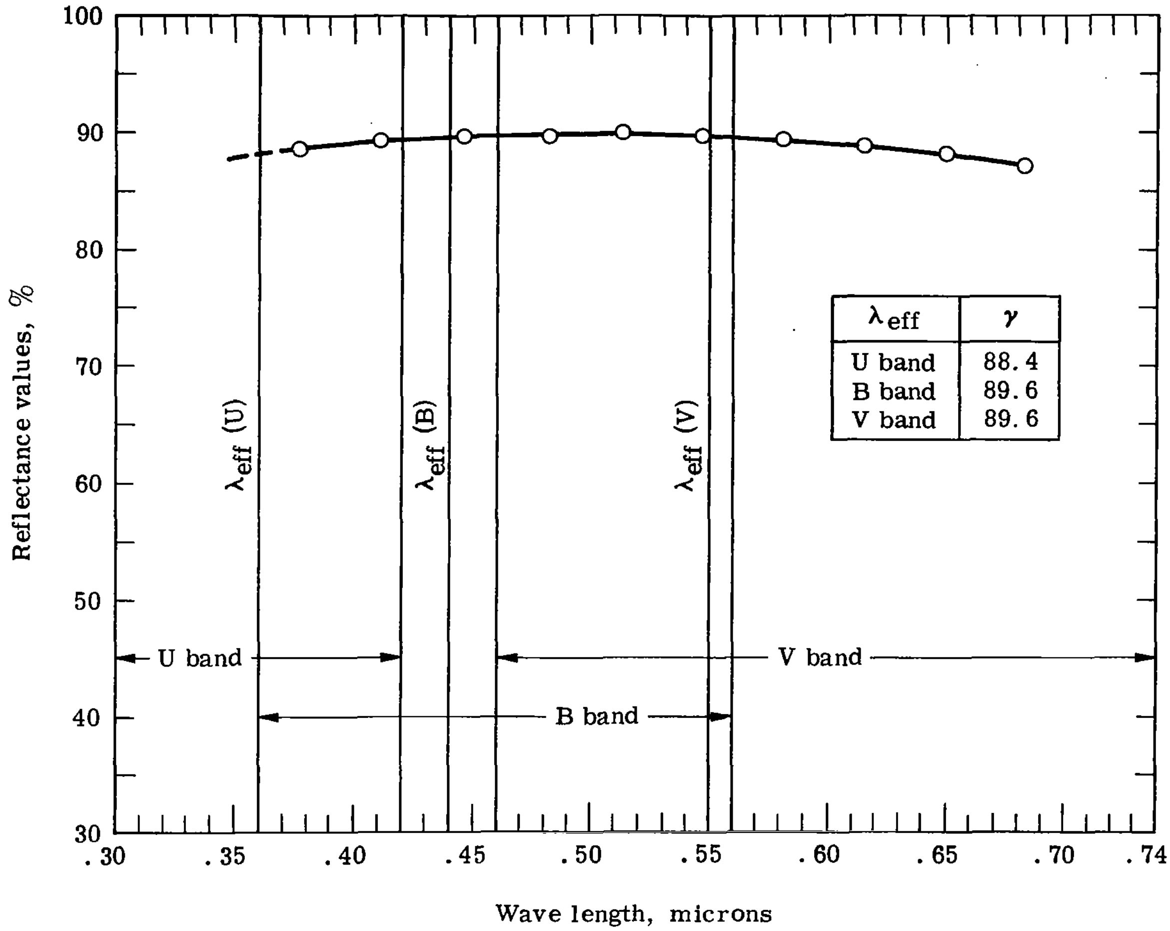

Figure 4. - Absolute reflectance values of PAGEOS I aluminized Mylar material (ground measurements).

U band	88.4 percent
B band	89.6 percent
V band	89.6 percent

These reflectance values were subsequently adopted as γ for the radius of curvature determinations (eq. 19).

Laboratory spectrophotometer values for the diffuse component of reflectance for PAGEOS I material in various wave length regions are as follows:

3600 Å	3.7 percent
4200 Å	3.4 percent
5500 Å	3.0 percent

This shows that the expected value for specularity is in the 96-97 percent region for these bands.

Statistical Evaluation

General. - In this program, an equation is used to provide an indirect,derived value of a system's parameter, which cannot be directly measured. Into this equation are substituted numbers, usually obtained by direct or indirect observation. These numbers often possess a difficult property - they are unpredictable, random variables. Therefore, the derived value is also a random variable. To alleviate this random variability of single measurements, the average of several observations is used. The question then arises as to the precision of estimation by such averages in the equations. The derivations below provide the statistical basis of the criterion equations for satisfaction of the specified precisions. The basic question answered in each case is this: is the sample size of observations large enough so that the averages computed from the equations are within the required tolerance precisions of the actual parameters? Obviously, the results are only as good as the quality of the original measurements; if some systematic bias has been introduced by the equipment or by some constants in the equations, then the statistical methods herein cannot and do not discover nor eliminate this unknown factor. The statistical analysis is given in appendix B. A discussion of the method of assessment of each parameter follows.

Specularity. - In this report, the specular component of the reflected light is called specularity, and is expressed as a percentage of the total reflected light. Specularity, S, is estimated by:

$$S = \frac{A_{sp}}{A_{sp} + B_d}, \tag{21}$$

where A_{sp} and B_d are regression coefficients of a line fitted to illuminance and $f(\psi)$, using a sample size of N observed data points.

To judge if this estimate, S, is within two percent of the "true value"* with 96 percent confidence, a measure of the random variability of S is first needed. This measure is the standard deviation of S, σ_S, which can be derived by using Gaussian propagation of error (see ref. 9).

$$\sigma_S = \left[\left(\frac{\partial S}{\partial A_{sp}}\right)^2 \sigma_{A_{sp}}{}^2 + \left(\frac{\partial S}{\partial B_d}\right)^2 \sigma_{B_d}{}^2\right]^{1/2}$$

$$\sigma_S = \frac{\left[A_{sp}^2 \sigma_{B_d}^2 + B_d^2 \sigma_{A_{sp}}^2\right]^{1/2}}{\left(A_{sp} + B_d\right)^2} \tag{22}$$

*"True value" is that parameter number obtained by an infinite number of unbiased, randomly varying quantities.

The coefficient of variation $C_v(S)$ of S will be needed in the rationale of the next step, so it is repeated from reference 9:

$$C_v(S) = \frac{\sigma_S}{S} = \frac{\left[A_{sp}^2 \sigma_{B_d}^2 + B_d^2 \ \sigma_{A_{sp}}^2\right]^{1/2}}{A_{sp}(A_{sp} + B_d)} \quad (23)$$

The regression coefficients A_{sp} and B_d are normally distributed if the original variables entering the regression fit are also normally distributed. However, the ratio of normal variables such as $A_{sp}/(A_{sp} + B_d)$ is not, in general, normally distributed. Therefore, to devise a test to show whether the specularity estimate, S, meets the required precision, a method was used that does not depend on any assumption about the distribution. This method which is based upon the Tchebycheff inequality, is:

$$P_r \left[|\bar{x} - \mu| < \rho\mu \right] > 1 - \frac{\sigma^2}{N(\rho\mu)^2} \quad (24)$$

where x is a sample estimator of the true parameter, μ; N is sample size; ρ is percent error of μ, which is specified (two percent for specularity and reflectance); σ is the standard deviation of the distribution from which the sample of measurements was drawn; and $P_r[\quad]$ signifies the probability of the statement within the brackets. But since σ^2/μ^2 is the coefficient of variation squared, then

$$P_r \left[|\bar{x} - \mu| < \rho\mu \right] > 1 - \frac{C_v^2(x)}{N\rho^2} = 0.96 \quad (25)$$

In this inequality, in terms of specularity, x is the estimate $S = A_{sp}/(A_{sp} + B_d)$; μ is the true value of S, S_t; and $C_v(S)$, which is computed from equation (23) and the right hand side of equation (25), must either exceed 0.96 (the desired confidence level), or if the right-hand side is solved for ρ it must not exceed 0.02 (from ±2 percent error). That is,

$$\frac{C_v(S)}{\sqrt{N(1 - 0.96)}} \leqq 0.02 \quad (26)$$

The meaning of the expression on the left of equation (26) is that the maximum percent error (with a confidence probability of 96 percent) is less than

$$\frac{C_v(S)}{\sqrt{N(1 - 0.96)}} \times 100. \quad (27)$$

It is worthy of mention that the Tchebycheff inequality is a very stringent criterion for judging the satisfaction of the required precisions. That is, a system must be much better in this case than if some distribution, such as the normal, were used.

Reflectance. - The reflectance, γ, is estimated by the following equation:

$$10^{-.4\,m} = K\gamma R_c^2 \quad (28)$$

where m is stellar magnitude, K is some constant, and R_c is radius of curvature. Taking logarithms, solving the equation for log γ, and using Gaussian propagation of error results in a coefficient of variation expression for reflectance, $C_v(\gamma)$, as follows:

$$C_v(\gamma)^2 = 0.16\sigma_m{}^2 + 4C_v(R_c)^2, \tag{29}$$

where σ_m is the standard deviation of stellar magnitude, m, for many repeated observations.

Now, since the estimating equation for γ is not a ratio and m and R_c are assumed to be normally distributed, we may justifiably use normal distribution properties. Therefore, a 2.06 standard deviation is commensurate with a 96 percent confidence level. Then, to meet a ±2 percent error requirement, it follows that computed values of $C_v(\gamma)$ from equation (29) for samples of size N must satisfy:

$$\frac{2.06\ C_v(\gamma)}{\sqrt{N}} \leq 0.02 \tag{30}$$

Radius of curvature. - The machine computations of the radius of curvature, R_c, provide the average, $\bar{R}_c$, for N sample size and also the standard deviation, σ_{R_c}. The coefficient of variation, $C_v(R_c)$, used in equation (28) for reflectance is simply:

$$C_v(R_c) = \frac{\sigma_{R_c}}{\bar{R}_c} \tag{31}$$

Also, since the required precision is in absolute values, ±0.7 feet, then the following inequality must be satisfied at the 96 percent confidence level:

$$\frac{2.06\sigma_{R_c}}{\sqrt{N}} < 0.7 \text{ feet.} \tag{32}$$

If this inequality is satisfied and no systematic non-random biases occur in the data, then it may be concluded that R_c is within 0.7 feet of the true radius of curvature.

Stellar magnitude. - The computer program provides values of m, the average for N measurements, and σ_m. Then the following must be satisfied:

$$\frac{2.06\sigma_m}{\sqrt{N}} < 0.2. \tag{33}$$

Summary. - Equations (26), (30), (32), and (33) interpret the desired accuracies in statistical terms.

DESCRIPTION OF EQUIPMENT

The NASA Satellite Photometric Observatory used in this study consists of an instrument room and observation deck mounted on a truck bed and component parts for data reduction and transmission.

Truck

The truck chassis (see fig. 5) provides the observatory the mobility to go anywhere accessible by standard automobile The truck is equipped with a support system that maximizes its operational stability. This support system consists of six jacks and pads that enable the entire observatory to be raised off its road suspension and, with the use of the mounted leveling devices, provide a method for precise leveling. Sway braces that interlock the supporting pads increase the observatory's stability. The truck is equipped with a power generator, mounted on the outside of the front section of the van.

Instrumentation Room

The front section of the van contains a general-purpose 28-Vdc power supply, a heater, an air conditioner, a hydraulic power unit for positioning of the observation deck, and the control system and instrumentation system equipment for operation of the observatory. The equipment is shown in figures 6 and 7.

Control system equipment includes a control assembly, which provides the control functions for the polar and declination axes of the telescope: power and operational amplifiers; and the power supplies required to drive the telescope control motors.

Instrumentation equipment includes a photometer, a recording oscillograph, a receiver for reception of standard time signals, a tape recorder for voice recording of each mission, a monitor assembly, and a signal-operated tone generator. The photometer provides both high-voltage power to the photomultiplier and selectable gain amplification of the photomultiplier output. The oscillograph permits analog recording of up to 18 data channels, with frequency response up to 3000 cps. Five channels have active galvanometers, and two others are used for reference lines. Each observation requires at least the recording of satellite intensity, time, filter number, gain number, and a reference line. A fifth galvanometer is used to record polarization or cross-track positions. The monitor assembly permits operator or automatic control of the sequencing of the filters, shutters, and the polarization analyzer located in the telescope instrumentation head. The signal-modulated tone generator bridges the output of the photometer to drive a speaker located on the outside of the instrumentation room wall. The audio frequency of the tone generator changes when the light intensity is large enough to be recorded by the photometer. Thus, all members of the observation crew can monitor the photometer output. In addition to indicating that the telescope is properly pointed, the tone modulation permits observers to judge whether the proper gain scale is being used and whether filter sequencing is progressing correctly.

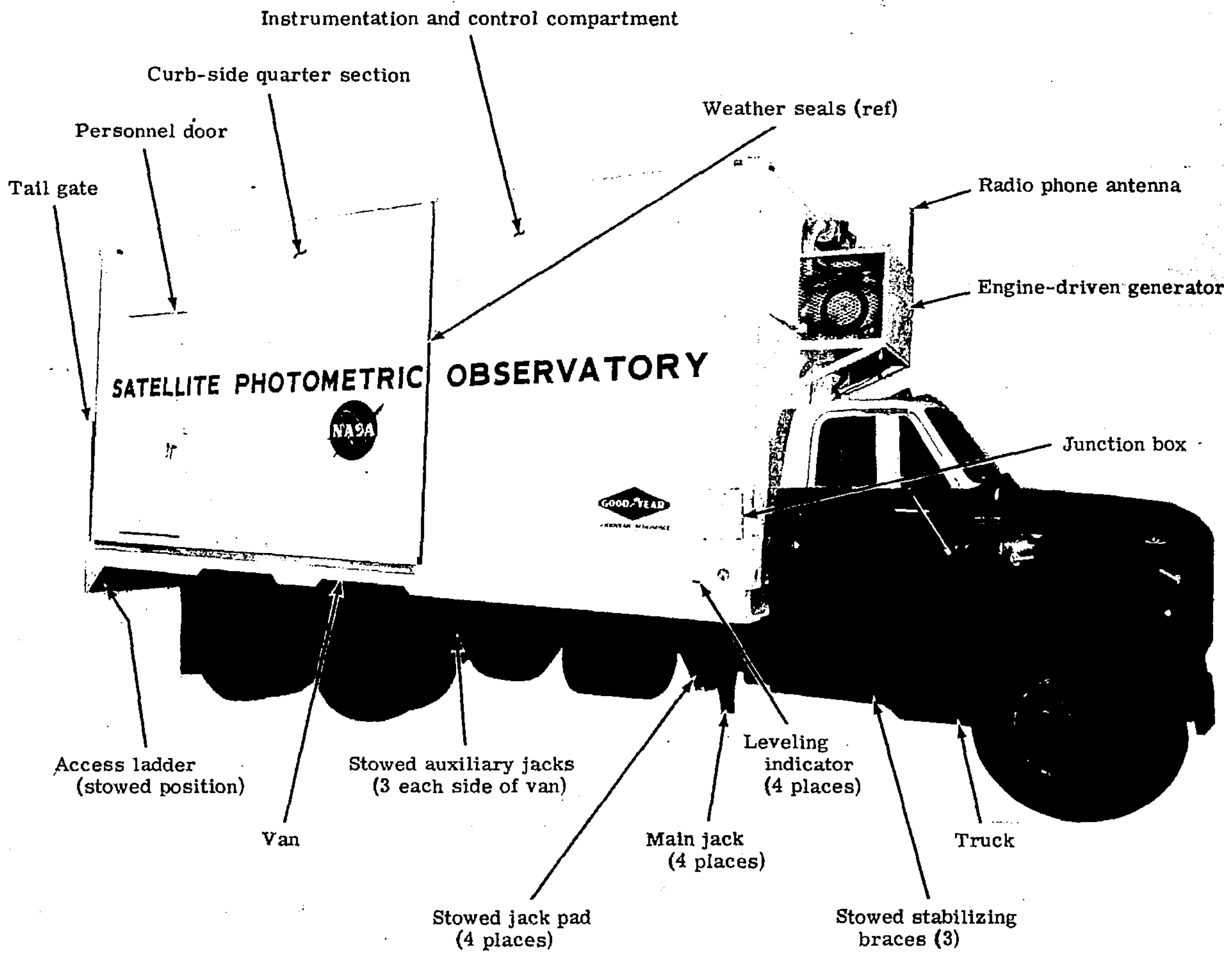

Figure 5. - NASA Mobile Photometric Observatory.

Observation Deck

The aft 12-foot section of the truck's van, as shown in figure 8, encloses the telescope complex.

Four hydraulic cylinders, two for each wall, are used to deploy the side walls of this section outward and downward to a horizontal position, forming an observation deck 25 feet wide by 16 feet long. The equipment on the observation deck includes the telescope complex (fig. 9), an associated control box, a folding table, a six-foot ladder, and an 11-foot ladder. The complex consists of a main telescope and three auxiliary telescopes mounted on a four-axis pedestal. The main telescope is a 24-inch Cassegrain, which can be converted to a 24-inch Newtonian telescope.

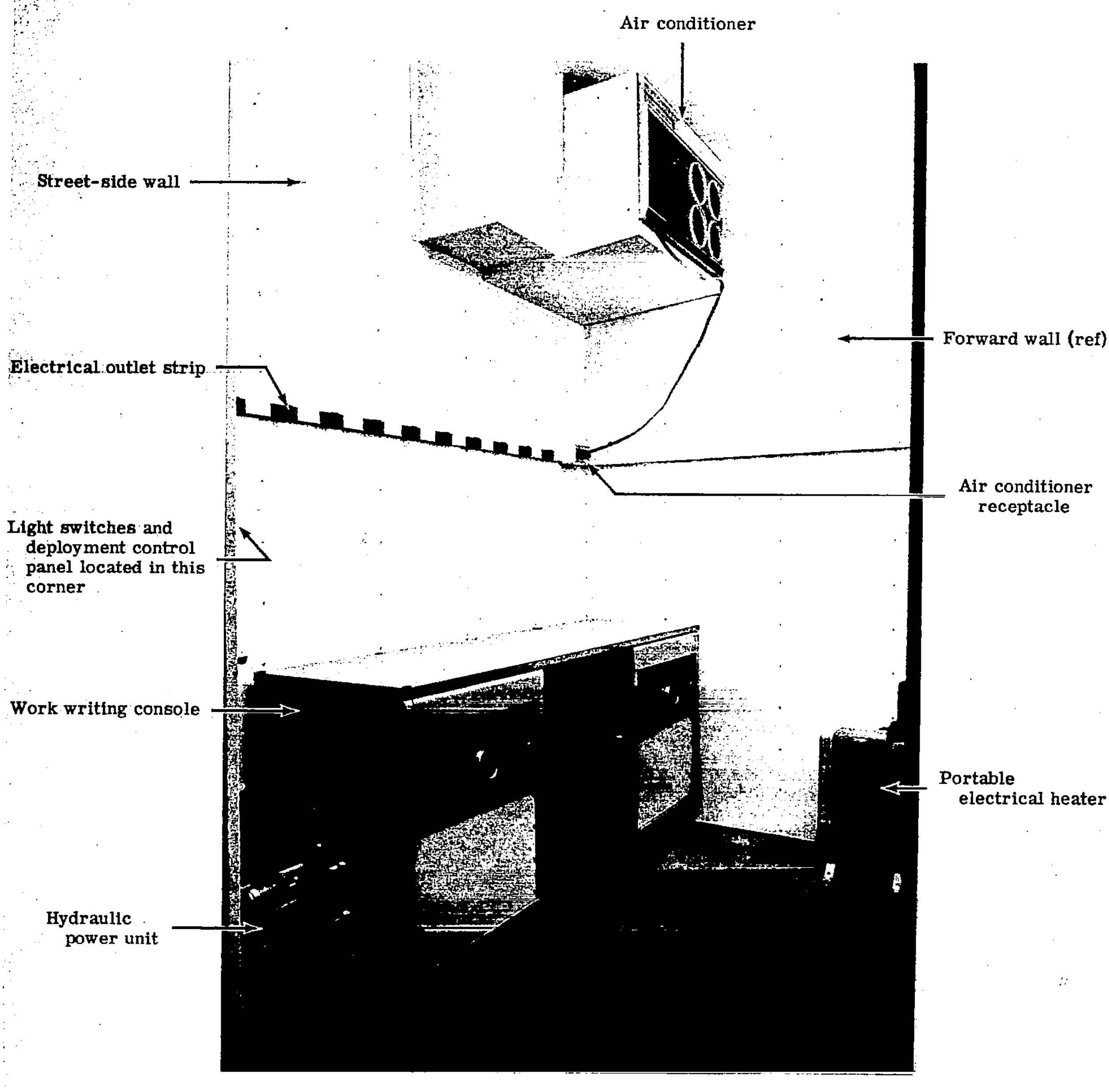

Figure 6. - Interior street-side wall of forward compartment.

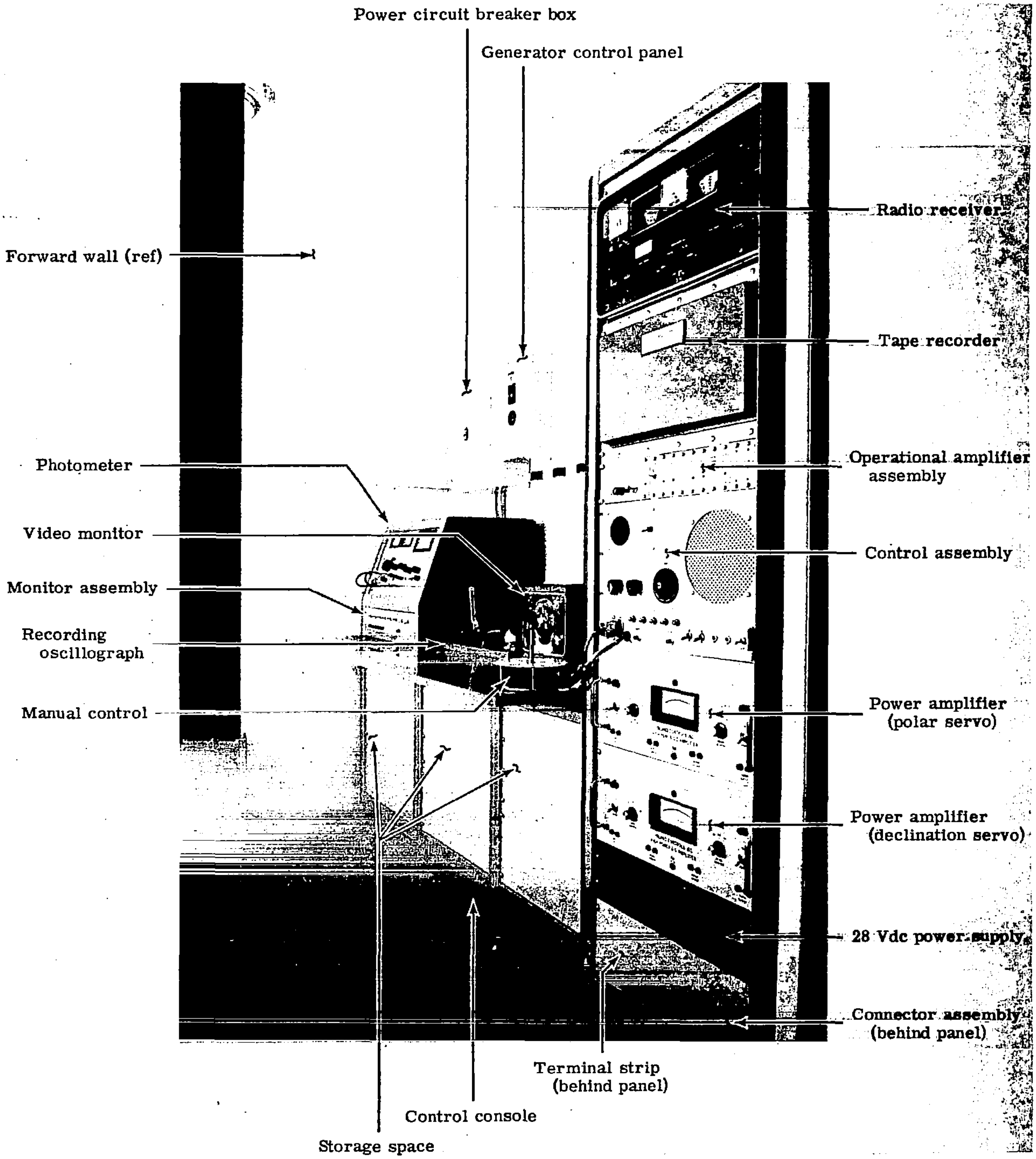

Figure 7. - Interior curb-side wall of forward compartment.

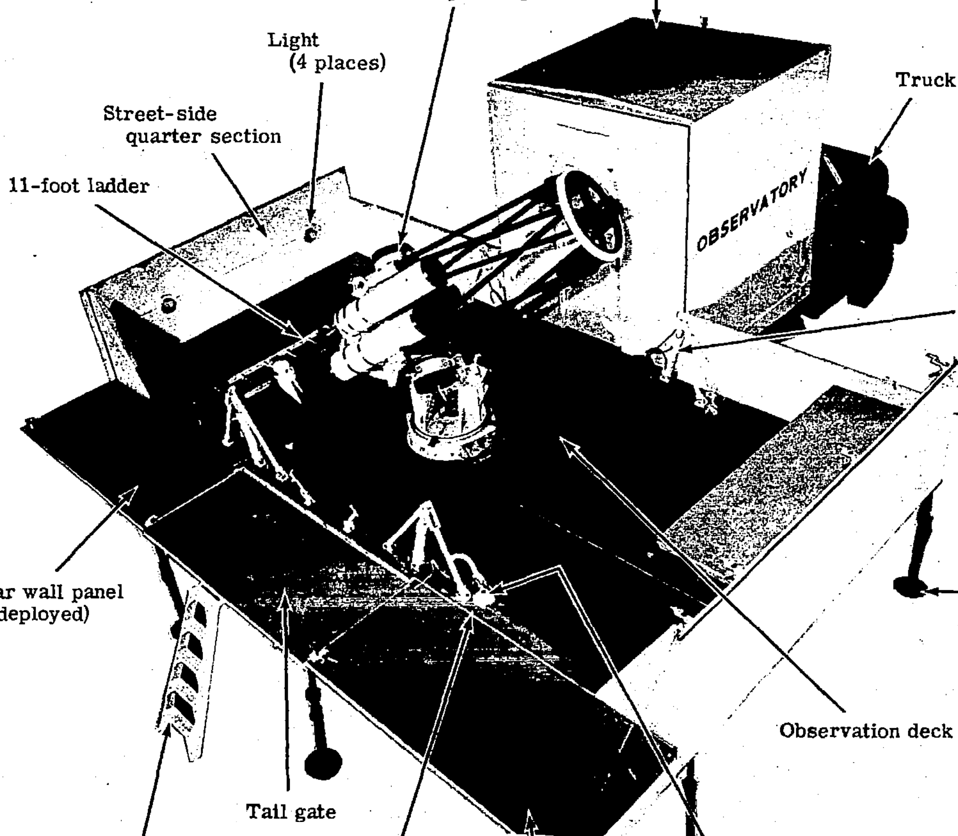

Figure 8. - Mobile Photometric Observatory in deployed configuration.

For photometry work, an instrument head is mounted on the main telescope in the Cassegrain mode. The instrument head incorporates a photomultiplier tube, a Fabry lens, selectable field stops ranging from 30 seconds of arc to 4 minutes of arc, sky background shutters, a depolarizer, a controllable color filter wheel with six filters, and a 360° rotational polarizer. The auxiliary telescopes are a 3-inch refractor, an 8-inch Newtonian, and an 8-inch Cassegrain.

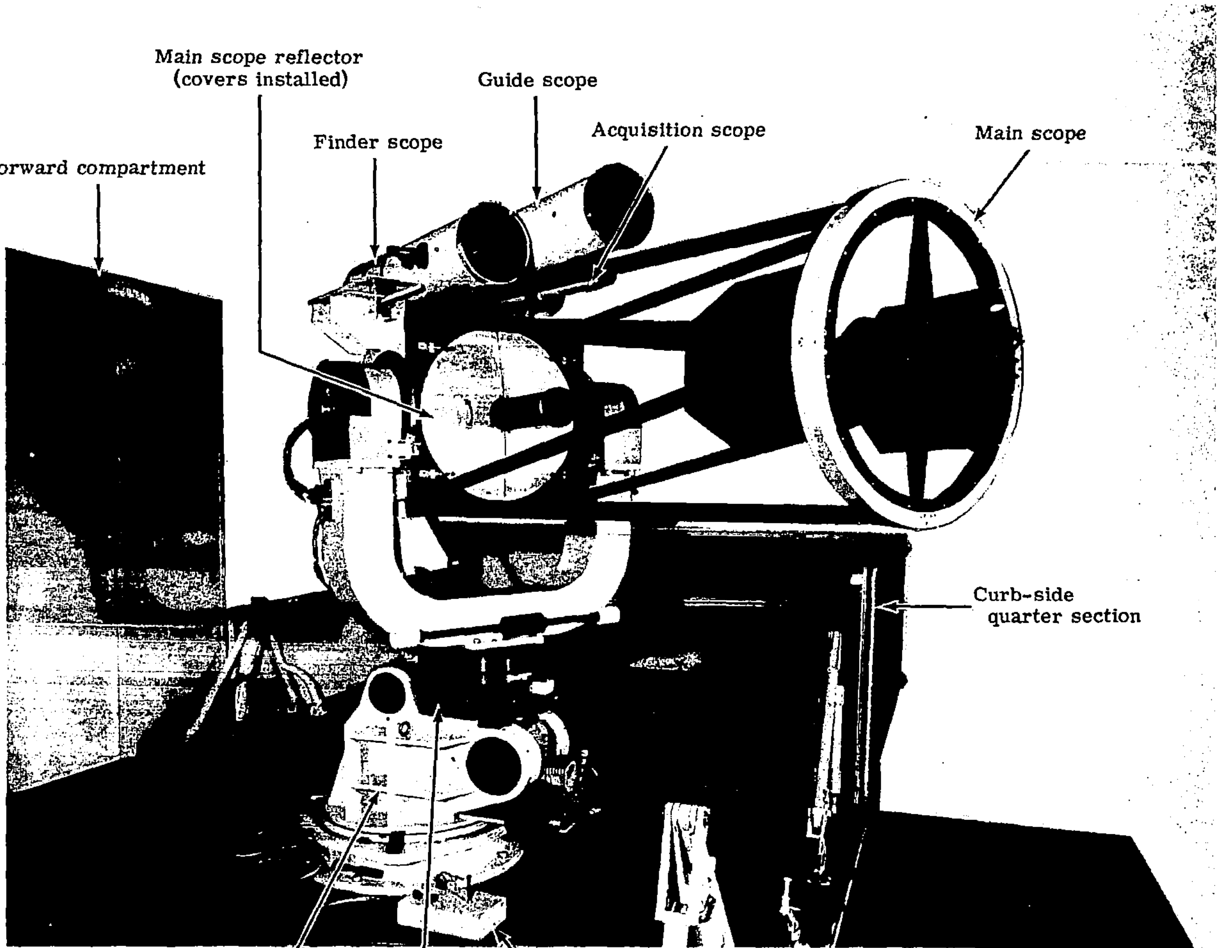

Figure 9. - Telescope complex.

Data Reduction and Transmission Equipment

The equipment used for field data reduction and transmission involved adaptation and installation of available standard equipment. The equipment consisted of a card punching machine, a transceiver unit coupled with a telephone signal unit, and a dataphone. This equipment permitted digital data transmission between the remote observation site and the computation center where corresponding equipment was maintained.

Site Selection

This program required that photometric measurements be made at a suitable observation site, somewhere in the southwestern part of continental United States, which would maximize the number of possible measurements of satellite size and surface characteristics throughout the 60-day period of field operations. Theoretical atmospheric extinction as a function of altitude above mean sea level was investigated for each of the three color bands (U, B, and V), as shown in figure 10, which is based on data in references 10 and 11.

After consideration of the foregoing factors, the optimum observing site was determined to be on Palomar Mountain, California (latitude N, 33 degrees, 18 minutes, 37 seconds; longitude W, 116 degrees, 50 minutes, 55 seconds; elevation 5640 feet above mean sea level). Time reception was obtained by use of a three-element, dipole array, designed for 10-megacycle signal reception from WWVH, Hawaii.

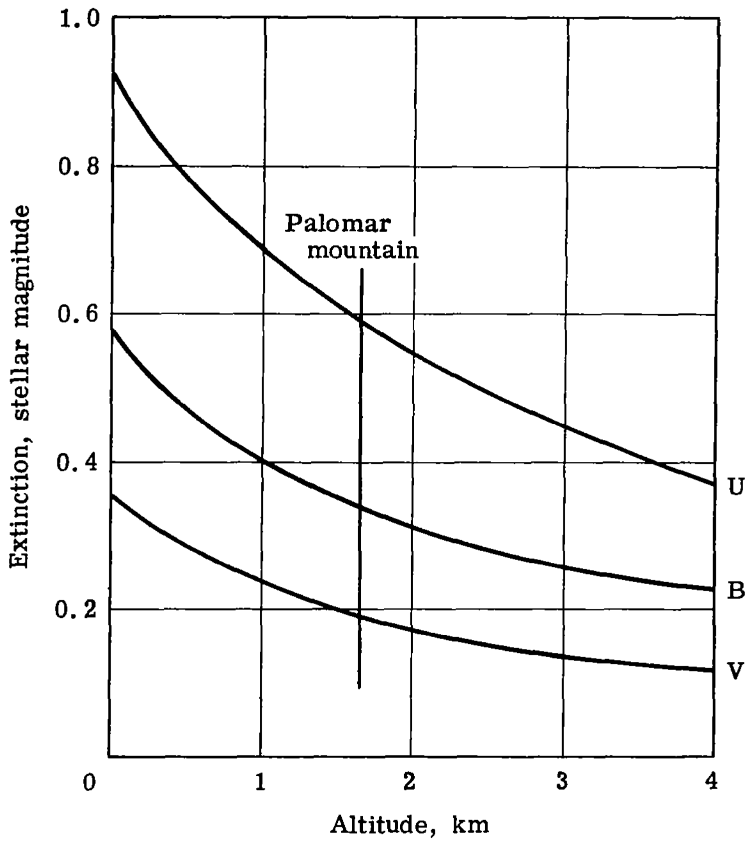

Figure 10. - Theoretical extinction versus altitude above mean sea level.

Preliminary Orbit Geometry Analysis

Preliminary orbital parameters for the PAGEOS I satellite, together with a projected right ascension of the ascending node of 331.5° were used to generate preliminary 60-day look-angle predictions for the chosen Palomar Mountain site. These computer predictions were compared with an earlier manual orbital analysis, which served to confirm the accuracy of both. It also determined the apparent orbital behavior of PAGEOS I as would be observed from Palomar, with respect to the earliest acquisition of the satellite, the adequate number of available passes, and the pass geometry (culmination times, elevations, angular velocities, and phase angles).

OPERATIONAL DESCRIPTION

Operation of the Mobile Observatory at a remote, temporary site includes functions that are peculiar to a remote operation and functions that are normal to satellite observations. The following sections describe, as sequentially as possible, the setup, preparation, observation procedures, data reduction, and data analysis required for a successful observation of the PAGEOS I satellite.

Orbital Analysis and Satellite Predictions

The actual lift-off time of the PAGEOS I satellite was received at Palomar from an official NASA observer present at the Western Test Range launch complex. This information, together with first-actual orbital parameters obtained from NASA-Goddard, permitted manual up-dating of the preliminary ephemeris in time to photometrically acquire the satellite as it first rose above Palomar's southern horizon on its fourth revolution.

For the first few days the PAGEOS I acquisitions were necessarily dependent upon manual corrections to the prelaunch ephemeris. Thereafter, as new orbital elements were received from the Smithsonian Astrophysical Observatory (SAO) in Cambridge, Massachusetts, highly accurate four-axis predictions for each pass were generated and transmitted to the field.

Observation Procedures

The procedure involved in tracking a satellite can be divided into four parts:

(1) Preparing the truck for observation

(2) Selecting and identifying the stars used for calibration

(3) Preparing for and observing the satellite

(4) Setting up for a positional point determination (required to correct the ephemeris for phase-angle determinations)

Preparing the truck for observation involved deploying the sides, positioning the telescope in azimuth and latitude, and turning on the instrumentation.

The stars used in correcting for atmospheric extinction were selected from the Arizona-Tonantzintla catalogue (ref. 3) according to the requirements proposed in Hardie's article, "Photoelectric Reductions" (ref. 1). These requirements were fulfilled in three groups for the determination of primary and secondary extinction coefficients and scale factors. The primary extinction coefficients were determined from five to seven stars which were selected from the satellite's predicted path with a B-V value equal to or less than ±0.4 of the sun's value. These stars were measured before and after each satellite pass (unless two satellite passes occurred one after the other). The second-order extinction coefficients were determined from several pairs of stars. The pairs were selected with a wide range in color and within three degrees of each other. The scale factors were determined from stars located near the zenith having a wide range in color. For stars in these last two groups, second order coefficients and scale factors were measured once a week. After the stars were selected, they were identified on the Skalnate-Pleso charts and listed according to right ascension. To aid in operational accuracy, a copy of this list was prepared for the instrumentation room with each title of the star calibration followed by the bright star catalogue number.

The procedure for observing the satellite required identifying the acquisition field, verifying that the four-axis predictions agreed with the right ascension and declination coordinates, and making a "dry-run" pass of the predicted orbit. The purpose of the dry-run pass was to guide personnel in setting up chairs, ladders, and tables for observer convenience in guiding on the satellite. In addition, it also provided a rapid identification of the sky background that would be photographed for positional determination.

After the dry-run was completed, the telescope was returned to the acquisition field a few minutes before acquisition time. Two observers watched for the satellite, one using the 3-inch refractor telescope and the other using a pair of 7 x 50 binoculars. After acquiring the satellite in the 3-inch refractor, the telescope's tracking rate was adjusted to correspond with the satellite's rate. An operator completed the observation of the satellite pass, observing the "on target" condition through the 8-inch Newtonian telescope and correcting the telescope position with the stick servo control.

The best procedure for making a positional point determination proved to be as follows. The camera was loaded and mounted, the tape recorder was started, and a stopwatch and a set of binoculars were ready for use. The first picture was a title sheet containing the following statements: (1) begin; (2) the name and acquisition time of the satellite; and (3) the universal date. The camera was then mounted with a cable release and a strobe light, which could be switched off and on, attached to its "electric eye." During an observation, pictures were taken of the satellite. The camera shutter was opened with the cable release and closed with a flash from the strobe light. The times of opening and closing the shutter were recorded on the tape, along with a description of the sky background. At the conclusion of an observation an edit picture was taken, recording the frame, a number indicating the sky background, and the time of opening and closing the shutter. A final edit picture was then taken showing the following: (1) end; (2) the name and time of acquisition of the satellite; and (3) the universal date. In addition, during the observation the 7 x 50 binoculars and stopwatch were also used to make a visual positional point determination when the satellite made a near-coincidence with a star.

Data Conversion

The recorded data for each UBV measurement was converted to a digital code and transmitted from the Palomar Mountain observation site to the computational center in Akron, Ohio. Appendix C shows samples of the control and data point information cards, and explains in detail the methods used to record the data. The data was preceded with a header card, which contained the date and title of the observation. The data consisted of filter number, time, intensity, and gain number. The coding for the data was as follows:

(1) The filters were numbered 1, 2, and 3 for the respective VUB sequence.

(2) The time was recorded in universal time to the nearest tenth of a second.

(3) The intensity was recorded in inches by using the level of the sky background as a baseline for each measurement. This eliminated measuring the sky background and subtracting it out later.

(4) The seventeen gain settings were numbered sequentially.

Key Punching and Closed Loop Check

The card punch machine was programmed for automatic duplication to reproduce any desired numbers, such as the hour, on the following card. The automatic skip was used to release the card at the end of the punching of the data code. This eliminated some of the typing and automatically fed the next card in at the conclusion of each data code. The typed data cards were then checked against the oscillograph sheets before transmission. This formed a closed loop check, since the cards were typed from worksheets that were made from the oscillograph sheets.

Computational Center Data Reduction

As soon as the data cards were received from the field, they were examined for possible errors by making complete listings of the data from all the cards. The lists were checked to determine that there were three points (U-B-V) for each of the calibration stars and complete U-B-V-U color sets for the observation of the PAGEOS I satellite.

After values of the various extinction coefficients had been obtained, computer program E-1213, "Satellite Photometer Program: U-B-V Stellar Magnitudes," was run, (see appendix D) using orbital elements corrected to the positional data taken during the pass. This program printed out universal time, altitude, phase angle, U-B-V normalized magnitudes, U-B-V extra-atmospheric magnitudes, etc. The sheets were examined for possible "bad" points (altitudes less than 20°) and these were removed. Computer program E-1214, "Specularity and Diffusivity Determinations: Radius of Curvature and Reflectance," was then run. This program printed out the following information:

(1) Mean normalized magnitudes

(2) Number of points

(3) Sigma of magnitudes

(4) Best-fit specular magnitude

(5) Specularity

(6) The individual points all with normalized magnitude, phase angle, best-fit diffuse magnitude, specular magnitude, and radius of curvature (R_c).

(7) Minimum and maximum radius of curvature.

(8) Mean radius of curvature.

(9) True mean specular magnitude.

(10) Average radius of curvature and sigma of R_c.

(11) Parametric solution of indicated reflectance, using an assumed radius of curvature.

(12) Figure of merit for specularity.

The various calculations of these parameters were handled in several ways:

(1) 3-color (UBV) determinations.

(2) Combined runs were made, i. e., all points were combined for a certain number of runs (approximately 10 runs were combined for a combination run).

(3) Single-color determinations were performed on various days.

Data Analysis

Data analysis began with the computer runs of the extinction coefficients (computer programs E-1960, E-1970, and E-1980) and the satellite observation (E-1213 and E-1214). It is obviously very important to obtain good values of the extinction coefficients before the computer runs of the satellite are begun; thus careful scrutiny of these coefficients was performed. As mentioned in the discussion of theory, there are ways to determine whether or not the values that have been calculated are valid.

Using orbital elements corrected to the pass by real-time tracking data, the computer program E-1213 was then performed and examined for altitude, phase angle, magnitudes, etc. The phase angles and magnitudes were examined to determine whether a particular observation would greatly bias the overall picture because of too small a range of phase angles or if magnitude bias existed because of too many or too few peaks in the reduced data.

When the examination of the E-1213 program was complete, the E-1214 program was performed to obtain mean normalized magnitudes, specularity, radius of curvature, etc. These values were tabulated, graphed, and examined to determine trends and various other characteristics of the day-to-day runs. Since the observations were performed in single color as well as U-B-V colors for the individual runs, these observations were analyzed for such parameters as periodicity and intensity variation. These phenomena are discussed under Results.

The next step in the data analysis was to perform combined runs of the U-B-V observations for the pre-shadow and post-shadow time periods. Five separate computer runs were performed for the various time periods.

The accuracy of results is always a most important factor in any experimental work. A so-called "goodness-of-fit" program was performed on a number of standard stars to gain an insight as to the accuracy of the equipment. A thorough statistical analysis was also performed.

RESULTS

Calibration

Second-order extinction coefficients. - The observations for the second-order calibration constants were performed on the following days: June 23 and 30; July 1, 6, 8, and 18; and August 5, 12, and 18, 1966. As noted in Table II, different second-order coefficients were used in the time periods 24 June to 6 July, 9 to 31 July, 5 to 16 August, and 17 to 22 August. The values used during the time period of 24 June to 6 July were average values from the first four sets of observations, i.e., 23 June, 30 June, 1 July, and 6 July. The observations of 18 July and 12 August were not considered to be of sufficient accuracy to use for the further calculations of calibration constants.

Scale factors. - Scale factor observations were performed on the following days: June 23 and 30; July 9 and 15; and August 6 and 13. Again, as was the case in obtaining satisfactory numbers for the second-order extinction coefficients early in the program, the scale factors provided numbers that were not considered to be of sufficient accuracy to use in the determination of primary extinction coefficients and satellite stellar magnitudes. For this reason the nominal values (see ref. 1) of $\epsilon = 0$, $\mu = 1$, and $\psi = 1$ were used until the 9 July 1966 observations. Starting with the observations on 9 July, excellent values of scale factors were obtained for the remainder of the time period in the field.

Primary extinction coefficients and zero-point terms. - Calibration procedures for primary extinction coefficients and zero-point terms were performed before and after each observation of the PAGEOS I satellite. This procedure is, beyond doubt, the most demanding of the three calibration programs, because it is performed each day; the values of the coefficients are highly significant in the calculation of the stellar magnitudes for the satellite; and the values of the primary extinction coefficients may vary by as much as a factor of two from pass-to-pass, as compared to the second-order coefficients and scale factors, which are comparatively constant.

Obtaining proper values for the coefficients is often a time-consuming job, requiring several reruns before a final set of constants is accepted. The selection of the final values come about through the use of several aids:

(1) The "transparency" and "seeing" was reported on a basis of a 1 to 5 rating for each observing day. (1 equals the poorest and 5 the clearest type of photometric observation conditions.)

(2) The best-fit straight line must have a standard error of residuals of less than 0.1.

(3) The variance of the individual k_v', k'_{b-v}, and k'_{u-b} values must be within a factor of 2 from values of $k_v' = 0.15$, $k'_{b-v} = 0.15$, and $k'_{u-b} = 0.30$, respectively. As can be noted from an examination of the values, there is some variance from this general rule, but the overall agreement is good.

TABLE II. - CALIBRATION CONSTANTS FOR PAGEOS I

Date (a)	2nd Order extinction coefficients		Transformation scale factor			Primary extinction coefficients			Zero-point terms			Remarks
	k''_{b-v}	k''_{u-b}	ϵ	μ	ψ	k'_v	k'_{b-v}	k'_{u-b}	ζ_v	ζ_{b-v}	ζ_{u-b}	
23 Jun 66	-0.0376	-0.0071	0.000	1.000	1.000	--	--	--	--	--	--	
24 Jun 66	-0.0376	-0.0071	0.000	1.000	1.000	0.220	0.072	0.503	-7.585	1.026	-0.192	
25 Jun 66	-0.0376	-0.0071	0.000	1.000	1.000	0.239	0.107	0.309	-7.603	1.059	-0.523	
26 Jun 66	-0.0376	-0.0071	0.000	1.000	1.000	0.311	0.026	0.269	-7.443	1.084	-0.575	
27 Jun 66	-0.0376	-0.0071	0.000	1.000	1.000	0.113	0.254	0.334	-7.782	1.275	-0.407	
28 Jun 66	-0.0376	-0.0071	0.000	1.000	1.000	0.338	0.216	0.224	-7.407	1.223	-0.725	
30 Jun 66	-0.0376	-0.0071	0.000	1.000	1.000	0.183	0.150	0.416	-7.399	1.138	-0.400	
1 Jul 66	-0.0376	-0.0071	0.000	1.000	1.000	0.136	0.108	0.271	-7.432	1.087	-0.568	
5 Jul 66	-0.0376	-0.0071	0.000	1.000	1.000	0.116	0.100	0.280	-6.852	1.074	-0.626	
6 Jul 66	-0.0376	-0.0071	0.000	1.000	1.000	0.119	0.102	0.321	-7.117	1.060	-0.531	
9 Jul 66	-0.0042	-0.0008	0.045	1.055	1.062	0.328	0.206	0.372	-6.816	1.154	-0.549	
10 Jul 66	-0.0042	-0.0008	0.045	1.055	1.062	0.154	0.275	0.308	-6.525	1.256	-0.653	
12 Jul 66	-0.0042	-0.0008	0.045	1.055	1.062	0.083	0.074	0.387	-6.850	1.054	-0.390	
13 Jul 66	-0.0042	-0.0008	0.045	1.055	1.062	0.142	--	--	-6.561	--	--	Continuous V observation
14 Jul 66	-0.0042	-0.0008	0.045	1.055	1.062	--	k'_b = 0.227	--	--	ζ_b = -5.746	--	Continuous B observation
15 Jul 66	-0.0042	-0.0008	0.045	1.055	1.062	--	--	k_u' = 0.485	--	--	ζ_u = -6.291	Continuous U observation
17 Jul 66	-0.0042	-0.0008	0.049	1.021	1.020	0.167	0.083	0.273	-6.913	1.059	-0.496	
18 Jul 66	-0.0042	-0.0008	0.049	1.021	1.020	0.178	0.043	0.303	-6.919	0.959	-0.474	
19 Jul 66	-0.0042	-0.0008	0.049	1.021	1.020	0.173	0.040	0.265	-6.819	0.974	-0.460	
20 Jul 66	-0.0042	-0.0008	0.049	1.021	1.020	0.132	0.114	0.321	-6.930	1.073	-0.424	
21 Jul 66	-0.0042	-0.0008	0.049	1.021	1.020	0.158	0.142	0.277	-6.892	1.091	-0.459	
22 Jul 66	-0.0042	-0.0008	0.049	1.021	1.020	0.221	0.118	0.307	-6.892	1.076	-0.508	
24 Jul 66	-0.0042	-0.0008	0.049	1.021	1.020	0.149	0.100	0.330	-6.937	1.017	-0.406	First pass
24 Jul 66	-0.0042	-0.0008	0.049	1.021	1.020	0.175	0.124	0.223	-6.966	1.077	-0.553	Second pass
25 Jul 66	-0.0042	-0.0008	0.049	1.021	1.020	0.109	0.220	0.192	-6.576	1.197	-0.636	
26 Jul 66	-0.0042	-0.0008	0.049	1.021	1.020	0.293	0.088	0.302	-6.142	0.983	-0.471	
27 Jul 66	-0.0042	-0.0008	0.049	1.021	1.020	0.363	0.053	0.283	-7.246	0.991	-0.475	
31 Jul 66	-0.0042	-0.0008	0.049	1.021	1.020	0.144	0.123	0.308	-6.625	1.116	-0.508	
5 Aug 66	-0.0469	-0.0143	0.054	0.960	1.043	0.215	0.143	0.333	-6.674	1.089	-0.464	First pass
5 Aug 66	-0.0469	-0.0143	0.054	0.960	1.043	0.215	0.096	0.259	-6.688	1.023	-0.608	Second pass
6 Aug 66	-0.0469	-0.0143	0.054	0.960	1.043	0.235	0.136	0.286	-6.744	1.053	-0.592	
7 Aug 66	-0.0469	-0.0143	0.054	0.960	1.043	0.240	0.166	0.386	-6.650	1.111	-0.442	First pass
7 Aug 66	-0.0469	-0.0143	0.054	0.960	1.043	0.217	0.087	0.336	-6.664	1.009	-0.491	Second pass
8 Aug 66	-0.0469	-0.0143	0.054	0.960	1.043	0.112	0.057	0.339	-6.594	0.970	-0.462	First pass
8 Aug 66	-0.0469	-0.0143	0.054	0.960	1.043	0.204	0.129	0.342	-6.519	1.067	-0.490	Second pass
9 Aug 66	-0.0469	-0.0143	0.054	0.960	1.043	0.084	0.169	0.489	-6.768	1.079	-0.292	First pass
9 Aug 66	-0.0469	-0.0143	0.054	0.960	1.043	0.199	0.067	0.394	-6.617	1.014	-0.391	Second pass
10 Aug 66	-0.0469	-0.0143	0.054	0.960	1.043	0.185	0.146	0.368	-6.860	1.097	-0.437	
11 Aug 66	-0.0469	-0.0143	0.054	0.960	1.043	0.213	0.107	0.417	-6.662	1.039	-0.362	
12 Aug 66	-0.0469	-0.0143	0.054	0.960	1.043	0.094	0.131	0.278	-6.680	1.129	-0.551	
13 Aug 66	-0.0469	-0.0143	0.054	0.960	1.043	0.167	0.179	0.270	-6.653	1.154	-0.548	
15 Aug 66	-0.0469	-0.0143	0.054	0.960	1.043	0.181	0.137	0.514	-6.425	1.085	-0.311	
16 Aug 66	-0.0469	-0.0143	0.054	0.960	1.043	0.239	0.175	0.434	-6.857	1.038	-0.458	First pass
16 Aug 66	-0.0469	-0.0143	0.054	0.960	1.043	0.337	0.074	0.394	-6.630	0.986	-0.474	Second pass
17 Aug 66	-0.0276	-0.0405	0.046	0.982	1.002	0.256	0.255	0.343	-6.829	1.187	-0.537	First pass
17 Aug 66	-0.0276	-0.0405	0.046	0.982	1.002	0.219	0.167	0.339	-6.771	1.135	-0.550	Second pass
18 Aug 66	-0.0276	-0.0405	0.046	0.982	1.002	0.113	0.197	0.331	-6.877	1.129	-0.586	First pass
18 Aug 66	-0.0276	-0.0405	0.046	0.982	1.002	0.310	0.164	0.485	-6.799	1.038	-0.353	Second pass
20 Aug 66	-0.0276	-0.0405	0.046	0.982	1.002	0.140	0.144	0.385	-7.019	1.124	-0.392	First pass
20 Aug 66	-0.0276	-0.0405	0.046	0.982	1.002	0.140	0.144	0.385	-7.019	1.124	-0.392	Second pass
21 Aug 66	-0.0276	-0.0405	0.046	0.982	1.002	0.200	0.085	0.362	-6.698	1.037	-0.447	First pass
21 Aug 66	-0.0276	-0.0405	0.046	0.982	1.002	0.200	0.085	0.362	-6.698	1.037	-0.447	Second pass
22 Aug 66	-0.0276	-0.0405	0.046	0.982	1.002	0.065	0.106	0.216	-6.811	1.075	-0.596	

[a] See tables VI, VII, and VIII for reasons observations were not taken on certain dates.

Statistical Error Analysis

As stated in the discussion of statistical evaluation in the theory section of this report, equations (26), (30), (32), and (33) must be satisfied to meet accuracy and confidence level requirements. The values on the left in these equations are reported in tables III and IV.

TABLE III. - PRE-SHADOW ERROR ANALYSIS (24 JUNE TO 12 JULY)

Band	Radius of curvature, R_c, %	Specularity, S, %	Reflectance, γ, %	Stellar magnitude, m
V	1.30	0.55	2.81	.027
U	.86	.26	1.88	.019
B	1.26	.52	2.76	.027

TABLE IV. - POST-SHADOW ERROR ANALYSIS

Period	Band	Radius of curvature, R_c, %	Specularity, S, %	Reflectance, γ, %	Stellar magnitude, m
17 July to 22 Aug (summary)	V	0.83	0.16	1.80	0.02
	U	.62	.08	1.34	.01
	B	.92	.17	1.99	.02
17 July to 27 July	V	1.85	0.59	4.00	0.04
	U	1.43	.29	3.04	.03
	B	2.31	.64	4.89	.04
5 Aug to 14 Aug	V	1.19	0.35	2.57	0.03
	U	.85	.18	1.83	.02
	B	1.14	.35	2.50	.03
15 Aug to 22 Aug	V	1.07	0.37	2.33	0.02
	U	.84	.21	1.83	.02
	B	1.17	.41	2.57	.03

Satellite Characteristics

Table I, which appears in the summary, presents the computer analysis of accumulated 1966 PAGEOS I UBV photometric data, based on various time periods: 24 June through 12 July 1966, (before the first earth-shadow contact, which occurred on 14 July), 17 through 27 July, 5 through 14 August, and 15 through 22 August 1966. The last three columns present the cumulative analysis of all the post-shadow UBV data (17 July through 22 August, 1966). For each period, a figure of merit for the specularity determinations is shown, computed as:

$$\frac{\left\{\sum_{1}^{n} \left[\overline{f(\psi)} - f(\psi)\right]^2\right\}^{1/2}}{\sigma_{R_c}/\bar{R}_c}$$

This expression, which increases with the number of data points and the range of phase angles observed and decreases with increased target scintillation, has been used as a weighting factor in combining computer determinations of specularity, as shown in table V. It follows from this specularity determination that the combined environment factors at the orbital height of PAGEOS I caused no measurable degradation (erosion) in the first two months following deployment.

TABLE V. - WEIGHTED AVERAGE PAGEOS I SPECULARITY DETERMINATIONS

	Optical band	N	Weighted average specularity
Pre-shadow	U + B + V	1071	100.8
Post-shadow	U + B + V	4063	97.0
Total mission	U	2565	98.9
Total mission	B	1285	97.2
Total mission	V	1284	98.8
Total mission	U + B + V	5134	98.4

With consideration given to prelaunch laboratory data on absolute reflectance versus wave length for "fresh and flat" PAGEOS I surface material, the following U, B, and V band reflectances were adopted for use in the local effective radius of curvature determinations:

Optical band	Adopted reflectance
U	0.884
B	0.896
V	0.896

The mean effective radii of curvature thus determined in each color and for each period are shown in table I. With N as a weighting factor, the total-mission weighted average effective radius of curvature was determined for the visual band (most dependable) reflectance to be 50.066 feet, indicating for the PAGEOS I satellite a mean diameter of 100.1 feet, to an accuracy within the required ±1.4 feet at a 96 percent confidence level. Indicated mean diameters from the blue and ultraviolet prelaunch reflectances are 98.9 and 95.1 feet, respectively. These are believed to differ from that obtained in the visual band because the actual U and B reflectances are somewhat lower than assumed. The B and U reflectances which reconcile the total mission photometric data to the V-band indicated diameter of 100 feet are 0.861 and 0.787, respectively. These indicated lower reflectances in the B and U bands are supported by the mean color indices (B-V = +0.66; U-V = +0.82) obtained for the sunlight reflected from PAGEOS I, which are in yellow excess over the true solar indices by two and 12 percent of the intensity, respectively.

Observation of the PAGEOS I Satellite

During the time period from 24 June to 22 August 1966, photometric observations were performed on 52 passes of the PAGEOS I satellite. A general survey of the reduced data is shown in tables VI, VII, and VIII and figures 11, 12, and 13. The tables also state why observations were not performed on certain days; these reasons include cloudy days and days when repairs and various other maintenance functions were being performed on the telescope and photometer facility. The distribution of PAGEOS I pass and observations according to data obtained is as follows:

(1) 45 U-B-V pass observations.

(2) Continuous V-band passes on 13 and 31 July 1966; first pass on 5 August, 11 August, and 18 August 1966.

(3) Continuous B-band on 14 July 1966.

(4) Continuous U-band pass on 15 July.

Continuous single-color observations were performed to show any periodicity in the maximum brightness of the satellite. This phenomena will be further discussed later in this section. In addition to the individual daily observation data, several combined runs were performed. Because the first shadow entry of the PAGEOS I satellite occurred on 14 July, this date or period is selected as the break-point for the combined runs. The pre-shadow combined computer run included observations from 24 June to 12 July 1966 - 12 passes in all. Values for this combined run are included in tables I, VI, VII, and VIII. During the first shadow entry period, continuous one-color observations were performed in U, B, and V colors. Beginning with the observation on 17 July, the first post-shadow U-B-V observations were performed.

After all data subsequent to 17 July 1966 had been received from the field, checked for accuracy, and reduced for individual passes, four separate combined runs were performed. Results are included in tables I, VI, VII, and VIII. These combined runs do not include continuous U-B-V band data. The four periodic combined runs included the following observation periods:

(1) 17 to 27 July - 11 passes

(2) 5 to 14 August - 11 passes

(3) 15 to 22 August - 11 passes

(4) 17 July to 22 August - 33 passes

TABLE VI. - PAGEOS I OBSERVATION DATA - ULTRAVIOLET (U) BAND

Date (1966)	Mean normalized magnitude	Sigma magnitude	Maximum magnitude	Minimum magnitude	Best-fit specular magnitude	True mean specular magnitude	Regression		Specularity, %	Maximum radius of curvature, ft	Minimum radius of curvature, ft	Average radius of curvature, ft
							A	B				
24 Jun	3.04	0.25	3.68	2.65	3.01	3.69	0.144	0.121	54.37	58.90	13.16	47.31
25 Jun	2.84	.11	3.10	2.60	2.84	3.02	.250	.046	84.33	55.86	44.98	50.69
26 Jun	3.10	.16	3.56	2.71	3.09	3.14	.225	.006	97.31	53.82	36.28	44.80
27 Jun	2.88	.23	3.31	2.15	2.85	3.32	.195	.078	71.52	75.34	37.45	48.24
28 Jun	3.11	.19	3.43	2.40	3.09	3.15	.223	.007	96.99	61.99	37.91	44.59
29 Jun	--	--	--	--	--	--	--	--	--	--	--	--
30 Jun	2.82	.10	2.94	2.66	2.81	2.67	.342	-.136	166.13	45.22	39.53	42.33
1 Jul	2.99	.21	3.39	2.47	2.97	--	.283	-.046	119.61	55.34	38.00	45.23
2 Jul	--	--	--	--	--	--	--	--	--	--	--	--
3 Jul	--	--	--	--	--	--	--	--	--	--	--	--
4 Jul	--	--	--	--	--	--	--	--	--	--	--	--
5 Jul	2.94	.15	3.26	2.47	2.93	2.90	.280	-.016	105.90	58.66	42.46	47.92
6 Jul	3.07	.20	3.44	2.58	3.06	2.89	.281	-.043	118.17	53.32	39.27	45.42
7 Jul	--	--	--	--	--	--	--	--	--	--	--	--
8 Jul	--	--	--	--	--	--	--	--	--	--	--	--
9 Jul	3.03	.19	3.35	2.64	3.01	3.08	.237	.009	96.23	55.82	39.01	46.18
10 Jul	2.94	.23	3.69	2.19	2.91	2.79	.312	-.029	110.32	65.30	38.78	49.42
11 Jul	--	--	--	--	--	--	--	--	--	--	--	--
12 Jul	3.02	.22	3.55	2.58	3.00	2.96	.267	-.022	108.85	55.14	36.50	46.02
13 Jul	--	--	--	--	--	--	--	--	--	--	--	--
14 Jul	--	--	--	--	--	--	--	--	--	--	--	--
15 Jul[1′]	2.94	.34	3.64	2.07	2.88	3.26	.214	.070	75.38	74.83	29.93	48.82
15 Jul[1″]	3.09	.25	3.64	2.49	3.07	3.41	.180	.060	74.82	61.01	32.07	45.36
16 Jul	--	--	--	--	--	--	--	--	--	--	--	--
17 Jul	3.05	.42	3.64	1.27	2.94	3.45	.202	.052	79.40	112.26	25.06	44.73
18 Jul	2.98	.31	3.60	2.30	2.93	2.97	.271	-.002	100.74	64.86	35.57	47.91
19 Jul	3.03	.37	3.79	1.69	2.95	3.22	.225	.026	89.63	87.83	26.52	45.47
20 Jul	3.11	.36	3.67	1.40	3.03	3.60	.170	.052	76.57	105.67	20.63	42.04
21 Jul	3.02	.31	3.89	2.17	2.97	3.18	.225	.019	92.19	68.39	25.74	45.32
22 Jul	3.02	.33	3.76	2.40	2.97	3.07	.249	.006	97.68	61.18	32.83	46.41
23 Jul	--	--	--	--	--	--	--	--	--	--	--	--
24 Jul[1]	3.00	.28	3.59	2.11	2.96	3.32	.198	.060	76.67	73.57	28.28	46.63
24 Jul[2]	2.99	.45	5.08	1.92	2.91	3.23	.223	.030	88.11	77.65	13.11	46.06
25 Jul	2.97	.22	3.66	2.40	2.95	3.04	.250	.015	94.26	61.84	34.72	47.57
26 Jul	3.01	.27	3.63	2.15	2.98	3.27	.206	.031	87.07	68.77	28.88	44.65
27 Jul	2.97	.24	3.58	2.36	2.94	3.46	.173	.049	77.81	63.24	29.75	43.40
28 Jul	--	--	--	--	--	--	--	--	--	--	--	--
29 Jul	--	--	--	--	--	--	--	--	--	--	--	--

Note: The superscript 1 and 2 following the date (first column) indicate first pass and second pass.

TABLE VI. - Continued.

Date (1966)	Mean radius of curvature, ft	Sigma radius of curvature, ft	Reflectance	Figure of merit	Phase angle range, deg		No. of points	Remarks
					From	To		
24 Jun	46.22	8.12	.755	3.77	75.28	118.11	34	
25 Jun	50.61	2.88	.906	6.06	70.32	103.18	16	
26 Jun	44.66	3.47	.705	9.59	66.75	111.75	49	
27 Jun	47.80	6.83	.808	6.16	61.97	108.86	37	
28 Jun	44.41	4.25	.697	11.14	57.54	108.80	50	
29 Jun	--	--	--	--	--	--	--	No observation; clouds
30 Jun	42.30	1.56	.633	3.12	110.05	127.88	18	Small change in phase angle range
1 Jul	45.05	4.03	.718	7.07	88.59	130.12	56	
2 Jul	--	--	--	--	--	--	--	No observation; telescope under repair
3 Jul	--	--	--	--	--	--	--	No observation; telescope under repair
4 Jul	--	--	--	--	--	--	--	No observation; telescope under repair
5 Jul	47.82	3.11	.809	15.97	71.87	125.37	62	
6 Jul	45.30	3.28	.726	16.71	61.25	123.70	52	
7 Jul	--	--	--	--	--	--	--	No observation; clouds
8 Jul	--	--	--	--	--	--	--	No observation; low pass only
9 Jul	45.98	4.31	.748	10.63	48.46	98.94	44	
10 Jul	49.22	4.52	.857	21.16	44.08	119.68	70	
11 Jul	--	--	--	--	--	--	--	No observation; clouds
12 Jul	45.81	4.36	.742	7.22	78.14	122.60	46	
13 Jul	--	--	--	--	--	--	--	Continuous V band observation only
14 Jul	--	--	--	--	--	--	--	Continuous B band observation only
15 Jul[1']	47.87	9.63	.811	10.75	59.67	123.30	174	Continuous U band observation only; peaks in
15 Jul[1'']	44.95	5.96	.714	13.24	59.67	123.30	117	Continuous U band observation only; peaks removed
16 Jul	--	--	--	--	--	--	--	No observation; telescope under repair
17 Jul	42.85	14.84	.649	4.37	51.57	115.78	60	
18 Jul	47.42	6.92	.795	8.62	47.80	107.72	46	
19 Jul	44.51	10.10	.701	7.31	43.76	107.21	64	
20 Jul	40.51	12.41	.580	4.94	39.24	101.45	54	
21 Jul	44.70	7.50	.706	9.49	34.80	94.08	68	
22 Jul	45.84	7.19	.743	15.56	30.16	118.24	58	
23 Jul	--	--	--	--	--	--	--	No observation; clouds
24 Jul[1]	45.99	7.80	.748	6.29	59.72	109.58	58	
24 Jul[2]	44.84	9.96	.711	10.63	20.96	105.50	74	
25 Jul	47.29	5.09	.791	14.06	59.36	118.82	84	
26 Jul	44.09	7.07	.687	11.51	22.18	92.46	80	
27 Jul	42.91	6.45	.651	11.01	10.42	87.13	62	
28 Jul	--	--	--	--	--	--	--	No observation; clouds
29 Jul	--	--	--	--	--	--	--	No observation; clouds

TABLE VI. - Continued.

Date (1966)	Mean normalized magnitude	Sigma magnitude	Maximum magnitude	Minimum magnitude	Best-fit specular magnitude	True mean specular magnitude	Regression		Specularity, %	Maximum radius of curvature, ft	Minimum radius of curvature, ft	Average radius of curvature, ft
							A	B				
30 Jul	--	--	--	--	--	--	--	--	--	--	--	--
31 Jul	--	--	--	--	--	--	--	--	--	--	--	--
1 Aug	--	--	--	--	--	--	--	--	--	--	--	--
2 Aug	--	--	--	--	--	--	--	--	--	--	--	--
3 Aug	--	--	--	--	--	--	--	--	--	--	--	--
4 Aug	--	--	--	--	--	--	--	--	--	--	--	--
5 Aug[1]	--	--	--	--	--	--	--	--	--	--	--	--
5 Aug[2]	2.85	0.22	3.50	2.02	2.83	2.82	0.305	-0.006	101.94	73.22	38.28	50.55
6 Aug	2.86	.14	3.35	2.53	2.85	2.92	.273	.009	96.87	57.38	38.10	49.27
7 Aug[1]	2.92	.24	3.53	2.43	2.89	2.82	.305	-.019	106.65	59.39	38.65	49.44
7 Aug[2]	2.93	.19	3.45	2.52	2.92	3.02	.252	.012	95.36	57.25	36.35	47.61
8 Aug[1]	3.02	.19	3.48	2.53	3.00	3.09	.236	.011	95.40	58.60	36.72	46.06
8 Aug[2]	2.91	.23	3.41	2.34	2.88	2.89	.286	-.003	101.01	63.08	38.84	49.18
9 Aug[1]	2.88	.19	3.42	2.41	2.86	2.90	.282	.003	99.06	61.31	38.04	49.41
9 Aug[2]	2.94	.19	3.41	2.51	2.92	2.94	.271	.000	99.97	58.48	38.67	48.25
10 Aug	2.93	.30	3.54	2.31	2.89	3.03	.256	.016	94.12	64.39	33.51	47.93
11 Aug	--	--	--	--	--	--	--	--	--	--	--	--
12 Aug	2.81	.18	3.15	2.43	2.80	2.57	.378	-.056	117.40	60.35	46.80	52.59
13 Aug	2.90	.30	3.55	2.36	2.86	3.08	.246	.042	85.44	63.66	34.09	49.27
14 Aug	--	--	--	--	--	--	--	--	--	--	--	--
15 Aug	2.88	.21	3.47	2.30	2.86	2.84	.297	-.007	102.53	64.13	38.10	49.80
16 Aug[1]	2.94	.29	4.23	2.38	2.90	2.56	.383	-.080	126.51	61.38	34.69	51.00
16 Aug[2]	2.97	.26	3.53	2.28	2.94	2.91	.280	-.012	104.61	63.84	37.29	47.78
17 Aug[1]	3.01	.20	3.67	2.66	2.99	3.14	.226	.023	90.76	54.46	34.18	46.13
17 Aug[2]	2.94	.23	3.51	2.43	2.91	2.97	.266	.005	98.01	60.72	36.90	48.14
18 Aug[1]	--	--	--	--	--	--	--	--	--	--	--	--
18 Aug[2]	2.96	.24	3.62	2.43	2.93	2.82	.303	-.024	108.46	59.40	37.28	48.88
19 Aug	--	--	--	--	--	--	--	--	--	--	--	--
20 Aug[1]	2.93	.21	3.45	2.47	2.91	2.96	.267	.004	98.38	59.50	37.40	48.17
20 Aug[2]	2.91	.19	3.37	2.42	2.89	2.92	.277	.001	99.49	61.07	39.26	48.83
21 Aug[1]	2.91	.21	3.45	2.34	2.89	3.02	.253	.017	93.80	64.09	35.85	48.02
21 Aug[2]	2.92	.17	3.22	2.63	2.91	2.88	.286	-.006	102.24	55.79	42.81	49.01
22 Aug	2.94	.25	3.43	2.43	2.91	3.13	.233	.029	89.07	60.91	34.87	46.88
24 Jun-12 Jul	3.00	.21	3.69	2.15	2.98	2.96	.266	-.009	103.40	68.91	34.00	47.15
17 Jul-27 Jul	3.01	.33	5.08	1.27	2.96	3.17	.231	.022	91.28	106.67	2.23	45.92
5 Aug-14 Aug	2.91	.23	3.55	2.02	2.88	2.93	.274	.005	98.38	73.56	35.83	48.78
15 Aug-22 Aug	2.94	.23	4.23	2.28	2.91	2.92	.278	-.003	101.05	64.70	26.92	48.48
17 Jul-22 Aug	2.95	.28	5.08	1.27	2.92	3.02	.257	.010	96.18	104.83	13.44	47.64
5 Aug-22 Aug	2.92	.23	4.23	2.02	2.90	2.93	.275	.002	99.32	73.46	26.24	48.61

TABLE VI. - Concluded.

Date (1966)	Mean radius of curvature, ft	Sigma radius of curvature, ft	Reflectance	Figure of merit	Phase angle range, deg		No. of points	Remarks
					From	To		
30 Jul	--	--	--	--	--	--	--	No observation; clouds
31 Jul	--	--	--	--	--	--	--	Continuous V band observation only
1 Aug	--	--	--	--	--	--	--	No observation; telescope under repair
2 Aug	--	--	--	--	--	--	--	No observation; telescope under repair
3 Aug	--	--	--	--	--	--	--	No observation; telescope under repair
4 Aug	--	--	--	--	--	--	--	No observation; telescope under repair
5 Aug[1]	--	--	--	--	--	--	--	Continuous V band observation only
5 Aug[2]	50.31	5.03	0.895	20.18	20.48	94.92	98	
6 Aug	49.16	3.30	.854	25.28	15.38	91.98	62	
7 Aug[1]	49.22	4.64	.857	14.16	40.86	109.91	40	
7 Aug[2]	47.40	4.32	.794	15.89	13.51	94.77	40	
8 Aug[1]	45.86	4.22	.744	18.21	40.87	107.41	74	
8 Aug[2]	48.91	5.19	.846	16.31	17.31	88.70	78	
9 Aug[1]	49.21	4.44	.856	19.54	34.91	102.83	78	
9 Aug[2]	48.06	4.19	.817	16.27	19.95	82.81	66	
10 Aug	47.39	7.20	.794	9.58	31.48	99.47	50	
11 Aug	--	--	--	--	--	--	--	Continuous V band observation only
12 Aug	52.49	3.36	.974	8.17	55.50	88.11	30	
13 Aug	48.64	7.80	.836	8.54	52.71	114.98	68	
14 Aug	--	--	--	--	--	--	--	No observation; clouds
15 Aug	49.60	4.57	.870	22.94	26.36	109.09	82	
16 Aug[1]	50.84	3.96	.914	16.90	44.66	100.88	64	
16 Aug[2]	47.48	5.41	.797	10.92	50.08	112.54	58	
17 Aug[1]	45.90	4.57	.745	13.12	44.87	107.47	56	
17 Aug[2]	47.85	5.31	.810	18.91	24.65	108.85	78	
18 Aug[1]	--	--	--	--	--	--	--	Continuous V band observation only
18 Aug[2]	48.67	4.53	.838	14.39	38.71	98.88	64	
19 Aug	--	--	--	--	--	--	--	No observation; clouds
20 Aug[1]	47.93	4.84	.812	10.64	41.44	93.28	48	
20 Aug[2]	48.64	4.37	.837	12.22	28.94	81.52	51	
21 Aug[1]	47.77	4.99	.807	10.17	36.82	89.50	48	
21 Aug[2]	48.88	3.62	.845	13.04	32.16	78.78	48	
22 Aug	46.46	6.27	.763	6.26	45.86	89.62	42	
24 Jun-12 Jul	46.94	4.55	.779	43.48	44.08	130.12	534	Combined run; pre-shadow
17 Jul-27 Jul	45.11	8.47	.720	33.96	10.42	118.82	708	Combined run; post-shadow
5 Aug-14 Aug	48.51	5.20	.832	52.78	13.51	114.98	684	Combined run; post-shadow
15 Aug-22 Aug	48.22	4.98	.822	47.86	24.65	112.54	639	Combined run; post-shadow
17 Jul-22 Aug	47.24	6.47	.789	71.92	13.51	118.82	2031	Combined run(s); total post-shadow
5 Aug-22 Aug	48.34	5.11	.826	71.35	13.51	114.98	1323	Combined run(s); post-shadow

TABLE VII. - PAGEOS I OBSERVATION DATA - BLUE (B) BAND

Date (1966)	Mean normalized magnitude	Sigma magnitude	Maximum magnitude	Minimum magnitude	Best-fit specular magnitude	True mean specular magnitude	Regression		Specularity, %	Maximum radius of curvature, ft	Minimum radius of curvature, ft	Average radius of curvature, ft
							A	B				
24 Jun	2.82	0.11	3.06	2.61	2.82	2.99	0.257	0.047	84.58	54.94	41.93	49.68
25 Jun	2.68	.09	2.85	2.53	2.67	2.97	.260	.085	75.29	55.60	49.23	52.99
26 Jun	2.97	.22	3.60	2.49	2.95	2.99	.261	.003	98.83	57.48	34.07	46.08
27 Jun	2.71	.24	3.24	2.22	2.69	3.16	.229	.088	72.14	65.82	28.31	50.17
28 Jun	2.93	.22	3.24	2.42	2.91	3.15	.226	.043	83.94	59.01	38.29	46.42
29 Jun	--	--	--	--	--	--	--	--	--	--	--	--
30 Jun	2.83	.10	3.02	2.69	2.83	2.97	.260	.120	68.32	59.41	51.37	55.53
1 Jul	2.81	.30	3.84	2.28	2.77	2.90	.289	.048	85.65	65.44	28.94	51.85
2 Jul	--	--	--	--	--	--	--	--	--	--	--	--
3 Jul	--	--	--	--	--	--	--	--	--	--	--	--
4 Jul	--	--	--	--	--	--	--	--	--	--	--	--
5 Jul	2.83	.15	3.28	2.55	2.82	2.98	.261	.050	83.94	56.79	41.85	50.14
6 Jul	2.78	.20	3.21	2.37	2.76	--	.357	-.045	114.58	60.70	42.12	50.20
7 Jul	--	--	--	--	--	--	--	--	--	--	--	--
8 Jul	--	--	--	--	--	--	--	--	--	--	--	--
9 Jul	2.86	.18	3.15	2.45	2.84	2.84	.297	-.004	101.26	58.39	42.62	48.71
10 Jul	2.83	.15	3.14	2.56	2.82	2.79	.309	-.008	102.62	55.08	42.86	49.42
11 Jul	--	--	--	--	--	--	--	--	--	--	--	--
12 Jul	2.89	.27	3.27	2.29	2.85	2.78	.318	-.042	115.27	60.83	40.78	47.07
13 Jul	--	--	--	--	--	--	--	--	--	--	--	--
14 Jul[1']	2.87	.32	3.51	2.08	2.82	3.10	.245	.066	78.83	72.56	32.07	49.54
14 Jul[1"]	3.03	.20	3.51	2.58	3.01	3.20	.214	.045	82.57	55.27	35.61	45.73
15 Jul	--	--	--	--	--	--	--	--	--	--	--	--
16 Jul	--	--	--	--	--	--	--	--	--	--	--	--
17 Jul	2.81	.45	3.37	1.18	2.69	3.21	.255	.065	79.74	112.38	26.03	48.31
18 Jul	2.85	.30	3.52	2.08	2.80	3.20	.226	.061	78.69	70.70	30.97	47.47
19 Jul	2.81	.38	3.41	1.68	2.73	3.03	.270	.035	88.40	84.70	32.26	48.46
20 Jul	3.00	.28	3.52	2.04	2.96	3.24	.214	.034	86.37	70.76	33.14	44.06
21 Jul	2.91	.26	3.60	2.42	2.88	3.12	.236	.026	90.13	57.69	33.50	45.52
22 Jul	2.89	.40	3.59	2.15	2.82	2.99	.274	.016	94.52	68.27	33.41	47.48
23 Jul	--	--	--	--	--	--	--	--	--	--	--	--
24 Jul[1]	2.85	.32	3.56	2.22	2.81	2.76	.327	-.024	107.78	62.99	35.51	48.99
24 Jul[2]	2.76	.44	3.68	1.48	2.66	2.71	.358	-.008	102.19	90.03	33.55	51.98
25 Jul	2.80	.38	4.49	2.00	2.74	3.14	.230	.088	72.26	73.94	19.99	50.58
26 Jul	2.80	.32	3.32	1.88	2.74	3.05	.259	.035	87.96	75.55	33.95	47.86
27 Jul	2.76	.40	3.66	1.66	2.68	4.08	.117	.118	49.63	96.11	11.24	42.67
28 Jul	--	--	--	--	--	--	--	--	--	--	--	--

TABLE VII. - Continued.

Date (1966)	Mean radius of curvature, ft	Sigma radius of curvature, ft	Reflectance	Figure of merit	Phase angle range, deg		No. of points	Remarks
					From	To		
24 Jun	49.61	2.68	0.882	8.33	75.59	117.83	17	
25 Jun	52.94	2.16	1.005	6.00	70.45	103.94	8	Small number of points
26 Jun	45.83	4.75	.753	5.11	66.86	111.55	26	
27 Jun	49.48	7.86	.877	3.96	62.04	108.76	19	
28 Jun	46.09	5.67	.761	6.12	58.10	108.65	25	
29 Jun	--	--	--	--	--	--	--	No observation; clouds
30 Jun	55.47	2.63	1.102	1.62	111.60	126.90	9	Small number of points and phase angle change
1 Jul	51.28	7.29	.942	3.16	88.82	130.03	28	
2 Jul	--	--	--	--	--	--	--	No observation; telescope under repair
3 Jul	--	--	--	--	--	--	--	No observation; telescope under repair
4 Jul	--	--	--	--	--	--	--	No observation; telescope under repair
5 Jul	50.00	3.67	.896	9.97	72.52	125.26	31	
6 Jul	50.06	3.84	.898	11.21	61.40	123.19	26	
7 Jul	--	--	--	--	--	--	--	No observation; clouds
8 Jul	--	--	--	--	--	--	--	No observation; low pass only
9 Jul	48.54	4.11	.845	8.30	48.69	98.71	22	
10 Jul	49.32	3.19	.872	21.21	44.08	119.35	35	
11 Jul	--	--	--	--	--	--	--	No observation; clouds
12 Jul	46.72	5.52	.784	4.12	78.75	122.09	23	
13 Jul	--	--	--	--	--	--	--	Continuous V band observation only
14 Jul[1']	48.80	8.73	.854	8.05	65.70	127.63	74	Continuous B band observation only; peaks in
14 Jul[1'']	45.51	4.44	.742	11.91	65.70	127.63	50	Continuous B band observation only; peaks removed
15 Jul	--	--	--	--	--	--	--	Continuous U band observation only
16 Jul	--	--	--	--	--	--	--	No observation; telescope under repair
17 Jul	46.11	16.38	.762	3.03	51.61	115.62	30	
18 Jul	46.67	8.98	.781	4.66	47.91	107.61	23	
19 Jul	47.36	10.83	.804	5.14	43.78	106.70	32	
20 Jul	43.49	7.43	.678	6.19	39.25	102.64	27	
21 Jul	45.04	6.50	.727	7.82	34.82	93.81	34	
22 Jul	46.57	9.33	.777	8.67	30.17	118.07	29	
23 Jul	--	--	--	--	--	--	--	No observation; clouds
24 Jul[1]	48.53	6.78	.844	5.38	60.02	109.39	29	
24 Jul[2]	50.94	11.06	.930	7.65	20.96	104.97	37	
25 Jul	49.65	8.91	.884	6.05	59.58	118.61	42	
26 Jul	47.05	9.23	.793	6.69	22.59	92.13	40	
27 Jul	38.93	18.39	.543	2.68	11.01	86.79	31	
28 Jul	--	--	--	--	--	--	--	No observation; clouds

TABLE VII. - Continued.

Date (1966)	Mean normalized magnitude	Sigma magnitude	Maximum magnitude	Minimum magnitude	Best-fit specular magnitude	True mean specular magnitude	Regression		Specularity, %	Maximum radius of curvature, ft	Minimum radius of curvature, ft	Average radius of curvature, ft
							A	B				
29 Jul	--	--	--	--	--	--	--	--	--	--	--	--
30 Jul	--	--	--	--	--	--	--	--	--	--	--	--
31 Jul	--	--	--	--	--	--	--	--	--	--	--	--
1 Aug	--	--	--	--	--	--	--	--	--	--	--	--
2 Aug	--	--	--	--	--	--	--	--	--	--	--	--
3 Aug	--	--	--	--	--	--	--	--	--	--	--	--
4 Aug	--	--	--	--	--	--	--	--	--	--	--	--
5 Aug[1]	--	--	--	--	--	--	--	--	--	--	--	--
5 Aug[2]	2.77	0.20	3.24	2.25	2.75	2.68	0.345	-0.016	104.87	64.34	42.76	51.31
6 Aug	2.74	.19	3.08	2.34	2.73	2.76	.321	.002	99.31	61.16	43.21	50.82
7 Aug[1]	2.78	.17	3.07	2.46	2.77	2.81	.305	.006	98.09	57.99	43.23	49.93
7 Aug[2]	2.76	.21	3.29	2.43	2.75	2.81	.305	.008	97.37	58.63	38.55	50.07
8 Aug[1]	2.83	.16	3.19	2.35	2.82	2.87	.288	.007	97.53	60.97	40.79	48.67
8 Aug[2]	2.76	.27	3.22	2.20	2.73	2.80	.314	.006	98.12	65.34	39.93	50.40
9 Aug[1]	2.75	.20	3.21	2.31	2.74	2.90	.282	.028	90.86	61.73	37.51	49.74
9 Aug[2]	2.82	.20	3.42	2.46	2.81	2.79	.312	-.006	101.89	58.16	37.94	49.52
10 Aug	2.75	.26	3.20	2.11	2.71	2.76	.324	.003	98.99	67.99	41.09	50.95
11 Aug	--	--	--	--	--	--	--	--	--	--	--	--
12 Aug	2.67	.18	3.00	2.34	2.65	2.41	.438	-.071	119.21	60.92	48.63	54.34
13 Aug	2.74	.29	3.22	2.22	2.70	2.80	.316	.018	94.56	64.80	40.27	51.37
14 Aug	--	--	--	--	--	--	--	--	--	--	--	--
15 Aug	2.75	.20	3.27	2.26	2.73	2.80	.308	.012	96.19	63.66	39.12	50.56
16 Aug[1]	2.83	.20	3.43	2.44	2.82	2.68	.342	-.032	110.33	58.92	39.43	49.84
16 Aug[2]	2.81	.24	3.37	2.36	2.79	2.67	.348	-.040	112.91	58.08	40.04	49.62
17 Aug[1]	2.76	.19	3.11	2.31	2.74	2.74	.326	-.004	101.22	61.82	42.79	50.75
17 Aug[2]	2.76	.27	3.40	2.23	2.73	2.81	.310	.010	96.89	64.90	37.04	50.40
18 Aug[1]	--	--	--	--	--	--	--	--	--	--	--	--
18 Aug[2]	2.76	.27	3.34	2.28	2.73	2.69	.345	-.014	104.34	62.30	39.01	51.32
19 Aug	--	--	--	--	--	--	--	--	--	--	--	--
20 Aug[1]	2.81	.19	3.32	2.55	2.79	2.67	.344	-.027	108.54	55.74	41.12	50.44
20 Aug[2]	2.75	.21	3.19	2.26	2.73	2.74	.326	-.000	100.15	63.46	41.46	50.96
21 Aug[1]	2.77	.23	3.49	2.46	2.75	2.83	.302	.010	96.65	57.51	34.97	49.93
21 Aug[2]	2.75	.17	3.09	2.24	2.73	2.55	.385	-.035	110.07	63.97	45.25	52.99
22 Aug	2.79	.24	3.41	2.30	2.76	2.99	.263	.036	87.88	62.65	32.72	48.50
24 Jun-12 Jul	2.84	.22	3.84	2.22	2.82	2.85	.297	.002	99.33	65.03	30.78	49.05
17 Jul-27 Jul	2.83	.37	4.49	1.18	2.77	3.03	.268	.031	89.66	108.04	18.75	48.04
5 Aug-14 Aug	2.77	.22	3.42	2.11	2.74	2.77	.318	.001	99.82	67.95	37.00	50.45
15 Aug-22 Aug	2.77	.23	3.49	2.23	2.75	2.77	.318	-.000	100.12	64.23	36.03	50.34
17 Jul-22 Aug	2.79	.28	4.49	1.18	2.75	2.86	.298	.013	95.85	105.79	21.26	49.54
5 Aug-22 Aug	2.77	.22	3.49	2.11	2.75	2.77	.318	.000	99.91	67.94	35.96	50.39

TABLE VII. - Concluded.

Date (1966)	Mean radius of curvature, ft	Sigma radius of curvature, ft	Reflectance	Figure of merit	Phase angle range, deg		No. of points	Remarks
					From	To		
29 Jul	--	--	--	--	--	--	--	No observation; clouds
30 Jul	--	--	--	--	--	--	--	No observation; clouds
31 Jul	--	--	--	--	--	--	--	Continuous V band observation only
1 Aug	--	--	--	--	--	--	--	No observation; telescope under repair
2 Aug	--	--	--	--	--	--	--	No observation; telescope under repair
3 Aug	--	--	--	--	--	--	--	No observation; telescope under repair
4 Aug	--	--	--	--	--	--	--	No observation; telescope under repair
5 Aug[1]	--	--	--	--	--	--	--	Continuous V band observation only
5 Aug[2]	51.14	4.16	0.937	17.51	20.98	94.64	49	
6 Aug	50.63	4.48	.919	13.59	16.30	91.73	31	
7 Aug[1]	49.77	3.98	.888	11.79	41.43	109.70	20	
7 Aug[2]	49.84	4.74	.890	10.78	14.27	94.54	20	
8 Aug[1]	48.52	3.80	.844	15.09	41.15	107.10	37	
8 Aug[2]	50.00	6.42	.896	9.56	17.92	88.51	39	
9 Aug[1]	49.48	5.05	.877	12.24	35.21	102.63	39	
9 Aug[2]	49.33	4.25	.872	11.67	20.49	82.57	33	
10 Aug	50.58	6.32	.917	8.21	31.74	99.21	25	
11 Aug	--	--	--	--	--	--	--	Continuous V band observation only
12 Aug	54.23	3.52	1.054	5.66	56.37	87.84	15	
13 Aug	50.83	7.41	.926	6.61	53.47	114.57	34	
14 Aug	--	--	--	--	--	--	--	No observation; clouds
15 Aug	50.33	4.84	.908	15.48	26.92	108.84	41	
16 Aug[1]	49.69	3.76	.885	12.29	45.08	100.68	32	
16 Aug[2]	49.40	4.71	.875	9.19	51.11	112.22	29	
17 Aug[1]	50.56	4.44	.916	10.48	45.52	107.31	28	
17 Aug[2]	50.01	6.21	.896	11.97	25.24	108.52	39	
18 Aug[1]	--	--	--	--	--	--	--	Continuous V band observation only
18 Aug[2]	50.98	5.86	.931	8.25	39.34	96.55	32	
19 Aug	--	--	--	--	--	--	--	No observation; clouds
20 Aug[1]	50.31	3.58	.907	10.67	42.18	93.04	24	
20 Aug[2]	50.73	4.94	.922	8.17	29.39	82.01	26	
21 Aug[1]	49.63	5.25	.883	6.83	49.07	89.13	24	
21 Aug[2]	52.88	3.47	1.002	10.38	32.67	78.59	24	
22 Aug	48.08	6.29	.828	4.55	46.73	89.17	21	
24 Jun- 12 Jul	48.81	4.94	.854	29.50	44.08	130.03	269	Combined run - pre-shadow
17 Jul- 27 Jul	47.08	10.13	.794	21.04	11.01	118.61	354	Combined run - post-shadow
5 Aug- 14 Aug	50.19	5.18	.903	38.76	14.27	114.57	342	Combined run - post-shadow
15 Aug- 22 Aug	50.08	5.13	.899	34.02	25.24	112.22	320	Combined run - post-shadow
17 Jul- 22 Aug	49.06	7.08	.863	48.35	11.01	118.61	1016	Combined run(s) - total post-shadow
5 Aug- 22 Aug	50.13	5.14	.901	51.92	14.77	114.57	662	Combined run(s) - post-shadow

TABLE VIII. - PAGEOS I OBSERVATION DATA - VISUAL (V) BAND

Date (1966)	Mean normalized magnitude	Sigma magnitude	Maximum magnitude	Minimum magnitude	Best-fit specular magnitude	True mean specular magnitude	Regression		Specularity, %	Maximum radius of curvature, ft	Minimum radius of curvature, ft	Average radius of curvature, ft
							A	B				
24 Jun	2.20	0.11	2.37	2.00	2.19	2.44	0.424	0.121	77.79	54.23	43.81	49.55
25 Jun	1.95	.29	2.31	1.25	1.90	1.94	.700	-.007	101.08	75.47	46.33	55.33
26 Jun	2.18	.15	2.42	1.80	2.17	2.45	.426	.104	80.34	59.75	41.45	48.73
27 Jun	2.03	.19	2.39	1.55	2.01	2.36	.464	.135	77.49	66.15	45.11	51.70
28 Jun	2.26	.17	2.61	1.84	2.24	2.37	.457	.042	91.55	57.74	38.83	47.29
29 Jun	--	--	--	--	--	--	--	--	--	--	--	--
30 Jun	2.13	.11	2.29	1.96	2.12	1.91	.689	-.392	232.45	39.52	34.35	36.54
1 Jul	2.13	.21	2.53	1.75	2.12	2.20	.538	.065	89.22	61.42	42.73	51.90
2 Jul	--	--	--	--	--	--	--	--	--	--	--	--
3 Jul	--	--	--	--	--	--	--	--	--	--	--	--
4 Jul	--	--	--	--	--	--	--	--	--	--	--	--
5 Jul	2.14	.17	2.38	1.64	2.13	2.12	.573	-.010	101.85	62.58	44.87	50.20
6 Jul	2.24	.23	2.71	1.85	2.22	2.12	.577	-.060	111.52	56.30	39.49	48.12
7 Jul	--	--	--	--	--	--	--	--	--	--	--	--
8 Jul	--	--	--	--	--	--	--	--	--	--	--	--
9 Jul	2.18	.16	2.55	1.91	2.17	2.35	.464	.058	88.85	54.71	38.51	48.40
10 Jul	2.24	.26	2.69	1.34	2.21	2.30	.496	.022	95.79	72.78	39.37	47.90
11 Jul	--	--	--	--	--	--	--	--	--	--	--	--
12 Jul	2.24	.25	2.63	1.69	2.21	2.11	.586	-.094	119.15	59.20	38.73	46.86
13 Jul[1']	2.04	.36	2.64	1.30	1.98	2.02	.657	-.014	102.16	73.25	39.50	53.13
13 Jul[1'']	2.23	.21	2.64	1.67	2.21	2.32	.481	.062	88.52	64.81	41.44	49.27
14 Jul	--	--	--	--	--	--	--	--	--	--	--	--
15 Jul	--	--	--	--	--	--	--	--	--	--	--	--
16 Jul	--	--	--	--	--	--	--	--	--	--	--	--
17 Jul	2.21	.48	2.92	.33	2.06	2.91	.397	.163	70.93	129.79	17.77	45.73
18 Jul	2.28	.30	2.82	1.67	2.24	2.36	.477	.027	94.73	62.86	35.44	47.15
19 Jul	2.24	.33	2.77	1.30	2.19	2.45	.451	.055	89.10	74.48	32.75	46.69
20 Jul	2.29	.27	2.74	1.82	2.25	2.17	.557	-.038	107.34	57.18	39.52	47.87
21 Jul	2.22	.39	2.83	.87	2.14	2.57	.428	.074	85.17	92.52	26.82	45.82
22 Jul	2.11	.38	2.83	1.23	2.04	2.00	.668	-.039	106.26	74.30	36.42	52.35
23 Jul	--	--	--	--	--	--	--	--	--	--	--	--
24 Jul[1]	2.01	.31	2.58	1.24	1.97	1.95	.688	-.033	105.11	74.12	40.58	53.61
24 Jul[2]	2.18	.37	2.89	1.28	2.12	1.95	.689	-.069	111.10	71.55	39.53	52.14
25 Jul	2.19	.26	2.98	1.73	2.16	2.12	.583	-.036	106.65	60.14	35.82	49.18
26 Jul	2.20	.30	2.83	1.67	2.16	2.17	.563	-.011	101.93	62.08	36.70	49.30
27 Jul	2.15	.25	2.61	1.66	2.12	2.55	.401	.087	82.09	61.77	31.53	46.17
28 Jul	--	--	--	--	--	--	--	--	--	--	--	--
29 Jul	--	--	--	--	--	--	--	--	--	--	--	--
30 Jul	--	--	--	--	--	--	--	--	--	--	--	--

TABLE VIII. - Continued.

Date (1966)	Mean radius of curvature, ft	Sigma radius of curvature, ft	Reflectance	Figure of merit	Phase angle range, deg		No. of points	Remarks
					From	To		
24 Jun	49.50	2.27	0.878	10.07	75.47	118.28	17	
25 Jun	54.81	8.14	1.077	1.70	70.54	104.75	8	Small number of points
26 Jun	48.55	4.18	.845	6.12	66.80	111.16	25	
27 Jun	51.42	5.54	.948	5.78	62.01	108.59	19	
28 Jun	47.13	4.01	.796	8.87	57.73	108.46	25	
29 Jun	--	--	--	--	--	--	--	No observation; clouds
30 Jun	36.51	1.34	.478	2.20	111.06	127.48	9	Small no. of points and phase angle change
1 Jul	51.64	5.14	.956	4.51	88.70	129.88	28	
2 Jul	--	--	--	--	--	--	--	No observation; telescope under repair
3 Jul	--	--	--	--	--	--	--	No observation; telescope under repair
4 Jul	--	--	--	--	--	--	--	No observation; telescope under repair
5 Jul	50.04	4.12	.897	8.92	72.32	125.12	31	
6 Jul	47.92	4.36	.823	9.44	61.30	122.51	26	
7 Jul	--	--	--	--	--	--	--	No observation; clouds
8 Jul	--	--	--	--	--	--	--	No observation; low pass only
9 Jul	48.23	3.97	.834	8.51	48.64	98.45	22	
10 Jul	47.52	6.41	.809	10.20	44.08	118.87	35	
11 Jul	--	--	--	--	--	--	--	No observation; clouds
12 Jul	46.62	4.86	.779	4.67	78.59	121.73	23	
13 Jul[1']	52.42	8.90	.985	6.52	70.78	126.26	47	Continuous V band obs only; peaks in
13 Jul[1'']	49.01	5.26	.861	8.61	70.78	126.26	33	Continuous V band obs only; peaks removed
14 Jul	--	--	--	--	--	--	--	Continuous B band observation only
15 Jul	--	--	--	--	--	--	--	Continuous U band observation only
16 Jul	--	--	--	--	--	--	--	No observation; telescope under repair
17 Jul	41.80	20.82	.626	2.25	51.59	115.41	30	
18 Jul	46.65	6.95	.780	5.98	47.89	107.47	23	
19 Jul	45.88	9.00	.755	5.92	43.77	106.46	32	
20 Jul	47.57	5.33	.811	9.26	39.25	102.11	27	
21 Jul	44.42	12.07	.707	4.21	34.82	93.60	34	
22 Jul	51.66	8.49	.956	10.49	30.17	117.89	29	
23 Jul	--	--	--	--	--	--	--	No observation; clouds
24 Jul[1]	53.12	7.39	1.011	5.41	59.91	109.16	29	
24 Jul[2]	51.62	7.39	.955	11.45	20.96	104.71	37	
25 Jul	48.89	5.15	.857	10.15	59.44	118.23	42	
26 Jul	48.86	6.46	.856	9.82	22.37	91.94	40	
27 Jul	45.58	7.13	.745	7.48	10.52	86.47	31	
28 Jul	--	--	--	--	--	--	--	No observation; clouds
29 Jul	--	--	--	--	--	--	--	No observation; clouds
30 Jul	--	--	--	--	--	--	--	No observation; clouds

TABLE VIII. - Continued.

Date (1966)	Mean normalized magnitude	Sigma magnitude	Maximum magnitude	Minimum magnitude	Best-fit specular magnitude	True mean specular magnitude	Regression		Specularity, %	Maximum radius of curvature, ft	Minimum radius of curvature, ft	Average radius of curvature, ft
							A	B				
31 Jul[1']	2.06	0.36	2.77	1.24	2.00	1.93	0.704	-0.049	107.52	75.43	41.51	53.54
31 Jul[1'']	2.27	.23	2.77	1.83	2.24	2.13	.569	-.043	108.16	57.20	40.73	48.33
1 Aug	--	--	--	--	--	--	--	--	--	--	--	--
2 Aug	--	--	--	--	--	--	--	--	--	--	--	--
3 Aug	--	--	--	--	--	--	--	--	--	--	--	--
4 Aug	--	--	--	--	--	--	--	--	--	--	--	--
5 Aug[1']	2.05	.23	2.71	1.26	2.02	2.05	.621	-.000	100.08	74.93	38.37	52.34
5 Aug[1'']	2.17	.16	2.71	1.87	2.16	2.13	.569	-.016	102.95	56.72	39.23	49.61
5 Aug[2]	2.12	.21	2.64	1.63	2.10	2.07	.607	-.018	103.03	63.74	40.10	51.11
6 Aug	2.09	.14	2.51	1.88	2.08	2.08	.592	-.002	100.35	56.35	42.27	51.25
7 Aug[1]	2.14	.27	2.96	1.80	2.11	2.25	.522	.039	93.12	58.01	33.06	49.71
7 Aug[2]	2.08	.16	2.50	1.87	2.07	2.14	.562	.020	96.60	55.50	41.51	50.86
8 Aug[1]	2.16	.20	2.69	1.70	2.14	2.26	.509	.036	93.41	61.88	37.01	49.14
8 Aug[2]	2.10	.23	2.56	1.65	2.07	2.10	.591	.001	99.81	62.65	41.01	51.18
9 Aug[1]	2.14	.18	2.53	1.68	2.13	2.33	.477	.061	88.67	62.10	38.39	48.87
9 Aug[2]	2.14	.21	2.65	1.78	2.12	2.15	.564	.003	99.47	58.89	39.31	50.13
10 Aug	2.13	.30	2.66	1.45	2.08	2.26	.525	.044	92.32	69.09	37.13	49.81
11 Aug	2.07	.20	2.44	1.47	2.05	2.40	.452	.092	83.11	67.43	37.12	48.98
12 Aug	2.00	.18	2.30	1.64	1.99	1.75	.803	-.124	118.30	62.45	50.16	54.98
13 Aug	2.09	.31	2.73	1.52	2.05	2.27	.522	.086	85.80	67.35	36.70	51.44
14 Aug	--	--	--	--	--	--	--	--	--	--	--	--
15 Aug	2.08	.17	2.64	1.80	2.07	2.12	.575	.016	97.24	58.46	39.17	51.26
16 Aug[1]	2.16	.20	2.67	1.73	2.14	1.95	.670	-.085	114.61	59.89	42.16	51.02
16 Aug[2]	2.14	.25	2.60	1.46	2.11	1.96	.672	-.097	116.92	64.32	42.70	50.45
17 Aug[1]	2.09	.21	2.59	1.70	2.07	2.12	.581	.010	98.28	61.31	40.47	51.16
17 Aug[2]	2.09	.19	2.57	1.76	2.07	2.16	.554	.028	95.16	58.75	39.06	50.83
18 Aug[1]	2.23	.22	3.00	1.74	2.21	2.40	.450	.055	89.05	59.12	32.03	47.25
18 Aug[2]	2.05	.18	2.46	1.62	2.03	2.06	.609	.005	99.18	63.50	42.79	52.23
19 Aug	--	--	--	--	--	--	--	--	--	--	--	--
20 Aug[1]	2.12	.17	2.47	1.83	2.11	2.22	.525	.034	93.92	57.47	40.65	49.81
20 Aug[2]	2.12	.16	2.55	1.86	2.11	2.13	.568	.004	99.25	56.73	40.94	50.43
21 Aug[1]	2.10	.18	2.55	1.75	2.09	2.28	.498	.056	89.84	60.42	39.53	49.56
21 Aug[2]	2.10	.20	2.39	1.67	2.09	2.41	.447	.079	85.06	61.98	38.75	48.18
22 Aug	2.18	.21	2.58	1.72	2.16	2.59	.382	.116	76.73	61.96	33.58	46.58
24 Jun-12 Jul	2.18	.21	2.71	1.25	2.16	2.19	.541	.008	98.53	76.03	38.46	49.52
17 Jul-27 Jul	2.19	.34	2.98	.33	2.13	2.18	.566	-.003	100.45	114.47	34.12	49.51
5 Aug-14 Aug	2.11	.23	2.96	1.45	2.09	2.16	.562	.014	97.58	68.69	33.78	50.45
15 Aug-22 Aug	2.11	.20	2.67	1.46	2.09	2.13	.571	.008	98.54	68.64	38.69	50.70
17 Jul-22 Aug	2.14	.27	2.98	.33	2.10	2.16	.567	.006	98.98	115.02	33.64	50.21
5 Aug-22 Aug	2.11	.21	2.96	1.45	2.09	2.14	.566	.012	98.01	68.79	33.85	50.57

TABLE VIII. - Concluded.

Date (1966)	Mean radius of curvature, ft	Sigma radius of curvature, ft	Reflectance	Figure of merit	Phase angle range, deg		No. of points	Remarks
					From	To		
31 Jul[1']	52.97	7.95	1.005	10.48	35.57	94.00	78	Continuous V band obs only; peaks in
31 Jul[1"]	48.13	4.32	.830	14.19	35.57	94.00	52	Continuous V band obs only; peaks removed
1 Aug	--	--	--	--	--	--	--	No observation; telescope under repair
2 Aug	--	--	--	--	--	--	--	No observation; telescope under repair
3 Aug	--	--	--	--	--	--	--	No observation; telescope under repair
4 Aug	--	--	--	--	--	--	--	No observation; telescope under repair
5 Aug[1']	52.03	5.80	.970	11.45	48.72	110.49	60	Continuous V band obs only; peaks in
5 Aug[1"]	49.50	3.28	.878	15.66	48.72	110.49	40	Continuous V band obs only; peaks removed
5 Aug[2]	50.89	4.73	.928	15.31	20.63	94.38	49	
6 Aug	51.14	3.23	.937	19.02	15.87	91.45	31	
7 Aug[1]	49.28	6.14	.870	7.60	41.30	109.43	20	
7 Aug[2]	50.71	3.76	.922	13.79	14.03	94.26	20	
8 Aug[1]	48.91	4.69	.857	12.33	40.99	106.85	37	
8 Aug[2]	50.90	5.32	.929	11.71	17.65	88.26	39	
9 Aug[1]	48.67	4.39	.849	13.85	35.02	102.39	39	
9 Aug[2]	49.90	4.65	.893	10.75	20.26	82.26	33	
10 Aug	49.24	7.75	.869	6.54	31.56	98.94	25	
11 Aug	48.65	5.91	.848	14.93	27.72	88.97	103	Continuous V band observation only
12 Aug	54.87	3.59	1.079	5.64	56.71	87.50	15	
13 Aug	50.71	8.58	.921	5.75	53.00	114.37	34	
14 Aug	--	--	--	--	--	--	--	No observation; clouds
15 Aug	51.09	4.09	.936	18.69	26.67	108.62	41	
16 Aug[1]	50.88	3.66	.928	12.93	44.90	100.34	32	
16 Aug[2]	50.22	4.90	.904	9.03	50.44	111.97	29	
17 Aug[1]	50.91	5.07	.929	9.24	45.30	107.08	28	
17 Aug[2]	50.61	4.67	.918	16.06	24.93	108.28	39	
18 Aug[1]	46.93	5.41	.789	18.65	36.94	104.16	127	Continuous V band observation only
18 Aug[2]	52.04	4.41	.971	11.17	38.99	96.26	32	
19 Aug	--	--	--	--	--	--	--	No observation; clouds
20 Aug[1]	49.61	4.33	.882	8.70	41.72	92.78	24	
20 Aug[2]	50.29	3.74	.906	10.64	29.13	81.75	26	
21 Aug[1]	49.35	4.52	.873	8.17	37.68	88.85	24	
21 Aug[2]	47.86	5.57	.821	5.88	32.28	78.32	24	
22 Aug	46.16	6.21	.764	4.43	46.20	88.96	21	
24 Jun-12 Jul	49.27	5.11	.870	28.76	44.08	129.88	268	Combined run - pre-shadow
17 Jul-27 Jul	48.88	8.37	.856	26.19	10.52	118.23	354	Combined run - post-shadow
5 Aug-14 Aug	50.17	5.37	.902	37.39	14.03	114.37	342	Combined run - post-shadow
15 Aug-22 Aug	50.49	4.71	.914	37.45	24.93	111.97	320	Combined run - post-shadow
17 Jul-22 Aug	49.82	6.46	.890	53.67	10.52	118.23	1016	Combined run(s) - total post-shadow
5 Aug-22 Aug	50.32	5.04	.908	53.17	14.03	114.37	662	Combined run(s) - post-shadow

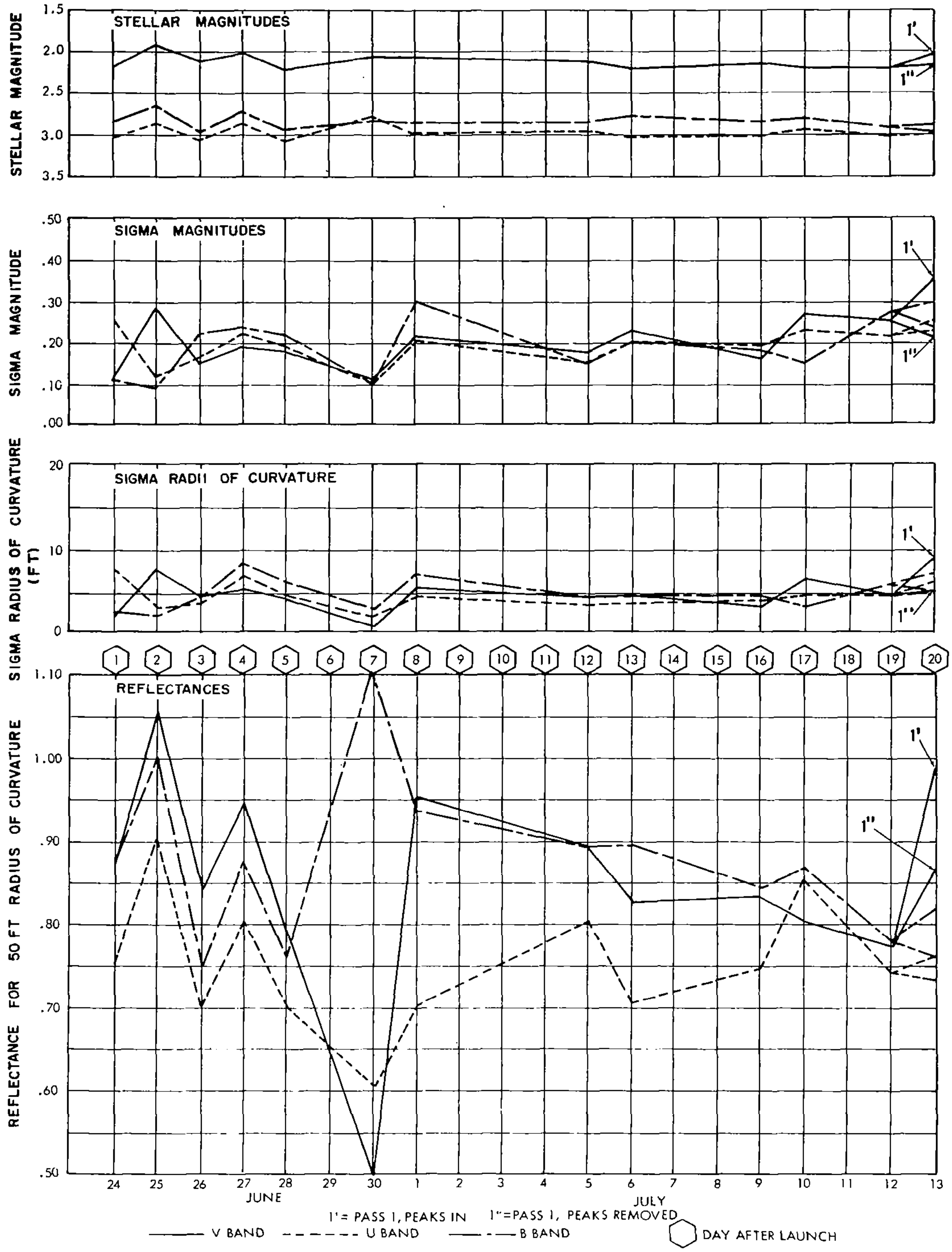

Note: Tables VI, VII, and VIII list days on which no observations were made.

Figure 11. - PAGEOS I UBV stellar magnitudes, sigma magnitudes and radii of curvature, and reflectances.

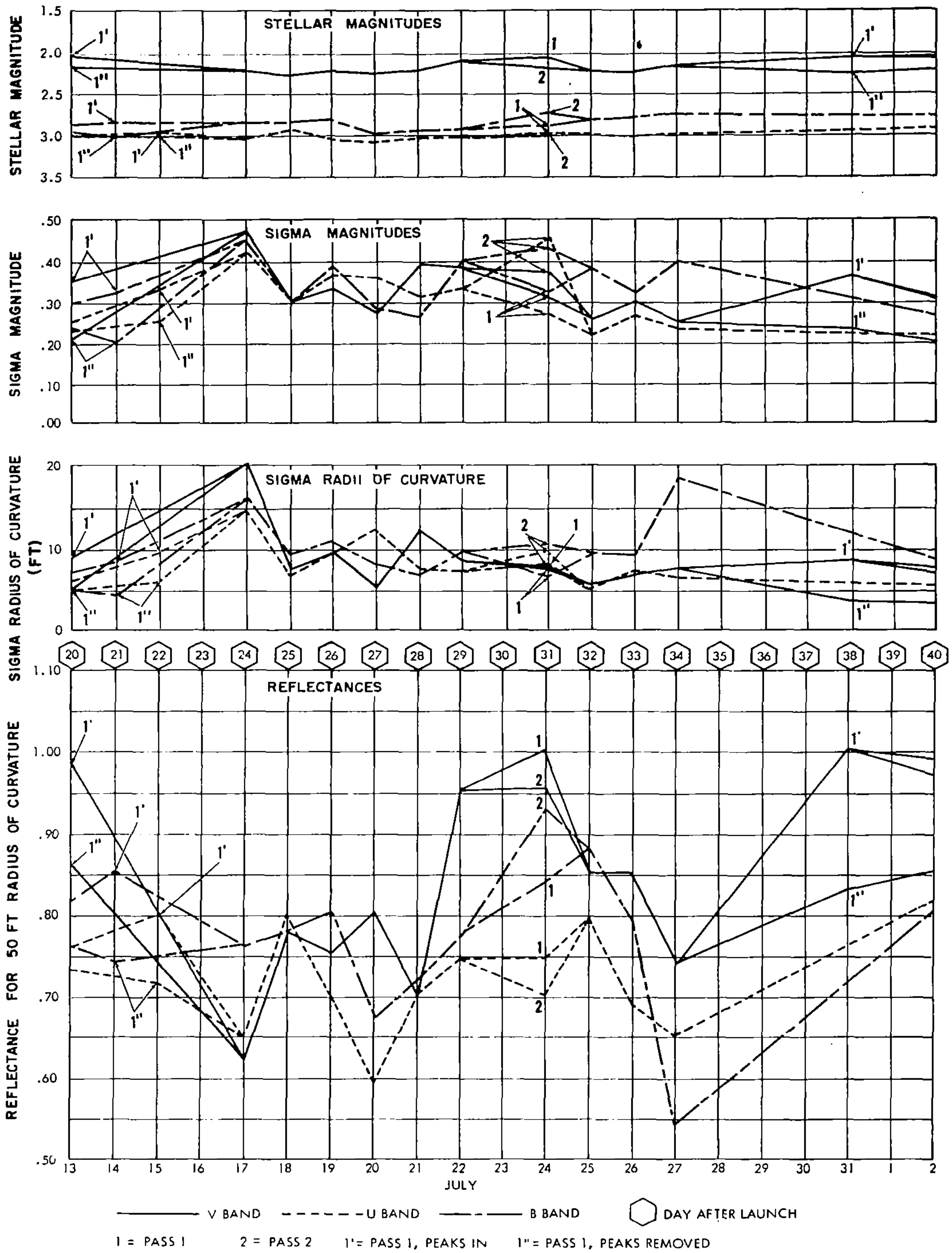

Figure 11. - Continued.

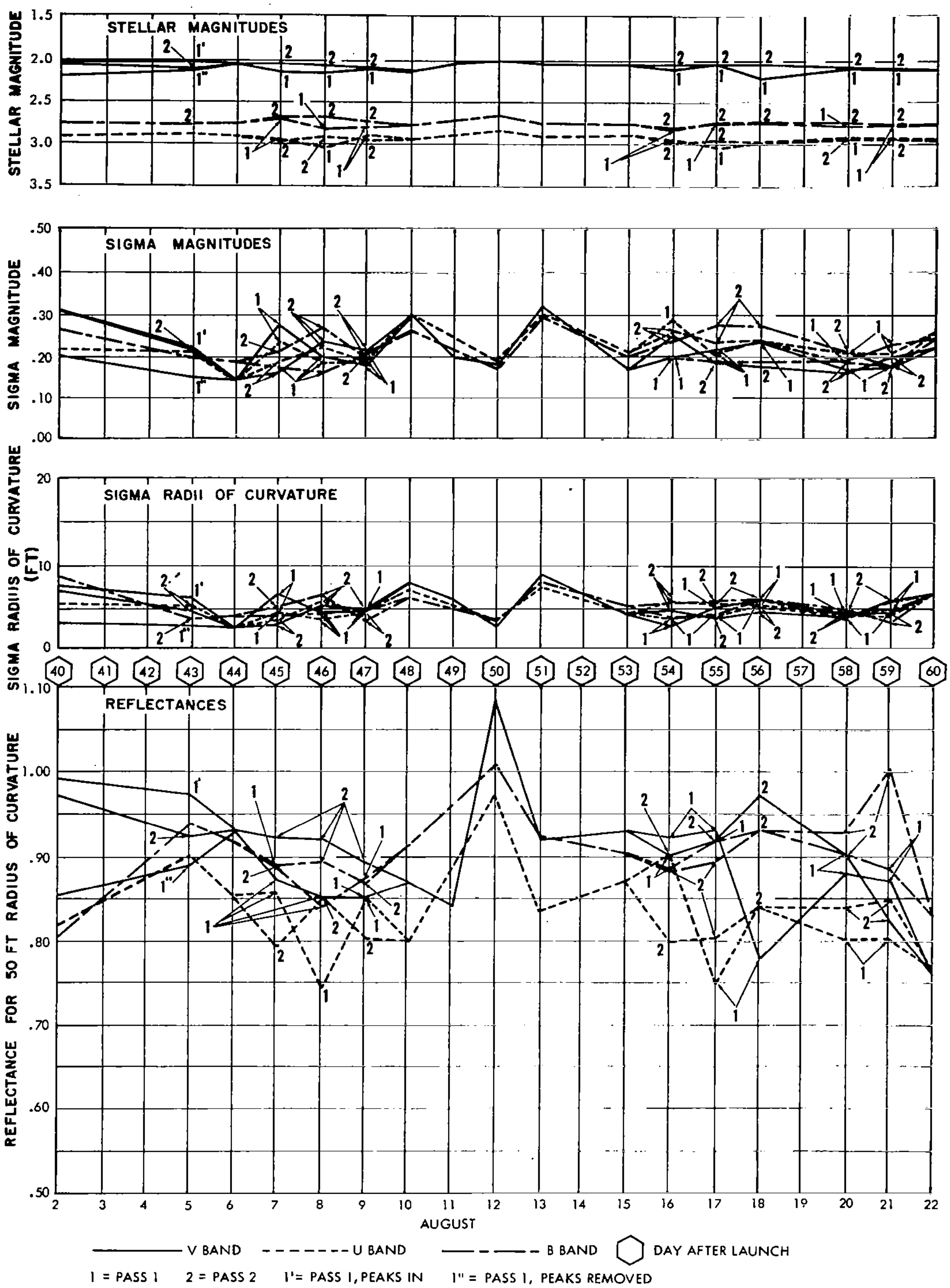

Figure 11. - Concluded.

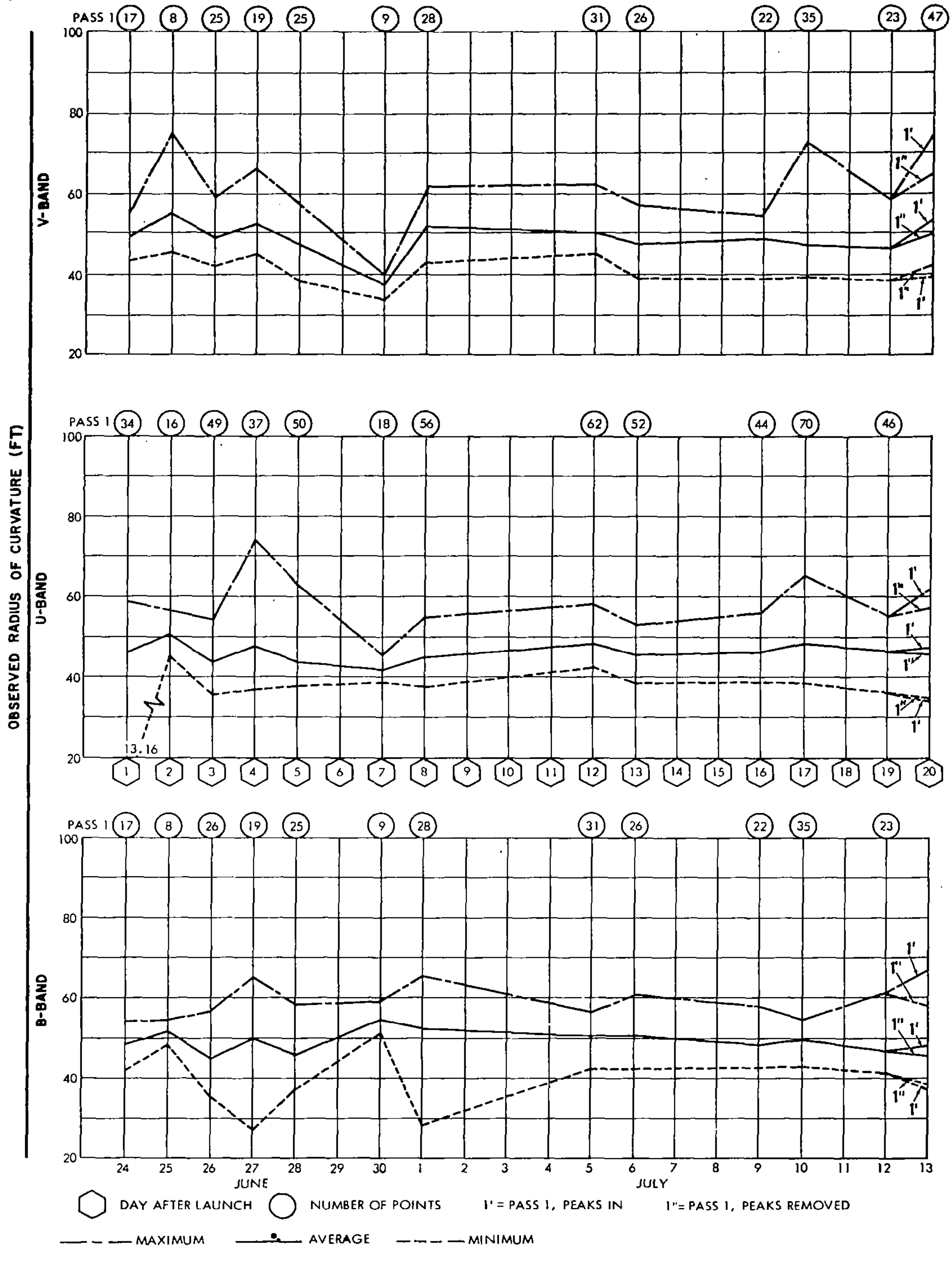

Figure 12. - PAGEOS I UBV radii of curvature.

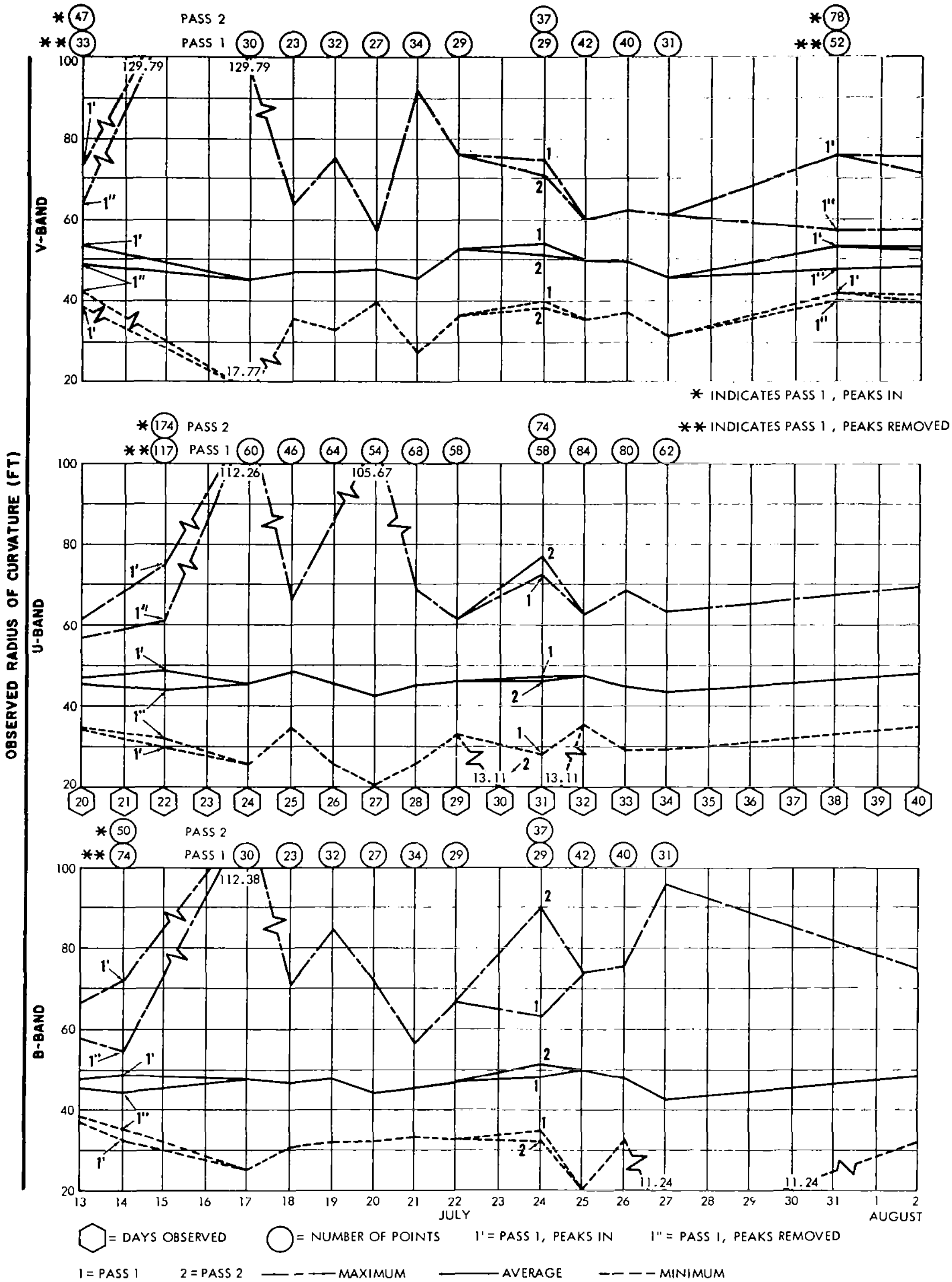

Figure 12. - Continued.

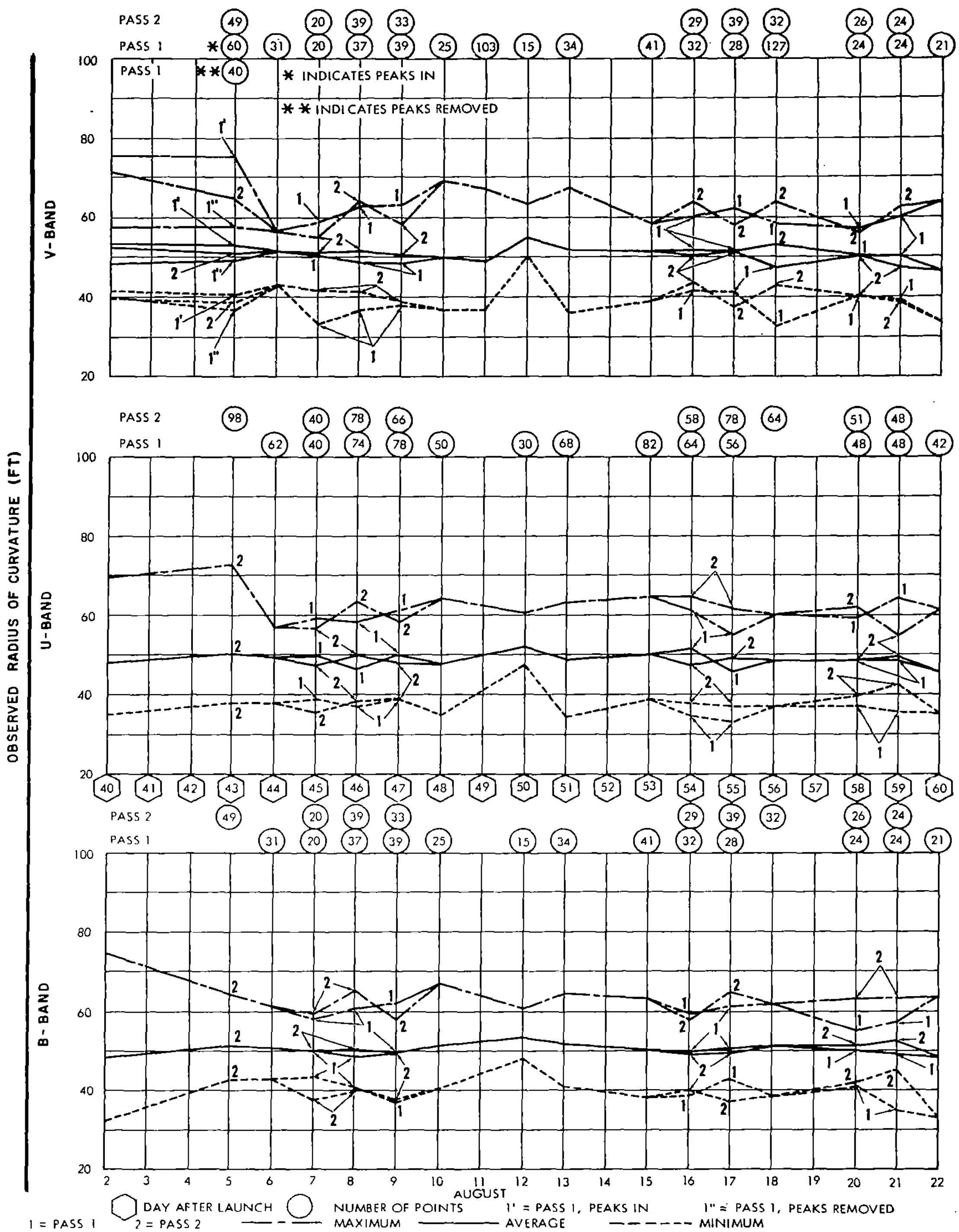

Figure 12. - Concluded.

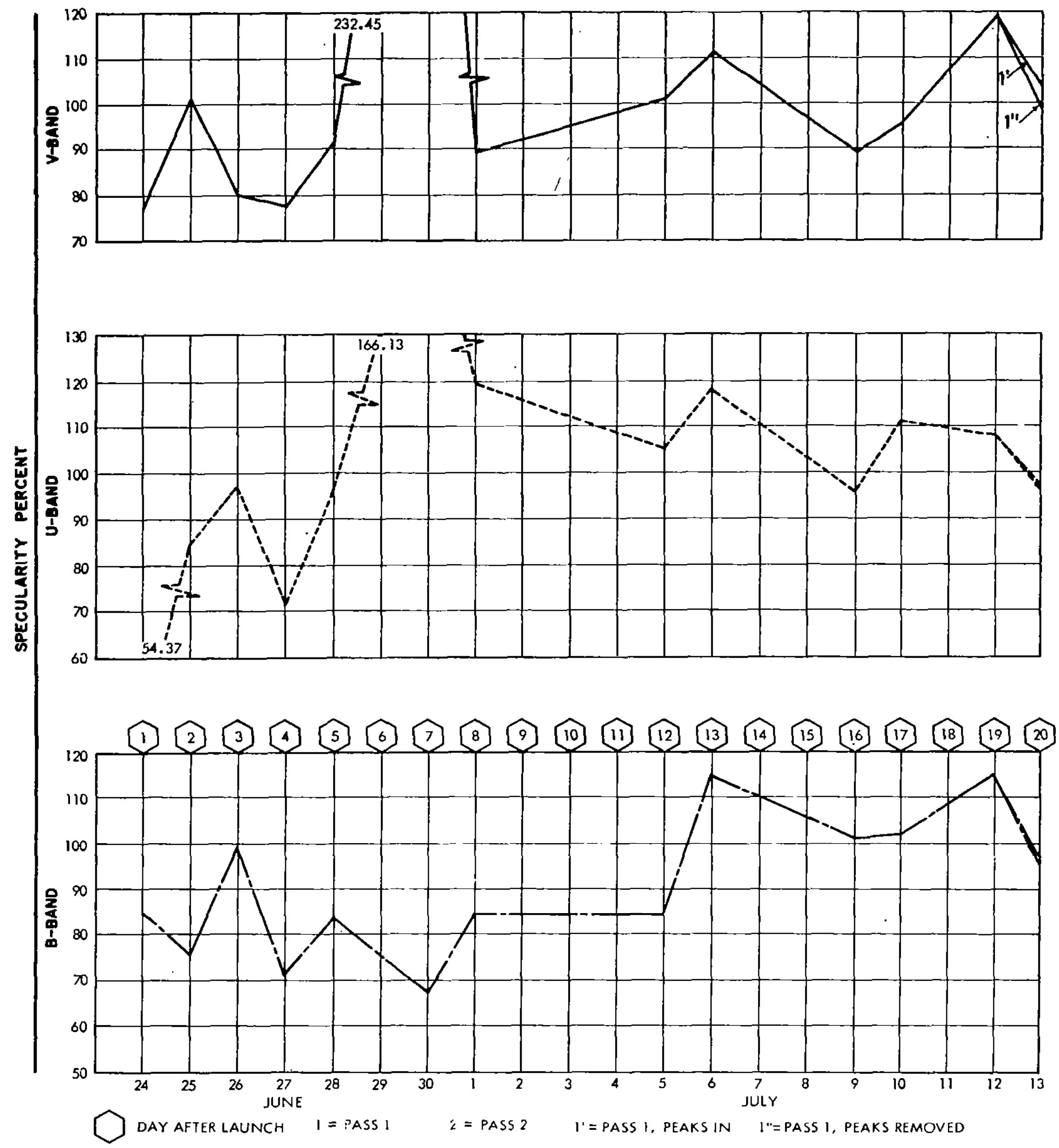

Note: Tables VI, VII, and VIII list days on which no observations were made.

Figure 13. - PAGEOS I UBV specularity.

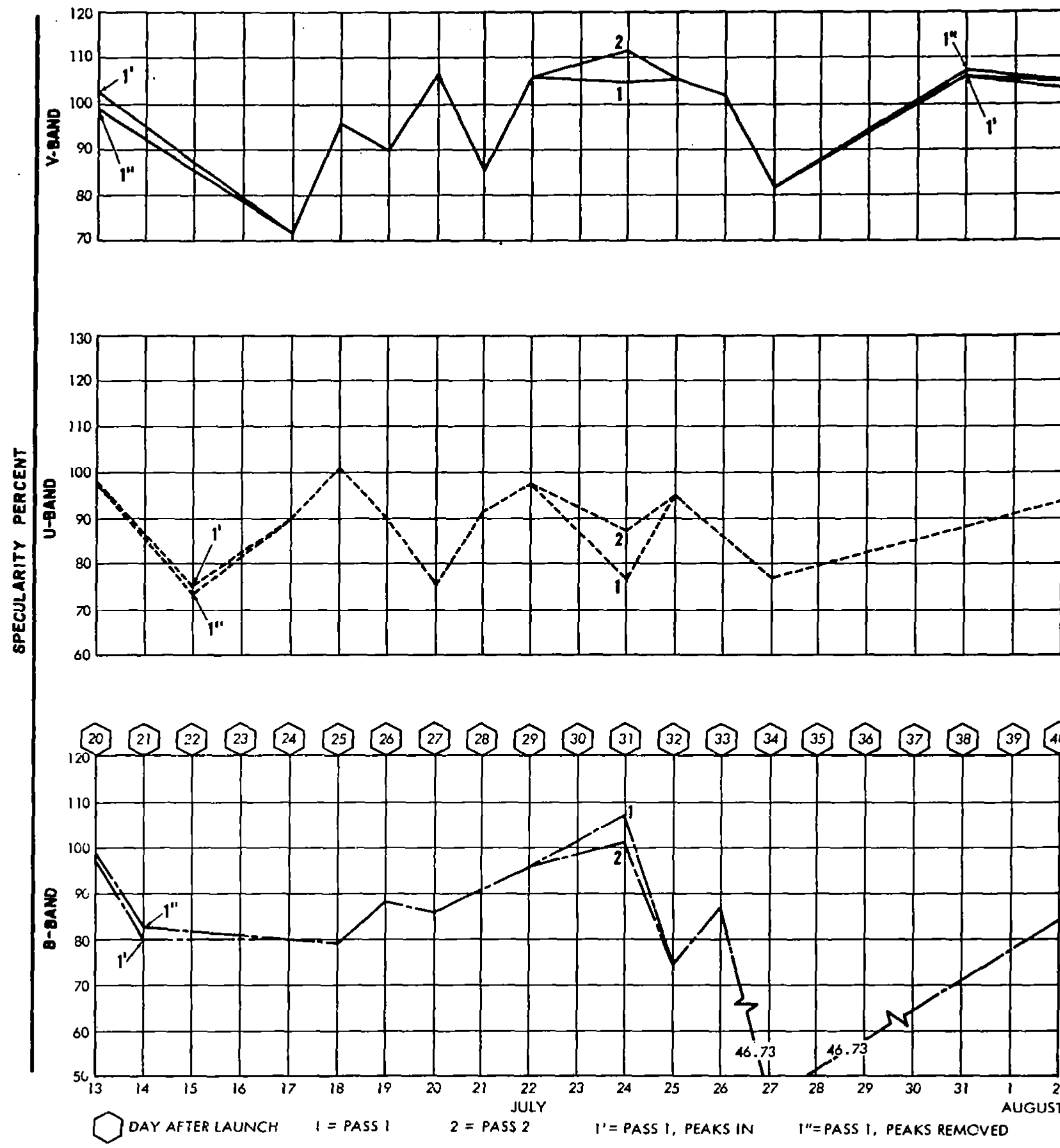

Figure 13. - Continued.

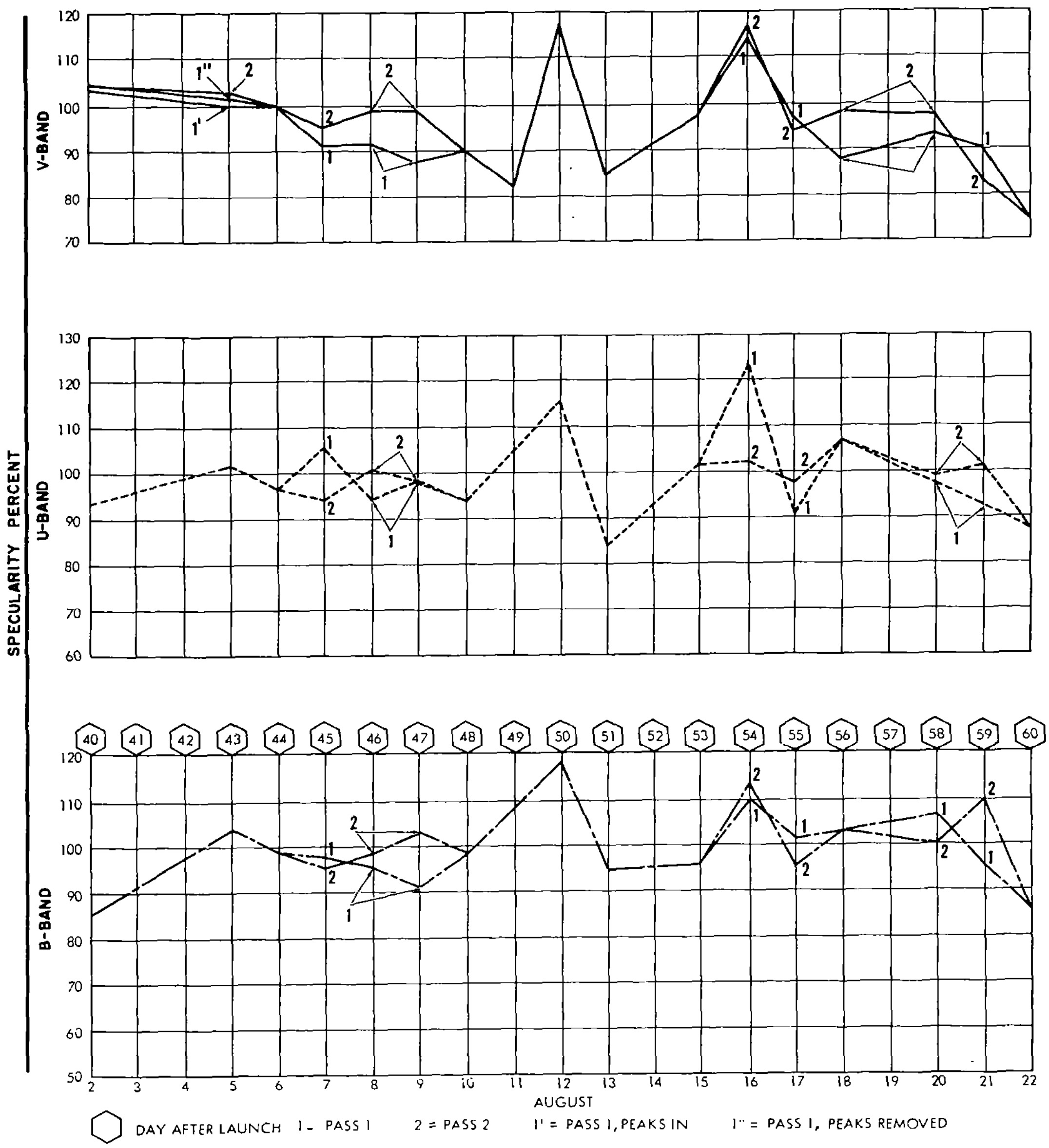

Figure 13. - Concluded.

These passes are summarized in table I. In comparing individual results, one may notice quite a wide variation between pre-shadow and post-shadow results, as well as in post-shadow results before and after 5 August. For instance, there are a large number of daily specularity values in excess of 100 percent for the U band in the pre-shadow time period, and thus a combined run value of greater than 100 percent is obtained. There is obviously some type of bias in this result, since the specularity cannot exceed 100 percent. However, if one recalls the method of calculating the specularity, i. e., plotting the illuminance ($4E/E_0$) as the ordinate against 8/3 Russell phase function as the abscissa and using the best-fit straight line to obtain the specularity (regression A_{sp} = intercept, regression B_d = slope), then one may see that values of greater than 100 percent may be obtained for individual passes. A combined run was performed for the pre-shadow period with the data for 25 June and 30 June removed, because it was thought that the extreme values obtained for these observations would create an unwarranted bias in the combined runs. Upon viewing this combined run for 10 passes instead of 12, it was discovered that the two additional runs changed the combined specularity values in all three colors by only one percent or less. If one examines the data for these two observations, it is possible to see the reasons for the extreme values:

(1) June 25 data - Too few points,combined with magnitude values which are far below the average, which indicates a bias in the number of peaks.

(2) June 30 data - Too few points, combined with a small change in phase angle for the observations. It has become quite apparent through examination of the various individual computer runs that these two parameters bias the data far more than any others. They are part of the "figure-of-merit" discussed elsewhere.

The continuous single-color observations were performed, as has been previously mentioned, to show periodicity and intensity variation in the PAGEOS I satellite. The method of reducing the raw single-color data was as follows:

(1) Major peaks were identified (1. 2 times trough level or greater, and with reasonable periodicity).

(2) Points of peaks were marked and straight lines drawn through rapidly rising or falling curve of data before and after peaks.

(3) Straight lines were drawn through trough data between the above peak lines.

(4) Data points were recorded at each end of trough and peaks added.

(5) Computer runs were made both with and without peaks.

The computer runs with and without peaks were performed for the 13, 14, 15, and 31 July runs and the V band run of 5 August. The V band observations of 11 and 18 August were reduced at 10-second intervals only because of lack of major peaks (the data is quite smooth), and thus the data is semi-random in nature. The single-color values of the various parameters, which are shown in tables VI, VII, and VIII, are also shown, in summary, in table IX. The first four V band observations (13 July, 31 July, 5 August, and 11 August) give magnitudes that vary by only 0. 02 magnitude for the "peaks-in" computer runs. The V band run of 18 August gives a value of stellar magnitude which appears like that of the "peaks removed." This is certainly indicative of a smoothing effect on the satellite. This latter phenomenon was calculated by removing the peak intensity points from the previous computer runs.

There is a marked improvement in both sigma magnitude and sigma radius of curvature, which is definitely a sign of smoothing. The sigma radius of curvature for the "peaks-in" run for 13 and 31 July 1966 are in excess of 8 feet, while those of 5, 11, and 18 August 1966 are in the 5 to 6 foot range.

Trends

The photometric data taken of PAGEOS I during the initial 60-day surveillance mission has defined the optical characteristics of the satellite, and will henceforth serve as a bench mark for any future PAGEOS I trend studies - whether for engineering or environmental science purposes. In this initial period, the only clearly apparent trend pertains to target scintillation and consists of a growth and later partial subsidence in the standard deviations of the normalized magnitudes and local effective radii of curvature (see figs. 12 and 13 and tables I and VI through VIII). An increase in the values of these surface anomaly parameters occurring in mid-July is time-correlated with the satellite's initial encounter with the earth's shadow, and therefore is very likely the consequence of thermal shocks upon the still gas-filled balloon at eclipse entry and exit. The subsequent decrease in these same parameters in early August, after PAGEOS I had been in orbit about six weeks, is probably due to the loss of most of the satellite's inflation gas - or particularly, the more volatile of the two sublimating powders. (A dynamic analysis of the orbital behavior of PAGEOS I, similar to the analysis of Echo I in reference 12, would provide for comparison an indicated time-history of the satellite's mass.)

Computer Printouts

A complete computer printout is shown in appendix D. Included are printouts for the scale factors (E-1970) of 13 August 1966, the primary extinction coefficients for 17 August 1966 (E-1980), and the second pass of the PAGEOS I satellite on 17 August 1966 (E-1213 and E-1214).

Satellite Scintillation

Low-frequency satellite scintillation is easily differentiated from atmospheric scintillation in the case of the PAGEOS I satellite. Satellite scintillation, as distinct from atmospheric scintillation, pertains to intensity variations contributed solely by the satellite.

The atmospheric scintillation is constant over the range of dc to 10 cps (as established by the recording galvanometer). In most cases, 3σ deviation of the peaks is contained in an envelope of ±10 percent of the stellar calibration readings. There is then a high degree of confidence that variation in signal greater than 20 percent of value at frequencies less than 0.5 cps is contributed by the satellite.

Substantial signal variation in the frequency band of 0.05 to 0.5 cps did occur in some of the data runs. All raw data reduction for U-B-V band measurements was made by taking the average signal level during the sample interval. This interval ranged from 1 to 10 seconds. Since this reduction technique masked out signal variation in the frequency range of 0.05 to 0.5 cps, some of the target scintillation was masked out in the U-B-V measurements.

Table IX presents the average and standard deviations of the reduced PAGEOS I normalized magnitudes and radii of curvature obtained during seven single-color observations (five passes observed in the continuous V mode and one pass each in continuous U and B), in which the raw data selected for reduction included extremes. The single-color data (except for the observations on 11 and 18 August 1966) was taken with one-third of the data being extremes.

TABLE IX. - SUMMARY OF DATA FOR CONTINUOUS-COLOR OBSERVATION

Color	Date	Magnitude	Sigma Magnitude	Specularity, %	Rad of curvature, ft	Sigma radius, ft	Reflectance[a]	Remarks
V	13 Jul 66	2.04	0.36	102.16	53.13	8.90	0.985	Peaks in
	13 Jul 66	2.23	0.21	88.52	49.27	5.26	0.861	Peaks removed
	31 Jul 66	2.06	0.36	107.52	53.54	7.95	1.005	Peaks in
	31 Jul 66	2.27	0.23	108.16	48.33	4.32	0.830	Peaks removed
	5 Aug 66	2.05	0.23	100.08	52.34	5.80	0.970	Peaks in
	5 Aug 66	2.17	0.16	102.95	49.61	3.28	0.878	Peaks removed
	11 Aug 66[b]	2.07	0.20	83.11	48.98	5.91	0.848	Peaks in
	18 Aug 66[c]	2.23	0.22	89.05	47.25	5.41	0.789	Peaks in
B	14 Jul 66	2.87	0.32	78.83	49.54	8.73	0.854	Peaks in
	14 Jul 66	3.03	0.20	82.57	45.73	4.44	0.742	Peaks removed
U	15 Jul 66	2.94	0.34	75.38	48.82	9.63	0.811	Peaks in
	15 Jul 66	3.09	0.25	74.82	45.36	5.96	0.714	Peaks removed

[a]When radius of curvature = 50 feet.
[b]Only one major peak in data; 85% tracking data taken every 10 seconds.
[c]Data very smooth; data taken every 10 seconds.

On 11 and 18 August 1966, so few peaks occurred that sufficient extreme data was not present to characterize a pass. For these two passes, data points were taken with a constant time period separating observation points. However, since this raw data selection philosophy for the three-color observations was consistently applied throughout the program, the values obtained for these parameters can be directly compared, as in figure 11 and table I. The consistency of the independent standard deviations of the radii of curvature in the three colors for each of the time periods shown in table I is an indication of their validity for comparison purposes.

Figures 14 and 15 present selected segments of the raw PAGEOS I data from two of the continuous V-band observations (13 July and 11 August) that are representative for these passes and illustrate the observed reduction in target scintillation in the latter part of the surveillance period.

The presence of some PAGEOS I intensity fluctuations prior to the initial encounter with the earth's shadow is not too surprising, since its twin and predecessor, Echo I, was visually observed to undergo several non-cyclic ±0.5 stellar magnitude variations during a pass on 18 August 1960, after only five days and 17 hours in orbit, and approximately six days before its first eclipse.

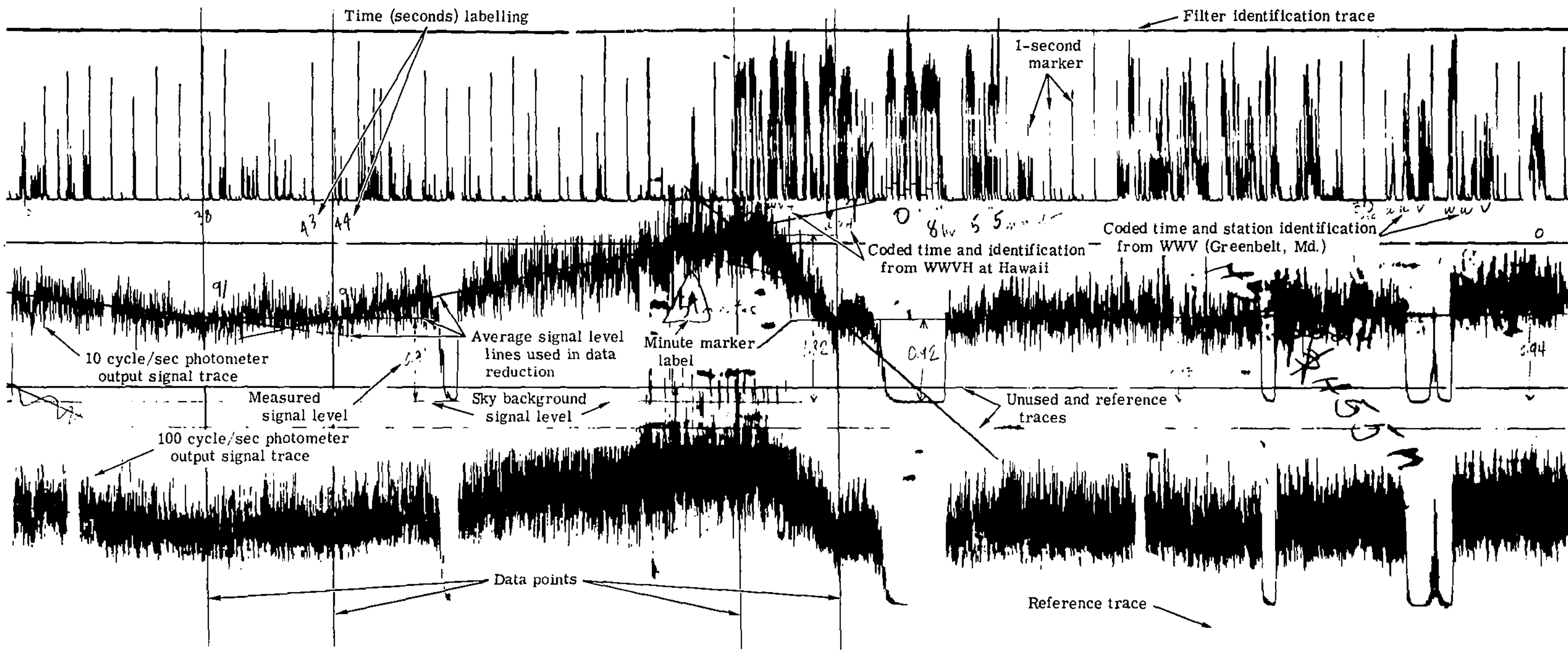

Figure 14. - Photometric data measurement in continuous V band - 13 July 1966. Satellite shows regular periodic peaks of intensity of reflected light.

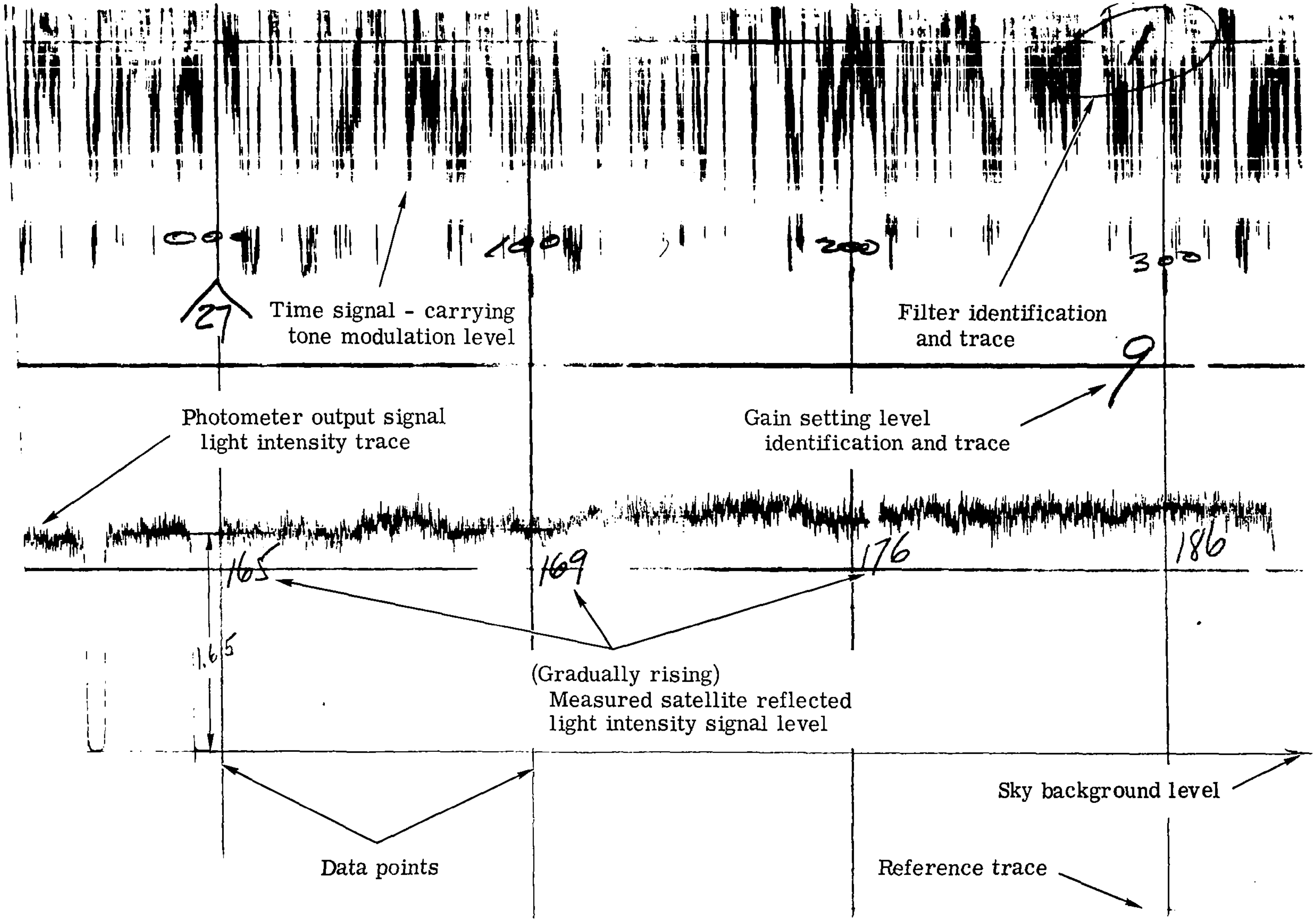

Figure 15. - Photometric data measurement in continuous V band - 11 August 1966.
Satellite exhibits relatively steady reflected light intensity.

Goodness-of-Fit Program

Computer program E-1981, "Test of Goodness of Fit," was developed to assist in the determination of the accuracy and repeatability of results. This program uses previously determined second-order extinction coefficients, scale factors, primary extinction coefficients, and zero-point terms to determine the accuracy and repeatability of the U-B-V photometric facility when observing standard stars. Five standard stars were chosen from the Arizona-Tonantzintla catalogue (ref. 3) to fulfill this test. The test required that measurements be performed at least twice: the first to determine the accuracy, and the second to determine the repeatability in each spectral region. Table X shows the individual values of tabular and calculated magnitudes and color indices for the stars. The calculated stellar accuracy and repeatability values in magnitudes for these stars are as follows:

Parameter	Spectral region		
	V	B-V	U-V
Absolute arithmetic average (accuracy)	0.036	0.014	0.028
Standard deviation ( )	.044	.017	.032
Absolute arithmetic average (repeatability)	.024	.022	.040

Since the tables are based on a very small sample size, in which the "accuracy" could change widely for different stars, a much larger sample of stars were chosen from several (six) primary extinction coefficient observations for the present contract and the identical type of tests were performed. The values of the tabular and measured values are depicted in table XI. The results shown, while not necessarily representative of the absolute accuracy of the facility, do show that the facility operates well within previously established requirements for magnitude accuracy and repeatability of standard stars. The calculated stellar magnitude accuracy and repeatability values for these stars are as follows:

Parameter	Spectral region		
	V	B-V	U-V
Accuracy (arithmetic average)	0.030	0.030	0.034
Accuracy (standard deviation)	.039	.039	.043
Repeatability (arithmetic average)	.049	.048	.051

TABLE X. - COMPARISON OF TABULAR AND MEASURED VALUES OF STANDARD STARS

Star	Test No.	Spectral region					
		V		B-V		U-B	
		Tabular value	Measured value	Tabular value	Measured value	Tabular value	Measured value
B.S. 7847	1	6.21	6.24	1.00	1.00	1.74	1.76
(44 Cygni)	2	6.21	6.23	1.00	0.99	1.74	1.71
B.S. 7770	1	5.16	5.15	0.65	0.66	1.13	1.16
(35 Cygni)	2	5.16	5.14	0.65	0.68	1.13	1.16
B.S. 7806	1	4.45	4.46	1.34	1.33	2.87	2.84
(39 Cygni)	2	4.45	4.48	1.34	1.31	2.87	2.86
B.S. 7796	1	2.23	2.16	0.67	0.67	1.21	1.24
(γ Cygni)	2	2.23	2.19	0.67	0.69	1.21	1.21
B.S. 7924	1	1.25	1.16	0.09	0.11	-0.12	-0.06
(α Cygni)	2	1.25	1.21	0.09	0.08	-0.12	-0.16

TABLE XI. - COMPARISON OF TABULAR AND MEASURED VALUES OF STANDARD STARS USED IN PAGEOS I CALIBRATION

Date	Star	Test No.	Spectral region					
			V		B-V		U-V	
			Tabular value	Measured value	Tabular value	Measured value	Tabular value	Measured value
20 Jul 66	B.S. 8115	1	3.19	3.15	1.00	0.96	1.76	1.75
		2	3.19	3.25	1.00	0.99	1.76	1.78
	B.S. 21	1	2.28	2.21	0.34	0.37	0.45	0.43
		2	2.28	2.30	0.34	0.33	0.45	0.42
	B.S. 163	1	4.39	4.33	0.87	0.87	1.34	1.32
		2	4.39	4.39	0.87	0.85	1.34	1.33
	B.S. 8684	1	3.48	3.45	0.94	0.96	1.61	1.65
		2	3.48	3.56	0.94	0.96	1.61	1.60
	B.S. 8665	1	4.19	4.15	0.51	0.50	0.47	0.46
		2	4.19	4.24	0.51	0.49	0.47	0.51
	B.S. 8905	1	4.44	4.35	0.61	0.65	0.79	0.82
		2	4.44	4.49	0.61	0.60	0.79	0.74
	B.S. 188	1	2.00	1.98	1.00	0.98	1.88	1.87
		2	2.00	2.10	1.00	1.04	1.88	1.91

TABLE XI. - Continued.

Date	Star	Test No.	Spectral Region					
			V		B-V		U-V	
			Tabular value	Measured value	Tabular value	Measured value	Tabular value	Measured value
10 Aug 66	B.S. 8115	1	3.19	3.24	1.00	0.98	1.76	1.69
		2	3.19	3.20	1.00	1.00	1.76	1.80
	B.S. 21	1	2.28	2.23	0.34	0.37	0.45	0.41
		2	2.28	2.25	0.34	0.31	0.45	0.45
	B.S. 8684	1	3.48	3.52	0.94	0.93	1.61	1.65
		2	3.48	3.48	0.94	0.92	1.61	1.66
	B.S. 8665	1	4.19	4.22	0.51	0.51	0.47	0.46
		2	4.19	4.25	0.51	0.47	0.47	0.45
	B.S. 163	1	4.39	4.36	0.87	0.90	1.34	1.30
		2	4.39	4.36	0.87	0.85	1.34	1.34
	B.S. 8905	1	4.44	4.42	0.61	0.68	0.79	0.77
		2	4.44	4.41	0.61	0.62	0.79	0.79
	B.S. 188	1	2.00	2.00	1.00	0.96	1.88	1.80
		2	2.00	2.02	1.00	1.04	1.55	2.02
13 Aug 66	B.S. 8115	1	3.19	3.20	1.00	0.99	1.76	1.74
		2	3.19	3.24	1.00	0.95	1.76	1.80
	B.S. 21	1	2.28	2.21	0.34	0.33	0.45	0.41
		2	2.28	2.31	0.34	0.30	0.45	0.46
	B.S. 163	1	4.39	4.33	0.87	0.87	1.34	1.32
		2	4.39	4.37	0.87	0.95	1.34	1.43
	B.S. 544	1	3.44	3.38	0.49	0.53	0.57	0.50
		2	3.44	3.44	0.49	0.44	0.57	0.53
	B.S. 8684	1	3.48	3.45	0.94	0.96	1.61	1.63
		2	3.48	3.52	0.94	0.92	1.61	1.59
	B.S. 8665	1	4.19	4.18	0.51	0.51	0.47	0.42
		2	4.19	4.26	0.51	0.53	0.47	0.50
17 Aug 66	B.S. 21	1	2.28	2.28	0.34	0.30	0.45	0.37
		2	2.28	2.24	0.34	0.40	0.45	0.42
	B.S. 8232	1	2.85	2.85	0.84	0.77	1.42	1.44
		2	2.85	2.84	0.84	0.84	1.42	1.46
	B.S. 7377	1	3.36	3.36	0.33	0.29	0.38	0.34
		2	3.36	3.37	0.33	0.34	0.38	0.38
	B.S. 7602	1	3.72	3.71	0.86	0.90	1.34	1.35
		2	3.72	3.72	0.86	0.88	1.34	1.35

TABLE XI. - Concluded.

Date	Star	Test No.	Spectral region					
			V		B-V		U-V	
			Tabular value	Measured value	Tabular value	Measured value	Tabular value	Measured value
17 Aug 66 (Cont)	B. S. 8684	1	3.48	3.50	0.94	0.90	1.61	1.57
		2	3.48	3.53	0.94	1.00	1.61	1.66
	B. S. 8115	1	3.19	3.15	1.00	0.96	1.76	1.82
	B. S. 8665	1	4.19	4.21	4.51	0.54	0.47	0.48
21 Aug 66	B. S. 21	1	2.28	2.20	0.34	0.37	0.45	0.42
		2	2.28	2.31	0.34	0.30	0.45	0.49
	B. S. 8684	1	3.48	3.47	0.94	0.94	1.61	1.60
		2	3.48	3.53	0.94	0.98	1.61	1.60
	B. S. 7602	1	3.72	3.69	0.86	0.89	1.34	1.35
		2	3.72	3.71	0.86	0.84	1.34	1.40
	B. S. 7377	1	3.36	3.30	0.33	0.29	0.38	0.39
		2	3.36	3.37	0.33	0.36	0.38	0.35
	B. S. 8232	1	2.85	2.86	0.84	0.79	1.42	1.43
		2	2.85	2.88	0.84	0.83	1.02	1.44
	B. S. 163	1	4.39	4.33	0.87	0.82	1.34	1.30
	B. S. 8115	1	3.19	3.22	1.00	0.93	1.76	1.80
	B. S. 8665	1	4.19	4.22	0.51	0.65	0.47	0.41
	B. S. 188	1	2.00	2.06	1.00	1.02	1.88	1.85
22 Aug 66	B. S. 21	1	2.28	2.26	0.34	0.40	0.45	0.47
		2	2.28	2.28	0.34	0.44	0.45	0.51
	B. S. 8684	1	3.48	3.51	0.94	0.86	1.61	1.50
		2	3.48	3.49	0.94	0.97	1.61	1.68
	B. S. 8665	1	4.19	4.19	0.51	0.49	0.47	0.51
		2	4.19	4.18	0.51	0.54	0.47	0.49
	B. S. 8905	1	4.44	4.43	0.61	0.56	0.79	0.75
		2	4.44	4.42	0.61	0.57	0.79	0.79
	B. S. 544	1	3.44	3.44	0.49	0.50	0.57	0.61
		2	3.44	3.45	0.49	0.46	0.57	0.53
	B. S. 163	1	4.39	4.33	0.87	0.89	1.34	1.37
		2	4.39	4.35	0.87	0.87	1.34	1.36
	B. S. 8115	1	3.19	3.20	1.00	1.00	1.76	1.70
	B. S. 27	1	5.04	5.03	0.40	0.35	0.66	0.59

CONCLUSIONS

General

The telescope-filter-photomultiplier system has given results which are in most cases in agreement with theory and previous observatory or laboratory measurements. The individual determinations of stellar magnitudes, as shown in the "Test of Goodness-of-Fit" computer program, have proved that the extinction coefficients, zero-point terms, and scale factors used in the various daily satellite observation programs are of high accuracy, even though the length of time between precalibration and postcalibration is in excess of good astronomical practice. There was no alternative to this practice in view of the long observation period of each pass of the PAGEOS I satellite.

The data for various parameters - mean normalized magnitude, specularity, radius of curvature, reflectance, etc - are at times controversial in the individual observations, but are seemingly of excellent quality when many data points are averaged in combined computer runs. The parameter that caused the most difficulty in the data reduction and analysis was the specularity, which exceeded the theoretical limit of 100 percent for several passes. This occurrence may be attributed to one or more of the following reasons:

(1) Too few data points

(2) Low variation of phase angle

(3) Biasing of the data by too many or too few peaks for a pass

(4) Satellite scintillation

When one views the combined post-shadow computer run, a different perspective is obtained:

(1) The B-V color index closely resembles that of the sun.

(2) The specularity is approximately 97 percent, in excellent agreement with expectations.

(3) The radius of curvature is approximately 50 feet in accordance with the design specifications.

Figures 11, 12, and 13 and the raw analog data on the oscillograph charts definitely show a smoothing effect on the data somewhere in the vicinity of 5 August, an effect which is most pronounced in the standard deviations of both mean normalized magnitude and radius of curvature. As far as the continuous V-band data is concerned, it was observed that the raw data was quite smooth for the 5, 11, and 18 August runs; whereas the observations of 13 and 31 July had definite periodicities (although random in time) between successive intensity maxima. The continuous B and U band data on 14 and 15 July respectively also showed definite periodicities.

Evaluation of Photometric Technique

When sophisticated photometric instrumentation is brought to bear on an orbiting spherical target, rather steady indications of the level of intensity of the light it reflects might be expected. Experience indicates, however, that this is never the case. The output signal representing the instantaneous light intensity is far more complex - constantly varying in various ways in response to the multitude of detail characteristics that seem to be always present to modify and affect the message received photometrically. With proper analysis and study the message received can be used to interpret the characteristics of the target satellite. Echo I, PAGEOS I, and Echo II satellites have all displayed this complex response. PAGEOS I, particularly, because it has had the most extensive and intensive examination, reveals in its photometric signal a variety and a wealth of information. The information content includes color characteristics and scintillation data. The color characteristics give some indication of the surface condition. Scintillation information is not completely separable with present techniques, but the content includes the following:

(1) Atmospheric scintillation, indicating the angular diameter of the area on the target object that is reflecting the light.

(2) Rapid target scintillation, indicating fine structure characteristics of the surface.

(3) Various slower target scintillations, indicating gross shape and surface characteristics, and indicating rotational or other movement of the entire satellite.

Furthermore, the above characteristics have both a static and a dynamic significance. Not only can the successive measured values be combined statistically to reinforce the precision and confidence level of the measured characteristics, but they can also be utilized in the context of their measured time sequence to study changes that are taking place and trends that are developing, thus giving a history as well as a static picture of the target satellite characteristics. This is particularly evident in the PAGEOS I photometric surveillance, where constant change was evident as a consequence of the immediate postlaunch era, the shadow entry period, and the post-shadow entry region, and the information was available with respect to phase angle, in three colors, and time-correlated. This information is of sufficient quantity that additional time and study would be required to completely consider all of the data collected and to obtain proper interpretation and definition regarding all the matters of interest.

Value of Continuous V Band

The intial concept for standard operations with multicolor photometry was to make use of U-B-V sequence measurements exclusively. However, early in the operations of the program it became evident that continuous V-band (or other single color) data was capable of conveying significant information that could be entirely missed in the exclusive U-B-V mode. As a result of this experience, it was ultimately decided that the schedule would include regular incorporation of single color band continuous measurements.

It appears from this experience that continuous single color band data is necessary to convey the full story regarding macrotexture, as well as dynamic motion, characteristics of satellites, and this data should be taken at regularly interspersed intervals to keep track of any changes occurring in these characteristics. In the case of PAGEOS I, this appeared in the very first runs in short records taken in continuous V band before going into the U-B-V mode. The changes that became apparent drew attention to the importance of making some measurements regularly in a continuous single color. This is well illustrated by the data records shown in figures 14 and 15. Figure 14 shows the satellite at a time when variations due to macrotexture effects, etc, are quite low (with a relatively steady rise due to phase and slant range predominating). Figure 15 shows the strong characteristic periodic signal rise encountered later, after shadow entry.

In general, it can be concluded that both multicolor and continuous single color photometric measurements are important. The former is necessary to record the color characteristics and microtexture of the satellite being observed, while the latter is needed for the macrotexture and dynamic characteristics. Therefore, both modes should normally be used, interspersed on a regular schedule devised to be appropriate for the particular satellite being observed and the measurement objectives.

Evaluation of Mobile Photometric Observatory

The observatory has successfully demonstrated its mobility without degradation of photometric capability. This demonstration encompassed not only self-transport of the observatory from Akron, Ohio to Palomar Mountain, California, but also included testing the unit over secondary roads at speeds up to 40 mph.

The observatory has demonstrated its ability to make photometric measurements of stars and of nominally spherical satellites. These measurements included satellites from first to seventh visual magnitudes (a light intensity ratio of more than 100) and stars from 0 to tenth visual magnitude (a light intensity ratio of 10 000).

The use of a two-minute field permits consistent tracking of satellites when the rate and position controls are used. For passes as long as 40 minutes, there was no indication that physical fatigue of the operator was contributing to errors in tracking continuity. The principal contributor to tracking outage time is operator difficulties when following the tracking telescope eyepiece. With the two-minute field stop, sky background contribution to the signal was negligible except during twilight conditions. The favorable sky at Palomar Mountain thus made data reduction an easier task, as measurements in the three colors could be made from the same base line.

APPENDIX A

ALBEDO CORRECTIONS OF GROUND-BASED PHOTOMETRIC OBSERVATIONS OF SATELLITES

Introduction

Accurate reduction of photometric measurement data from satellites requires determination of the stellar magnitude increment due to the earth's albedo in various observation bands. The satellite is assumed to be spherical and a specular reflector of solar energy.

Technical Discussion

The illuminance an observer on the earth sees from a satellite is due to two sources: the reflection of direct sun energy and the reflection of earth-reflected sun energy. The illuminance an observer sees is proportional to the illuminance that is incident on the satellite, because the spherical and specular satellite surface reflects incident energy equally in all directions. Consequently, the apparent stellar magnitude of the satellite can be written:

$$m = -2.5 \log K_n (E_e + E_s) + m_K \tag{A1}$$

where E_e and E_s are the incident illuminances due to the earth's albedo and the sun respectively, and K_n is a normalization factor relating the incident illuminance to that which an observer sees. The stellar magnitude of the satellite due to direct sun illumination alone can thus be written:

$$m_s = -2.5 \log K_n E_s + m_K \tag{A2}$$

The difference between these two expressions for stellar magnitude is the earth contribution and can be written as:

$$\begin{aligned} \Delta m &= m - m_s \\ &= -2.5 \log \left[1 + (E_e/E_s)\right] \end{aligned} \tag{A3}$$

Thus only the quantity E_e/E_s needs to be determined. The incident energy due to earth reflection is given by C_s a F. Values of F for various altitudes and α angles have been developed. The incident energy on a sphere due to direct solar illumination is $0.25C_s$. Consequently, the value of E_e/E_s is the ratio of these terms:

$$E_e/E_s = \frac{C_s \, a \, F}{0.25 C_s} = 4aF \tag{A4}$$

The stellar magnitude increments due to earthshine have been calculated for various α's and altitudes using the developed values of F and an assumed average earth reflectivity of 0.36. The results are shown in figure A1. The low angle cut-off points represent the points where the satellites appear on the horizon to an observer at local twilight.

In addition to the calculation of data, it was desirable to fit an equation to this data in order to integrate a correction term in the computerized data reduction process. To this end, the following equation was derived.

$$\Delta m_a = \left(\frac{403}{h} + 0.140 - 0.0272 \times 10^{-3} h\right) + \left(-\frac{411}{h} - 0.105 + 0.025 \times 10^{-3} h\right)\alpha + \left(\frac{107}{h} + 0.015 - 0.0049 \times 10^{-3} h\right)\alpha^2 \qquad \text{(A5)}$$

This equation is accurate to within 0.015 of a stellar magnitude at all altitudes and α's shown in figure A1. Figure A2 compares calculated and fitted data at the altitude extremes.

Equation (A5) presumes an earth albedo of 0.36, which is an average value over the earth and over the entire spectrum of solar energy. Local values vary drastically, (i.e., between 7 and 55 percent) depending on terrain and amount of cloud cover visible to the

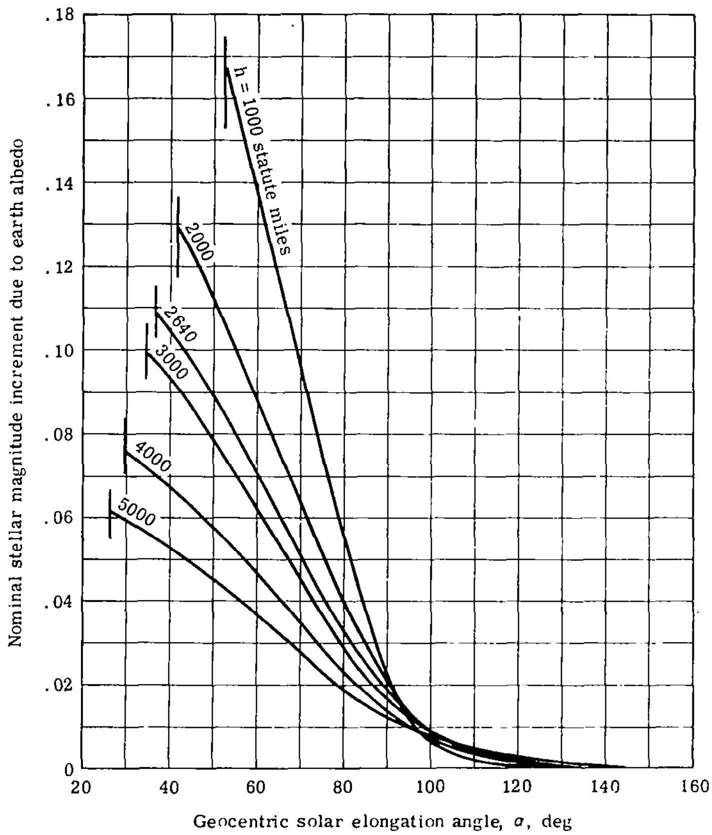

Figure A1. - Earth-reflected stellar magnitude increments.

satellite, as reported in reference 13 and confirmed by reference 14. This effect has been neglected, since it would be a difficult correction to make (weather conditions at time of observation would be required) and a large cap of the earth is viewed by PAGEOS I, damping out local variations.

Spectral variations are to be considered by use of a correction factor c:

$$a_b = 0.36c \text{ and } m_b \cong c \, \Delta \, m_a \tag{A6}$$

since E_e/E_s is considerably less than unity for the range considered. Figure A3 shows the system responses in the three bands considered, i.e., U, B, and V, located primarily in the near UV, blue, and the center of the visible portions of the spectrum, respectively (refs. 15 and 16 were used for information on the solar spectrum). Since the spectral albedo of the earth is not defined, estimates must be made from available data.

A number of references, including 13, 14, 17, 18, and 19, indicate the visual albedo (0.38 to 0.76 micron) to be 0.41 versus the 0.36 for the complete solar spectrum. Reference 20 presents the spectral absorptance of the atmosphere (no clouds), which shows that the ozone layer in the upper atmosphere absorbs essentially 100 percent of radiation below 0.33 micron and is transparent to longer wave lengths. The lower atmosphere, which has a number of absorption bands due to CO_2 and H_2O in the atmosphere, forms a fairly continuous

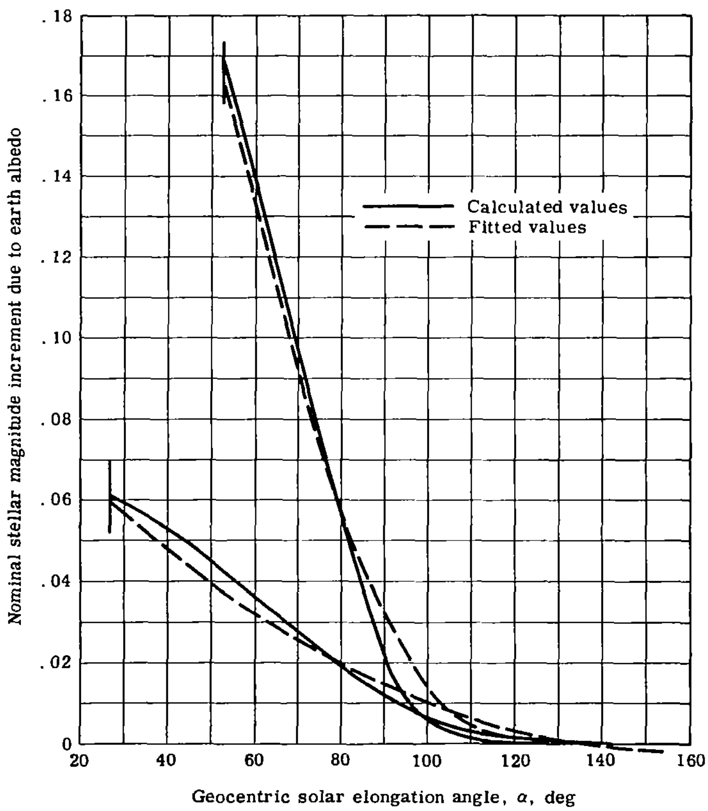

Figure A2. - Curve fit.

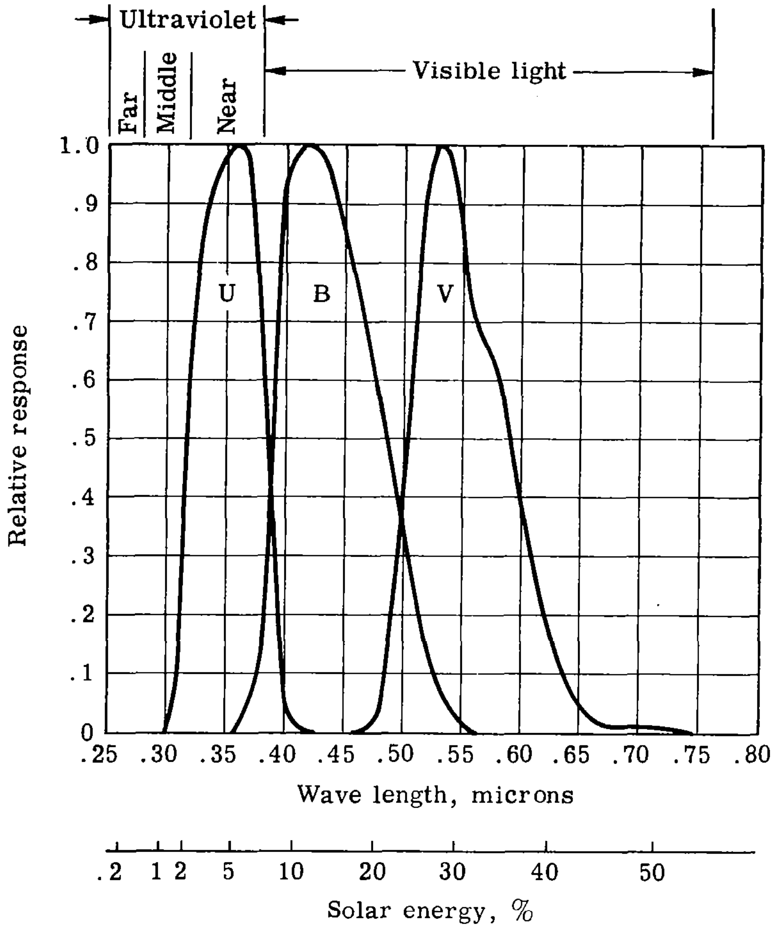

Figure A3. - UBV response functions.

curve for the three bands, with the longer wave lengths having a much larger absorptance. Reference 21 gives the following breakdown of the albedo and absorptance of the solar energy striking the earth: 24 percent reflected from clouds (51 percent cloudiness), 7 percent scattered back to space by air molecules and dust, and 4 percent reflected from ground to space (albedo 35 percent); and 65 percent reradiation occurring at longer wave lengths, made up of 47 percent absorbed by ground (including oceans), 13 percent by water vapor and dust, 3 percent by the ozone layer, and 2 percent by clouds. Rayleigh scattering accounts for the blue appearance of the sky.

Reference 22 reports on the spectral albedo of clouds, showing a constant albedo to wave lengths of 0.8 micron and decreasing values thereafter, with the visible and infrared solar values being 8 percent greater and less than the average value, respectively.

Photographs taken by astronauts, as well as Rayleigh scattering theory, show that the earth has a definite bluish color, except for ground features with high albedos such as desert areas (red), polar areas (white), and clouds (white).

Based upon the above information, Table AI was constructed to estimate albedo values for the three bands and the correction factor c for equation (A6). Recommended values of c are 1.2, 1.2, and 1.1 for the U, B, and V bands, respectively.

APPENDIX A

TABLE AI. - SPECTRAL ALBEDOS AND CORRECTION FACTORS

Band	Albedo				
	Clouds	Ground	Atm scattering	Total	c
Solar	0.25	0.04	0.07	0.36	1.0
Visible	.28	.04	.09	.41	1.1
U < 0.33 μ	0	0	0	0	0
U > 0.33 μ	.28	.03	.14	.45	1.2
U[a]	.24	.03	.12	.39[b]	1.1[b]
B	.28	.03	.12	.43	1.2
V	.28	.04	.09	.41	1.1

[a] 14 percent of energy below 0.33μ and 86 percent above 0.33μ.

[b] Valid for incident energy on satellite. Due to atmospheric attenuation of observations, value of total albedo of 0.43 (c = 1.2) should be used for photometric work.

Albedo varies not only with weather conditions but also with terrain, as discussed in references 13, 14, 17, 18, and 19.

Strong gradients in the value of albedo occur at coast lines, with oceans being poor reflectors except at low grazing angles and land areas being better reflectors but with large variations in values. Based upon the above references, a second correction factor (c') based on terrain may be included if desired. Table AII presents such data for observations from southern California.

A possible significant source of error in albedo corrections is the albedo variation with elongation angle α and altitude, as shown in figure A1 and approximated by equation (A5). The elongation angle dependence presumes a diffusely reflecting earth. Reflections from the earth are much more complex, involving such items as Rayleigh scattering, backscattering from ground surfaces, and some specular reflections from icecaps and oceans. An albedo model including these effects has not been developed, but the probable effect would be a flattening of the figure A1 curves so that albedo variation with elongation angle is not quite so pronounced.

TABLE AII. - ALBEDOS AND CORRECTION FACTORS FOR TERRAIN BENEATH SATELLITE

Terrain	Albedo	c'
Earth	0.36	1.0
Oceans	0.34	0.95
Arctic	0.44	1.20
North America[a]	0.38	1.05

[a] Excluding arctic regions, but including some desert regions.

APPENDIX A

Conclusions

An equation was developed that can be used to calculate the effect of earth albedo on the stellar magnitude increase of a specular and spherical satellite. The equation is valid over the range of 1000 to 5000 statute miles altitude and values of α from the point where the satellite appears on the horizon to an observer at twilight to where the satellite enters the umbra. Correction factors were developed to account for spectral albedo variations in the three bands as shown in table AI. Large variations (7 to 55 percent) in albedo occur for a given measurement due to weather conditions and type of terrain viewed by the satellite, with 36 percent being an average value for the entire solar spectrum. Possible sources of error in albedo corrections include the variation of the stellar magnitude increment with elongation angle α from predicted values due to non-diffuse reflections from the earth, and neglecting of diffuse reflections from the satellite in the albedo correction.

APPENDIX B

SAMPLE SIZE REQUIREMENTS FOR PAGEOS I SURVEILLANCE

Summary

The desired accuracies for the photometric determinations are as follows:

(1) Satellite stellar magnitude, m, to ±0.2 magnitudes.

(2) Solar reflectance, γ, to ±2 percent.

(3) Specularity, $A_{sp}/(A_{sp} + B_d)$, to ±2 percent.

(4) Satellite diameter to ±1.4 percent.

The following analysis derives the sample sizes necessary so that the averages for these determinations will be within the desired precision, when the individual measurements are not in each of the three bands.

The required number of observations per pass (that is, the statistical sample sizes, N, necessary to meet these desired accuracies) without calibration bias and with a confidence probability of 96 percent, are as follows: V-band, N_v - 15; U-band, N_u - 41; and B-band, N_b - 21. These are pessimistic overestimates of sample size based on assumptions made by the derivations.

The nightly calibrations introduce a bias into all the measurements of stellar magnitude in each of the three bands. However, from night to night this bias is not constant, but is a randomly varying quantity. Although these random biases may not average out to zero for a small sample of nights, tabulations of students' t distribution reveal that for a sample size of 30 nights the average of the sample is practically invariant and equal to the population mean. Since more than fifty nightly observations were made, it was assured that their pooled results completely canceled this source of error.

The minimum PAGEOS I visibility time required to obtain a successful observation (a significant number of data points in U, B, and V) is 5 minutes while the satellite remains above 20 degrees elevation. This permits the required number of data points.

Derivations

Specularity. - Sample sizes for specularity are estimated first. They are then verified to provide the required precision in the other parameters.

Because of the complex formulas used to estimate specularity, a general statistical approach will be used. A useful statistical tool is Tchebycheff's Inequality. This law states that for any random variable, x, of any arbitrary probability distribution, f(x), the sample mean, $\bar{x}$, will deviate from its true value, μ, by an amount exceeding a factor, K, of the standard deviation, σ, with a probability less than $1/K^2N$. In probability notation, where $P_r[\quad]$ means probability of occurrence of the statement in the brackets, the above description is:

$$P_r[|\bar{x} - \mu| > K\sigma] < \frac{1}{K^2N} \tag{B1}$$

Since the specified accuracy of ±2 percent must occur with a confidence probability, C, of 0.96, the specularity requirement may be symbolized similarly to equation (B1):

$$P_r[|\bar{x} - \mu| > \rho\mu] < 1 - C = 1 - 0.96 = 0.04 \tag{B2}$$

where ρ = proportion of μ, which is the true value estimated by x.

Therefore, from (B1) and (B2), $\rho\mu = K\sigma$; thus

$$K = \frac{\rho\mu}{\sigma} \tag{B3}$$

Also, from (B1) and (B2):

$$\frac{1}{K^2N} = 1 - C \tag{B4}$$

Now, substituting from (B3) into (B4) for K and solving for the sample size, N, we have:

$$N = \frac{(\sigma/\mu)^2}{\rho^2(1 - C)}$$

However, the coefficient of variation $C_v = \sigma/\mu$ and is a statistical measure of relative error. Thus

$$N = \frac{(C_v/\rho)^2}{1 - C} \tag{B5}$$

Equation (B5) is a parametric solution into which we may insert various relative coefficients of variation for given required accuracies. At a confidence level of 96 percent, and with ρ equal to 2 percent and 1 - C equal to 0.04, sample sizes can be calculated as follows:

C_v	N
1%	6.25 (7)
3%	56.25 (57)
5%	156.25 (157)
8%	400
10%	625

In reference 8, page 10, two regression coefficients, A_{sp} and B_d, are computed from repeated data points. The specularity, S, is then estimated by:

$$S = \frac{A_{sp}}{A_{sp} + B_d} \tag{B6}$$

APPENDIX B

To estimate what sample size we need in this regression to satisfy the required accuracy, we need the $C_v(S)$, the coefficient of variation of S. Thus, we first seek the standard deviation, σ_S, of S. To derive this we use Gaussian propagation of error (ref. 9 p. 118) to develop σ_S for specularity:

$$\sigma_S = \left[\left(\frac{\partial S}{\partial A_{sp}}\right)^2 \sigma_{A_{sp}}{}^2 + \left(\frac{\partial S}{\partial B_d}\right)^2 \sigma_{B_d}{}^2\right]^{1/2}$$

$$= (A_{sp} + B_d)^{-2} \left(B_d^2 \, \sigma_{A_{sp}}^2 + A_{sp}^2 \, \sigma_{B_d}^2\right)^{1/2}$$

Then the coefficient of variation is

$$C_v(S) = \frac{\sigma_S}{S} = \frac{1}{A_{sp}(A_{sp} + B_d)} \left(B_d^2 \, \sigma_{A_{sp}}^2 + A_{sp}^2 \, \sigma_{B_d}^2\right)^{1/2} \qquad \text{(B7)}$$

Given typical values of A and B, we need expressions for $\sigma_{A_{sp}}$ and σ_{B_d}. These are available from regression analyses (ref. 9, p. 535) as:

$$\sigma_{A_{sp}}^2 = \frac{\sigma^2}{N} \qquad \text{(B8)}$$

$$\sigma_{B_d}^2 = \frac{\sigma^2}{\Sigma N_i \, (x_i - \bar{x})^2} \qquad \text{(B9)}$$

Although values of the denominator of $\sigma_{B_d}^2$ are not available, an apparently safe assumption is to assume

$$\sigma_{B_d}^2 = \sigma_{A_{sp}}^2 = \sigma^2/N.$$

In this, σ^2, which is the standard error of residuals, is not known, but a pessimistic overestimate is possible from the dependent variable, $10^{-0.4m}$ (ref. 8, p. 10). To accomplish this we again use Gaussian propagation of error.

Let $f(m) = 10^{-0.4m}$, where m is stellar magnitude. Then:

$$\sigma_{f(m)}^2 = \left[\frac{\partial f}{\partial m}\right]^2 \sigma_m^2 = \left[(-0.4)\,(2.30259)\,10^{-0.4m}\right]^2 \sigma_m^2 \qquad \text{(B10)}$$

By assuming that the bracketed term equals unity, another pessimistic overestimate of σ is introduced.

Given typical values for all parameters, we are now in a position to estimate $C_v(S)$ and thus the required sample size, N, using the U band σ since it is highest:

$A_{sp} \cong 3.8$

$B_d \cong 0.12$

$2.5 \leq m \leq 3.0$

$\sigma = 0.10$

In equation (B10), σ is for individual values as is σ_S; thus in (B8) and (B9), N = 1; the final $C_v(S)$ equation into which we can substitute the above values is:

$$C_V(S) \cong \frac{\sigma_m}{A_{sp}(A_{sp} + B_d)} \left(B_d^2 + A_{sp}^2\right)^{1/2}$$

or

$$C_V(S) = 0.0255$$

Substituting this value into that for sample size N in equation (B5),

$$N = \frac{(C_V/\rho)^2}{1 - C} = \frac{(0.0255/0.02)^2}{1 - 0.96}$$

$$N = 41$$

Therefore, in the U band a sample of 41 data points in the regression fit for A_{sp} and B_d (ref. 8, p. 10) will give a specularity estimate that will be within ±2 percent of the true value with a confidence probability of 96 percent. This is the maximum that will be needed. Calculations for the other two bands, which have lower σ values, will result in smaller sample sizes. In the B band, by the same formulas, a sample size of $N_b = 21$ is required for ±2 percent accuracy on specularity. In the V band, $N_v = 15$.

Radius of curvature. - The sample sizes derived for specularity are now examined for satisfaction of the precision on radius of curvature, R_c. From the calculations in reference 8, it follows that

$$10^{-0.4m} = K \gamma R_c^2, \tag{B11}$$

where K is some constant.

The coefficient of variation of a variable y, $C_v(y)$, is defined to be the standard deviation, σ, divided by the mean, M:

$$C_v(y) = \sigma/M \tag{B12}$$

It is well known (see ref. 9, p. 248) that for an equation such as (B11):

$$0.16\sigma_m^2 = \overline{C_V(\gamma)^2} + \overline{4C_v(R_c)^2} \tag{B13}$$

APPENDIX B

In order to arrive at the sample sizes that will be necessary to meet the desired precision of estimates, the following assumptions are made.

First, in equation (B13) it is assumed that $C_V(\gamma) = 0$, which will give an overestimate of $C_V(R_c)$ and thus safely exaggerate the sample size. Also, from page 318 of reference 23 the following standard deviations are derivable. Reference 23 gives probable errors, p. e., for stellar photometry for z = 60 degrees (i. e., sec z = 2).

p. e. (V) = ±0.04

p. e. (B - V) = ±0.02

p. e. (U - B) = ±0.04

Therefore (for sec z = 2):

$$\sigma_v = \frac{0.04}{0.6745} = 0.06$$

$$\sigma_{b-v} = \frac{0.02}{0.6745} = 0.03$$

$$\sigma_{u-b} = \frac{0.04}{0.6745} = 0.06$$

Using the standard deviation of sums of random variables,

$$\sigma_b = \sqrt{\sigma_v^2 + \sigma_{b-v}^2} = \sqrt{(0.06)^2 + (0.03)^2} = 0.07$$

$$\sigma_u = \sqrt{\sigma_{u-b}^2 + \sigma_b^2} = 0.09$$

Thus, the three bands' standard deviations of stellar photometry for z = 60 degrees are:

$$\left.\begin{aligned} \sigma_v &= 0.06 \\ \sigma_u &= 0.09 \\ \sigma_b &= 0.07 \end{aligned}\right\} \text{ stellar magnitude} \qquad \text{(B14)}$$

Now, from the definition for the coefficient of variation, it follows for an average R_c of M_{R_c} = 50 ft and assuming that in equation (B13) $C_V(\gamma) = 0$:

$$0.4\sigma_m = 2C_V(R_c) = 2\left(\sigma_{R_c}/M_{R_c}\right)$$

or

$$\sigma_{R_c} = 0.2\sigma_m \cdot M_{R_c} \qquad \text{(B15)}$$

The nominal radius of curvature is $M_{R_c} = 50$ feet; therefore, in each of the three bands we have a standard deviation, $\sigma_{\bar{R}_c}$, of the estimator $\bar{R}_c$ of R_c:

$$\left.\begin{aligned} \sigma_v(R_c) &= 0.2\,(0.06)\,(50\text{ ft}) = 0.60 \\ \sigma_u(R_c) &= 0.2\,(0.09)\,(50\text{ ft}) = 1.0 \\ \sigma_b(R_c) &= 0.2\,(0.07)\,(50\text{ ft}) = 0.70 \end{aligned}\right\} \tag{B16}$$

An estimate of R_c can now be made by a pooled sample average, $\bar{R}_c$, of the three averages from each of the three bands. These three averages, $\bar{R}_c(V)$, $\bar{R}_c(U)$, and $\bar{R}_c(B)$, may be combined into an overall estimate of the true R_c with sample sizes N_v, N_u, and N_b in each:

$$\bar{R}_c = \frac{\bar{R}_c(V)N_v + \bar{R}_c(U)N_u + \bar{R}_c(B)N_b}{N_v + N_u + N_b} \tag{B17}$$

This $\bar{R}_c$ will have a standard deviation, $\sigma_{\bar{R}_c}$, given by:

$$\sigma_{\bar{R}_c} = \left[\frac{\sigma_{\bar{R}_{c(V)}}^2 \cdot N_v^2 + \sigma_{\bar{R}_{c(U)}}^2 \cdot N_u^2 + \sigma_{\bar{R}_{c(B)}}^2 \cdot N_b^2}{(N_v + N_u + N_b)^2}\right]^{1/2} \tag{B18}$$

But the standard error of any average $\bar{x}$ is, for sample size of N, related to the standard deviation, σ_{R_c}, of the individuals by:

$$\sigma_{\bar{x}}^2 = \frac{\sigma_x^2}{N}$$

Therefore, (B18) becomes:

$$\sigma_{\bar{R}_c} = \left[\frac{\sigma_v^2 \cdot N_v + \sigma_u^2 \cdot N_u + \sigma_b^2 \cdot N_b}{(N_v + N_u + N_b)^2}\right]^{1/2} \tag{B19}$$

Now, using the sample sizes $N_v = 15$, $N_u = 41$, and $N_b = 21$ for the specularity estimates, we must show that with a confidence probability of 96 percent the error in measuring R_c will be less than ±0.7 foot (2.06 standard deviation corresponds to 96 percent probability):

$$\sigma_{\bar{R}_c} = \left[\frac{(0.60)^2\,(15) + (1.0)^2\,(41) + (0.70)^2\,(21)}{(15 + 41 + 21)^2}\right]^{1/2} \tag{B20}$$

$$= 0.010 \text{ foot} \tag{B20a}$$

and $2.06\,\sigma_{\bar{R}_c} = 0.021$ foot, which is less than the target 0.7 foot. The requirements will easily be met by the sample sizes.

Stellar magnitude. - The requirement is ±0.2 with a confidence probability of 96 percent. This is equivalent to 2.06 standard deviations on the normal curve of error, or:

$$2.06 \frac{\sigma_m}{\sqrt{N_m}} \leq 0.2 \tag{B21}$$

Using the established sample sizes and the σ_m from equation (B14), the above inequality must be satisfied. For the three bands the left-hand side of equation (B21) is as follows:

V band: $2.06 \ (0.06/\sqrt{15}) = 0.032$

U band: $2.06 \ (0.09/\sqrt{41}) = 0.030$

B band: $2.06 \ (0.07/\sqrt{21}) = 0.031$

Therefore, stellar magnitude will be measured to the required precision by the established sample sizes.

Solar reflectance. - Using equation (B13), the coefficient of variation of γ may be expressed as a function of the variance of stellar magnitude, $\sigma_m{}^2$, and the coefficient of variation of radius of curvature estimates, R_c.

$$\left[C_v(\gamma)\right]^2 = 0.16\sigma_m{}^2 + 4\left[C_v(R_c)\right]^2 \tag{B22}$$

We must now show that the sample average $\bar{\gamma}$ in all three bands satisfies ±2 percent precision with 96 percent probability; that is,

$$2.06 \ C_v(\bar{\gamma}) \leq 0.02$$

or that all sample sizes meet

$$C_v(\bar{\gamma}) \quad 0.02/2.06 = 9.71 \times 10^{-3} \tag{B23}$$

To do this we note that for sample averages, equation (B22) becomes:

$$\left[C_v(\bar{\gamma})\right]^2 = 0.16 \ (\sigma_m{}^2/N) + 4 \left[C_v(\bar{R}_c)\right]^2 \tag{B24}$$

where N is sample size in each of the three bands.

From equations (B20) and (B20a) we have

$$C \ (\bar{R}_c) = \frac{\sigma_{\bar{R}_c}}{R_c} = \frac{0.010 \text{ foot}}{50 \text{ feet}} = 2 \times 10^{-4}$$

Then equation (B24) becomes

$$C \ (\bar{\gamma})^2 = 0.16(\sigma_m{}^2/N) + 16 \times 10^{-8} \tag{B25}$$

Substituting the three bands σ_m from equation (B14) and the established sample sizes in equation (B25) gives:

V band: $C_V(\bar{\gamma})_v = 5.0 \times 10^{-3}$

U band: $C_V(\bar{\gamma})_u = 6.0 \times 10^{-3}$

B band: $C_V(\bar{\gamma})_b = 6.1 \times 10^{-3}$

All three above satisfy the requirement of equation (B23). Therefore, the established sample sizes in each of the bands meet the required precisions.

Trend Analysis

The possibility exists that the satellite's parameters may change with time. This trend may be slight enough that the random variations existing in the experiment will tend to obscure it. Statistical methods that exist for detecting trend in the presence of "noise" (i. e., random variations) can be continuously applied to the data on each of the parameters to monitor and estimate the rate of change.

APPENDIX C

FILLING OUT CONTROL CARD I AND THE DATA POINT INFORMATION CARD

Control Card I

Columns 1, 2, 3, and 4. - The first four columns of control card I (fig. C1) are used to identify the data as part of one of the three calibration constant determinations or as part of the determination of satellite stellar magnitudes. The codes are as follows:

CAL6 - Determination of second-order extinction coefficients. These calibration constants are determined by repeatedly observing close pairs of stars having widely differing color indices through a wide range of altitudes.

CAL7 - Determination of scale factors for system transformation. Using the data from CAL6 determinations, these calibration constants are determined by observing a number of standard stars, ranging widely in color, through substantially the same air mass, preferably all near the zenith.

CAL8 - Determination of primary extinction coefficients and zero-point terms. Using determinations from both CAL6 and CAL7, these constants are determined by observing a number of high-z stars and low-z stars of spectral classes F-G-K, both before and after the satellite pass.

OBS3 - Determination of satellite stellar magnitude. This is computer program E-1213.

Columns 5 through 23. - The rest of the control card I columns are used as follows (terms are defined at the end of this appendix):

Columns 5 and 6 - Month (I2, right adjusted)

Columns 7 and 8 - Day (I2, right adjusted)

Columns 9 and 10 - Year (I2, right adjusted)

Columns 11 thru 28 - Not used

Columns 29 thru 48 - Header

(Remainder of columns not used.)

Data Point Information Card

The data point information card (fig. C2) is filled out for computer programs E-1960, 1970, and 1980 (calibration constant determinations). Columns are used as follows (terms are defined at the end of this appendix):

Column 1 - Filter number: V = 1, U = 2, B = 3 (I1)

Columns 2 and 3 - Hour UT (I2, right adjusted)

Columns 4 and 5 - Minute UT (I2, right adjusted)

	TYPE CAL OR OBS	PROG CODE	MO	DA	YR	GAIN TERMS V_1	U_1	B_1	V_2	U_2	B_2	HEADER COMMENTS	TEL. AZIMUTH DEG	MIN	TEL. ELEV DEG	MIN	SITE N. LAT DEG	MIN	SITE W. LONG DEG	MIN	SITE ELEV		OBSERVER
	1 2 3	4	5 6	7 8	9 0	1 2 3	4 5 6	7 8 9	0 1 2	3 4 5	6 7 8	9 0 1 2 3 4 5 6 7 8 9 0 1 2 3 4 5 6 7 8 9 0 1 2 3 4 5 6 7 8	9 0 1 2	3 4	5 6 7 8	9 0	1 2 3 4	5 6	7 8 9 0	1 2	3 4 5 6 7	8 9 0	
1																							
2																							
3																							
4																							
5																							
6																							
7																							
8																							
9																							
10																							
11																							
12																							
13																							
14																							
15																							
16																							
17																							
18																							
19																							
20																							

Figure C1. - Control card I.

DATA POINT INFORMATION FOR PROGRAMS

E1960 - E1970 - E1980 - E1213 - ______ - ______

BY ____________________

REFERENCE CONTROL CARD

MO ________ DAY ________ YR ________

HEADER COMMENTS ____________________

	FILTER NO	HR	MIN	SEC	INTENSITY	GAIN NO.	δ_1	δ_2	STAR IDENT NO. (B.S.)	PAIR NO.	POLARIZATION	
	1	2 3	4 5	6 7 8	9 0 1	2 3	4 5	6 7	8 9 0 1	2 3	4 5	6 7 8 9 0 1 2 3 4 5 6 7 8 9 0 1 2 3 4 5 6 7 8 9 0 1 2 3 4 5 6 7 8 9 0 1 2 3 4 5 6 7 8 9 0 1 2 3 4 5 6 7 8 9 0
1												
2												
3												
4												
5												
6												
7												
8												
9												
10												
11												
12												
13												
14												
15												
16												
17												
18												
19												
20												

Figure C2. - Data point information card.

Columns 6 thru 8 - Second UT (F3.1 dec pt 2 from left)

Columns 9 thru 11 - Intensity (F3.2 dec pt 1 from left)

Columns 12 and 13 - Gain No. 1 thru 15 (I2, right adjusted)
(F2.0, right adjusted)
(F2.0, right adjusted)

Columns 14 thru 17 - Not used

Columns 18 thru 21 - Bright Star No. (I4, right adjusted)

Columns 22 and 23 - Pair No. (I2, right adjusted)

Columns 24 and 25 - Not used

(Remainder of columns not used)

Columns 22 and 23 (Pair No.) are filled out when computer program E-1960, Second-Order Extinction Coefficients, is run. It should be noted that a set of U-B-V values (in any order) has to be entered on the DPI form. In addition, a set of U-B-V values for one star of the pair must be followed by a set of U-B-V values for the second star of the pair. If it is found that there are more sets of U-B-V values for one star of the pair than for the other, U-B-V values for the star with the lesser number of sets may be repeated. Likewise, U-B-V sets of three values must be used in sequence for calibration computer programs E-1970 and E-1980. It is proper to re-use individual U, B, or V values if it is found that one or two of the colors have fewer valid intensity values than the others.

Additional Forms

The Operations Data Sheet form (fig. C3) is used as an aid in setting circle determinations as well as a check on the stars which were used in the 3 calibration programs. The Maintenance Data Sheet (fig. C4) is a sheet for recording maintenance functions performed on the observatory.

Definition of Terms

Computer card format. -

Right adjusted	- Number must be in the right-most positions of the field allowed.
Iw (w is an interger)	- This specifies that an interger is to be right-adjusted in a field of size "w." Example: For I2, any number would have to be right-adjusted in a field of size 2. Given the number 3 to put in this field, one would get: [0 | 3]
Fw.d (w and d are intergers	- This specifies that a decimal number is to be put in a field of size "w" with "d" decimal places. Examples: For F4.0, given the number 23.8, one would get [0 | 0 | 2 | 4] . For F3.3, given the number 0.5678, one would get [5 | 6 | 8] .

APPENDIX C

OPERATIONS DATA SHEET

STARS USED IN PHOTOMETRIC CALIBRATION OBSERVATION

DATE ______________

SIGNATURE ______________

Calibration for
- ☐ Second-Order Extinction Coefficients
- ☐ Scale Factors for System Transformation
- ☐ Primary Extinction Coefficients and Zero Point Terms

Observing Estimated Time (U.T.)	Star Identity (B.S.)	Stellar Magnitude			Sidereal Time	Right Ascension	Local Hour Angle	Declination	Star Chart Number
		U	B	V					

Figure C3. - Operations data sheet.

Names of the Fields. -

Header - A verbal description of the type of observation or calibration for which the header is applicable.

Intensity - The reading which corresponds to a galvanometer deflection in inches.

Gain number - A gain setting used to compute a gain factor used in determining the gain. (See table C1.)

APPENDIX C

Date: ________________

MAINTENANCE DATA SHEET

Information To Be Entered:

(1) Maintenance Performed

(2) Parts Replaced

(3) Fueling, Servicing, Adjustments

(4) Supplies And Spare Parts Purchased

(5) Equipment Malfunctions

(6) Damage To Equipment

(7) Other

Figure C4. - Maintenance data sheet.

TABLE C1. - GAIN INFORMATION

Gain No.	Gain range	Gain factor	S
1	10 mA (10^{-2} A)	1	0
2	3	3.3	1.3072
3	1 (10^{-2} A)	10	2.5
4	0.3	33.3	3.8072
5	0.1 (10^{-4} A)	100	5.0
6	0.03	333	6.3072
7	10 μA (10^{-5} A)	1 000	7.5
8	3	3 333	8.8072
9	1 (10^{-6} A)	10 000	10.0
10	0.3	33 333	11.3072
11	0.1 (10^{-7} A)	100 000	12.5
12	0.03	333 333	13.8072
13	10 mμA (10^{-8} A)	1 000 000	15.0
14	3	3 333 333	16.3072
15	1 (10^{-9} A)	10 000 000	17.5
16	0.3	33 333 333	18.8072
17	0.1 (10^{-10} A)	100 000 000	20.0

APPENDIX D

DESCRIPTION OF COMPUTER PROGRAM PRINTOUT FOR PAGEOS I GROUND-BASED PHOTOMETRIC SURVEILLANCE

This appendix presents a computer printout for the second pass of the PAGEOS I satellite on 17 August 1966. The printout demonstrates the method of calculation of the various extinction coefficient and satellite parameters.

The five computer programs are as follows:

(1) Computer program E-1960, Second-Order Extinction Coefficients. The printout of the E-1960 program is not included. The last observation was performed on 17 August 1966. Values of k''_{b-v} = -0.02760 and k''_{u-b} = -0.04053 were obtained.

(2) Computer program E-1970, Transformation Scale Factors (table D1). The observation was performed on 13 August 1966. The values of the second-order coefficients performed on 17 August were used to calculate the new set of values for the scale factors, as may be verified in the table of calibration constants (table II of this report). The values in columns 4, 5, and 6 (DV/S_v, DU/S_u, and DB/S_b) refer to galvanometer deflection in inches/photometer gain position.

(3) Computer program E-1980, Primary Extinction Coefficients (table D2). This printout shows the standard stars and the calculated values used to obtain the primary extinction coefficients (k'_v, k'_{b-v}, k'_{u-b}) and the zero-point terms (ζ_v, ζ_{b-v}, and ζ_{u-b}). The "difference in dependent variable" denotes the amount of variation of the individual points from the best-fit straight line for the three spectral regions. The standard error of residuals for these differences is also shown.

(4) Computer program E-1213, Satellite Photometer Program: U-B-V Stellar Magnitude (table D3). The information on this run is for the most part self-explanatory; however, a few items require an explanation. The orbital elements shown at the start of the run are used to calculate the various satellite positions listed. UT refers to universal time (UT = EST + 5 hours). The last two columns (EA MAG and MAGO) are the stellar magnitudes. The column on the far right is the extra-atmospheric magnitude for the given slant range. The column second from the right (MAGO) refers to the extra-atmospheric magnitude, which is normalized for slant range to 2640 statute miles, with a correction factor for earth albedo included. This is the magnitude value which is used in the E-1214 program. The second line for each color band contains three terms. These refer to the correction factors - albedo (magnitudes), slant range (magnitudes), and the angle α (see appendix A).

(5) Computer program E-1214, Specularity and Diffusivity Determinations: Radius of Curvature and Reflectance (table D4). A very large number of parameters are printed out on this series, most of which are intermediate steps in the calculation of the parameters of interest. These include mean normalized magnitude, specularity, radius of curvature, and indicated reflectivity.

APPENDIX D

TABLE D1. - COMPUTER PROGRAM E-1970 PRINTOUT

SCALE FACTORS CALIBRATION PROGRAM (II) 8-13-66

STAR	Z	X	DV/S_v	DU/S_u	DB/S_b	VO	(B-V)O	(U-B)O	V-VO	B-V-(B-V)O	U-B-(U-B)O
5899	22.6	1.08314	0.89/10	1.50/13	0.53/10	11.27016	0.41714	2.35085	-6.49016	1.10286	-0.47085
6095	19.0	1.05740	2.24/10	1.61/10	1.26/ 9	10.27188	-0.86103	0.76845	-6.51188	1.13103	-0.56845
6148	16.1	1.04059	1.66/ 9	1.54/10	1.70/ 9	9.29255	-0.18268	1.16200	-6.52255	1.12268	-0.47200
6220	9.8	1.01464	0.88/ 9	2.78/11	0.92/ 9	9.98551	-0.20181	1.04840	-6.48551	1.12181	-0.43840
6410	8.9	1.01224	1.20/ 9	1.24/ 9	0.83/ 8	9.64912	-0.96652	0.48433	-6.52912	1.03652	-0.40433
6418	4.6	1.00324	1.22/ 9	2.91/12	0.78/ 9	9.63253	0.34862	2.17341	-6.47253	1.09138	-0.51341
6526	7.2	1.00790	1.26/10	2.70/13	0.82/10	10.90400	0.32818	2.19455	-6.49400	1.11182	-0.51455
6556	20.7	1.06907	1.05/ 8	2.75/ 9	2.03/ 8	8.59278	-0.89725	0.57989	-6.52278	1.03725	-0.46989
6703	6.0	1.00554	0.69/ 9	1.93/11	0.71/ 9	10.25096	-0.18271	1.17023	-6.54096	1.12271	-0.47023
6868	14.4	1.03239	0.80/10	3.75/14	1.28/11	11.39352	0.54709	2.44088	-6.43353	1.04291	-0.45087
6895	14.8	1.03424	0.61/ 9	2.87/12	0.48/ 9	10.38045	0.11251	1.63352	-6.52045	1.05749	-0.46352
7001	12.0	1.02237	0.72/ 6	2.35/ 7	1.75/ 6	6.50942	-1.14483	0.60218	-6.50942	1.14483	-0.57218
7178	14.8	1.03408	1.02/ 9	1.41/ 9	0.82/ 8	9.82230	-1.13823	0.31939	-6.59230	1.10823	-0.39939
7298	17.5	1.04827	1.19/10	2.97/10	1.02/ 9	10.96000	-1.33005	-0.16144	-6.58000	1.19005	-0.50856

NO. OF POINTS = 14

	CONST	SLOPES	SUM(X-XBAR)**2	STD ERROR OF RESIDUALS
v:	-6.54829	0.04585	5.55232	0.02880
b-v:	1.11506	-0.01843	5.55232	0.04471
u-b:	-0.48100	0.00173	5.07932	0.05388

DIFFERENCE IN DEP VAR. V-VO

-0.01157
0.02403
-0.01737
0.02059
0.01595
0.00973
-0.01174
0.01909
-0.03577
0.04186
-0.02581
0.03886
-0.04264
-0.02530

DIFFERENCE IN DEP VAR B-V-(B-V)O

0.01582
0.02094
0.02495
0.02371
-0.07725
0.00286
0.02330
-0.07524
0.02498
-0.04284
-0.03601
0.02977
-0.00739
0.07240

DIFFERENCE IN DEP VAR U-B-(U-B)O

0.00691
-0.05780
0.00781
0.04155
0.07653
-0.03527
-0.03645
0.01091
0.00956
0.02669
0.01546
-0.09123
0.08174
-0.02641

SYSTEM TRANSFORMATION SCALE FACTORS

EPS = 0.04585
MU = 0.98190
PSI = 1.00173

APPENDIX D

TABLE D2. - COMPUTER PROGRAM E-1980 PRINTOUT

PRIMARY EXTINCTION CALIBRATION PROGRAM (III) 8-17-66

STAR	Z	X	DV/s_v	DU/s_u	DB/s_b	(V+E(B-V)-V)	(MU(B-V)JX-(B-V))	(PSI(U-B)GX-(U-B))
8115	20.8	1.0694	0.90/ 9	1.88/11	0.90/ 9	6.96916	-1.00000	1.01696
7602	48.8	1.5164	1.64/10	1.31/11	1.62/10	7.08843	-0.84637	1.03350
7377	56.8	1.8235	2.07/10	1.19/10	1.01/ 9	7.17131	-0.87461	1.16468
8232	43.6	1.3793	1.11/ 9	0.96/10	1.26/ 9	7.07412	-0.98027	1.11495
8684	9.0	1.0124	0.66/ 9	1.77/11	0.70/ 9	7.01315	-1.00448	0.88675
21	28.3	1.1357	1.92/ 9	1.43/ 9	1.15/ 8	7.02625	-0.98436	0.89195
7602	60.7	2.0354	1.46/10	0.95/11	1.36/10	7.21466	-0.78011	1.23583
7377	68.9	2.7578	1.70/10	0.65/10	0.69/ 9	7.38512	-0.67678	1.47803
8232	51.6	1.6088	1.07/ 9	2.51/11	1.10/ 9	7.11397	-0.87079	1.13185
8684	16.9	1.0449	2.13/10	1.56/11	2.06/10	7.04826	-0.90335	0.89065
8665	26.7	1.1193	1.10/10	2.23/11	1.60/10	7.03601	-0.92179	0.91160
21	25.7	1.1093	2.02/ 9	1.45/ 9	1.11/ 8	6.97112	-0.88922	0.83491

NO. OF POINTS = 12

	-ZETA	SLOPES	SUM(X-XBAR)**2	STD ERROR OF RESIDUALS
v:	6.77071	0.21933	3.04803	0.02597
b-v:	-1.13483	0.16386	3.04803	0.04629
u-b	-0.55040	0.33993	3.04803	0.05779

DIFFERENCE IN DEP VAR V+E(B-V)-V	DIFFERENCE IN DEP VAR μ(B-V)JX-(B-V)	DIFFERENCE IN DEP VAR ψ(U-B)GX-(U-B)
-0.03611	-0.04039	0.10305
-0.01487	0.04000	-0.03235
0.00064	-0.03857	-0.00559
0.00088	-0.07145	0.09568
0.02039	-0.03553	-0.00778
0.00644	-0.03562	-0.04451
-0.00248	0.02122	-0.00645
0.00952	0.00616	-0.00983
-0.00960	0.00044	0.03459
0.04835	0.06026	-0.01496
0.01980	0.02963	-0.01928
-0.04291	0.06384	-0.09259

PRIMARY EXTINCTION COEFFICIENTS

K-PRIME V = 0.21933
K-PRIME B-V = 0.16683
K-PRIME U-B = 0.33934

ZERO POINT TERMS

ZETA V = -6.77071
ZETA B-V = 1.13483
ZETA U-B = -0.55040

TABLE D3. - COMPUTER PROGRAM E-1213 PRINTOUT

ORBITAL ELEMENTS

1966	8	5.000000	219.609985	-0.827800	333.229492	-0.086360	86.949295	1950.0
0.03336600	0.00069200	0.0	0.0	0.119453	7.938468	0.584500E-04	0.0	

STATION COORDINATES 33.31029 116.84860

CALIBRATION CONSTANTS

2ND ORDER EXTINCTION COEF.	-0.02760	-0.04053	
SYS. TRANS. SCALE FACTORS	0.04585	0.98190	1.00173
PRIMARY EXTINCTION COEF.	0.21933	0.16688	0.33934
ZERO POINT TERMS	-6.77071	1.13483	-0.55040

PAGEOS REDUCTION OF SATELLITE OBSERVATIONS 8-17-66 E1213

	UT	HT	LONG	LAT	ALT	AZ	SR	RA	DEC	PHASE	MAGO	EA MAG
V' 1966 8 17	9 20 55	2908.9	131.85	23.60	53.73	237.56	3266.3*	21 12.9	10.07	24.9	2.111	2.577
	0.0	-0.4664	142.3409									
U' 1966 8 17	9 20 51	2908.8	131.83	23.47	53.57	237.16	3269.5*	21 13.0	9.80	24.7	3.048	3.517
	0.0	-0.4685	142.4758									
B' 1966 8 17	9 21 1	2909.0	131.86	23.76	53.91	238.01	3262.6*	21 12.8	10.39	25.2	2.802	3.266
	0.0	-0.4639	142.1858									
U 1966 8 17	9 21 9	2909.1	131.87	24.01	54.19	238.73	3257.1*	21 12.5	10.89	25.7	2.750	3.210
	0.0	-0.4602	141.9457									
V' 1966 8 17	9 21 40	2909.7	131.95	24.98	55.25	241.70	3236.2*	21 11.6	12.88	27.7	1.970	2.416
	0.0	-0.4463	140.9855									
U 1966 8 17	9 21 37	2909.7	131.94	24.88	55.15	241.40	3238.2*	21 11.7	12.68	27.5	2.874	3.322
	0.0	-0.4476	141.0803									
B' 1966 8 17	9 21 45	2909.8	131.96	25.12	55.40	242.13	3233.5*	21 11.5	13.16	28.0	2.638	3.082
	0.0	-0.4444	140.8501									
U 1966 8 17	9 21 49	2909.9	131.97	25.25	55.53	242.56	3230.9*	21 11.3	13.43	28.2	3.003	3.446
	0.0	-0.4427	140.7202									
V' 1966 8 17	9 22 11	2910.2	132.01	25.91	56.21	244.73	3218.2*	21 10.6	14.80	29.6	2.199	2.633
	0.0	-0.4342	140.0644									
U' 1966 8 17	9 22 7	2910.2	132.00	25.79	56.09	244.33	3220.4*	21 10.8	14.55	29.3	3.049	3.484
	0.0	-0.4357	140.1846									
B' 1966 8 17	9 22 16	2910.3	132.02	26.07	56.36	245.26	3215.4*	21 10.5	15.12	29.9	2.765	3.198
	0.0	-0.4322	139.9094									
U 1966 8 17	9 22 20	2910.4	132.03	26.20	56.49	245.71	3213.0*	21 10.3	15.40	30.2	2.857	3.288
	0.0	-0.4306	139.7795									
V' 1966 8 17	9 22 43	2910.7	132.08	26.89	57.12	248.10	3201.3*	21 9.6	16.83	31.6	2.056	2.479
	0.0	-0.4228	139.0988									
U' 1966 8 17	9 22 39	2910.7	132.07	26.77	57.02	247.69	3203.3*	21 9.7	16.59	31.4	2.959	3.383
	0.0	-0.4241	139.2140									
B' 1966 8 17	9 22 48	2910.8	132.09	27.05	57.26	248.66	3198.8*	21 9.4	17.16	31.9	2.679	3.100
	0.0	-0.4211	138.9435									
U 1966 8 17	9 22 53	2910.8	132.10	27.18	57.38	249.16	3196.7*	21 9.2	17.44	32.2	2.781	3.200
	0.0	-0.4196	138.8083									
V 1966 8 17	9 23 16	2911.1	132.15	27.88	57.96	251.73	3186.4*	21 8.4	18.90	33.7	1.871	2.284
	0.0	-0.4126	138.1173									
U 1966 8 17	9 23 11	2911.0	132.14	27.74	57.84	251.20	3188.4*	21 8.6	18.61	33.4	2.608	3.022
	0.0	-0.4140	138.2577									
B 1966 8 17	9 23 21	2911.1	132.16	28.05	58.09	252.37	3184.1*	21 8.2	19.27	34.0	2.733	3.144
	0.0	-0.4110	137.9470									
U 1966 8 17	9 23 25	2911.2	132.17	28.17	58.18	252.83	3182.4*	21 8.0	19.52	34.3	3.036	3.446
	0.0	-0.4099	137.8271									
V 1966 8 17	9 23 47	2911.4	132.22	28.83	58.65	255.38	3174.3*	21 7.2	20.91	35.7	2.158	2.562
	0.0	-0.4043	137.1755									
U 1966 8 17	9 23 43	2911.3	132.21	28.73	58.58	254.98	3175.5*	21 7.3	20.69	35.5	3.073	3.478
	0.0	-0.4051	137.2762									
B 1966 8 17	9 23 52	2911.4	132.23	28.99	58.76	256.00	3172.4*	21 7.0	21.24	36.0	2.998	3.401
	0.0	-0.4031	137.0206									
U 1966 8 17	9 23 55	2911.4	132.24	29.10	58.83	256.42	3171.2*	21 6.9	21.46	36.2	3.233	3.635
	0.0	-0.4022	136.9153									
V 1966 8 17	9 24 19	2911.6	132.28	29.81	59.26	259.31	3163.9*	21 5.9	22.98	37.7	2.334	2.731
	0.0	-0.3972	136.2042									
U 1966 8 17	9 24 15	2911.5	132.27	29.68	59.18	258.76	3165.2*	21 6.1	22.69	37.5	3.404	3.802
	0.0	-0.3981	136.3395									
B 1966 8 17	9 24 25	2911.6	132.30	30.00	59.35	260.06	3162.2*	21 5.6	23.36	38.1	2.715	3.111
	0.0	-0.3961	136.0235									
U 1966 8 17	9 24 31	2911.6	132.31	30.18	59.45	260.81	3160.6*	21 5.4	23.75	38.5	2.684	3.079
	0.0	-0.3949	135.8435									
V 1966 8 17	9 25 1	2911.7	132.37	31.08	59.84	264.60	3153.9*	21 4.1	25.66	40.4	1.966	2.357
	0.0	-0.3903	134.9510									
U 1966 8 17	9 24 55	2911.7	132.36	30.90	59.78	263.85	3155.0*	21 4.3	25.28	40.1	2.619	3.010
	0.0	-0.3911	135.1267									
B 1966 8 17	9 25 6	2911.7	132.38	31.24	59.90	265.27	3152.9*	21 3.8	25.99	40.8	2.669	3.059
	0.0	-0.3896	134.7956									
U 1966 8 17	9 25 10	2911.7	132.39	31.36	59.94	265.81	3152.1*	21 3.6	26.26	41.0	2.974	3.363
	0.0	-0.3891	134.6705									

TABLE D3. - CONTINUED

PAGEOS REDUCTION OF SATELLITE OBSERVATIONS 8-17-66. E1213

		UT	HT	LONG	LAT	ALT	AZ	SR	RA	DEC	PHASE	MAGO	EA MAG
V	1966	8 17 9 25 31	2911.7	132.43	32.01	60.13	268.61	3148.9*	21 2.6	27.64	42.4	1.865	2.252
		0.0	-0.3869	134.0286									
U	1966	8 17 9 25 26	2911.7	132.42	31.84	60.09	267.88	3149.6*	21 2.9	27.28	42.1	2.747	3.134
		0.0	-0.3874	134.1942									
B	1966	8 17 9 25 36	2911.7	132.44	32.16	60.17	269.24	3148.3*	21 2.4	27.95	42.7	2.493	2.880
		0.0	-0.3865	133.8833									
U	1966	8 17 9 25 46	2911.7	132.45	32.46	60.23	270.55	3147.2*	21 1.9	28.58	43.4	3.304	3.689
		0.0	-0.3857	133.5875									
V	1966	8 17 9 26 9	2911.6	132.50	33.18	60.31	273.72	3145.6*	21 0.7	30.12	44.9	1.792	2.176
		0.0	-0.3846	132.8701									
U	1966	8 17 9 26 4	2911.7	132.49	33.00	60.30	272.94	3145.9*	21 1.0	29.74	44.6	2.725	3.109
		0.0	-0.3848	133.0458									
B	1966	8 17 9 26 15	2911.6	132.51	33.34	60.32	274.44	3145.4*	21 0.4	30.46	45.3	2.595	2.980
		0.0	-0.3845	132.7098									
U	1966	8 17 9 26 19	2911.6	132.52	33.47	60.33	275.01	3145.2*	21 0.1	30.74	45.6	2.869	3.253
		0.0	-0.3844	132.5795									
V	1966	8 17 9 26 44	2911.5	132.56	34.23	60.30	278.36	3145.3*	20 58.7	32.35	47.2	1.762	2.146
		0.0	-0.3844	131.8267									
U	1966	8 17 9 26 38	2911.5	132.55	34.04	60.32	277.53	3145.2*	20 59.1	31.95	46.8	2.763	3.147
		0.0	-0.3843	132.0124									
B	1966	8 17 9 26 51	2911.4	132.58	34.43	60.28	279.25	3145.6*	20 58.3	32.78	47.6	2.334	2.719
		0.0	-0.3846	131.6260									
U	1966	8 17 9 26 55	2911.4	132.58	34.57	60.26	279.85	3145.9*	20 58.1	33.07	47.9	2.839	3.224
		0.0	-0.3848	131.4906									
V	1966	8 17 9 27 23	2911.1	132.63	35.41	60.09	283.53	3148.3*	20 56.4	34.85	49.7	2.083	2.470
		0.0	-0.3865	130.6525									
U	1966	8 17 9 27 19	2911.2	132.63	35.29	60.12	283.00	3147.8*	20 56.6	34.60	49.5	2.895	3.281
		0.0	-0.3862	130.7730									
B	1966	8 17 9 27 29	2911.1	132.64	35.62	60.03	284.41	3149.1*	20 56.0	35.28	50.2	2.767	3.154
		0.0	-0.3870	130.4515									
U	1966	8 17 9 27 34	2911.0	132.65	35.77	59.98	285.06	3149.8*	20 55.6	35.60	50.5	2.902	3.289
		0.0	-0.3875	130.3009									
V	1966	8 17 9 27 58	2910.7	132.69	36.49	59.72	288.12	3153.8*	20 54.1	37.11	52.0	2.566	2.956
		0.0	-0.3902	129.5878									
U	1966	8 17 9 27 54	2910.8	132.69	36.36	59.77	287.57	3152.9*	20 54.4	36.84	51.8	3.294	3.684
		0.0	-0.3897	129.7182									
B	1966	8 17 9 28 3	2910.7	132.70	36.65	59.64	288.83	3154.9*	20 53.7	37.46	52.4	3.327	3.718
		0.0	-0.3910	129.4215									
U	1966	8 17 9 28 9	2910.6	132.71	36.82	59.57	289.53	3156.0*	20 53.3	37.81	52.8	3.192	3.584
		0.0	-0.3918	129.2564									
V	1966	8 17 9 28 34	2910.2	132.75	37.58	59.17	292.68	3162.2*	20 51.5	39.41	54.4	1.855	2.251
		0.0	-0.3961	128.4973									
U	1966	8 17 9 28 29	2910.3	132.74	37.44	59.25	292.10	3160.9*	20 51.8	39.11	54.1	2.444	2.839
		0.0	-0.3952	128.6378									
B	1966	8 17 9 28 41	2910.1	132.76	37.80	59.05	293.54	3164.2*	20 51.0	39.85	54.8	2.645	3.042
		0.0	-0.3974	128.2861									
U	1966	8 17 9 28 46	2910.0	132.77	37.96	58.95	294.20	3165.7*	20 50.6	40.19	55.2	2.599	2.997
		0.0	-0.3985	128.1254									
V	1966	8 17 9 29 15	2909.5	132.82	38.82	58.37	297.58	3175.0*	20 48.3	41.97	57.0	2.059	2.464
		0.0	-0.4048	127.2708									
U	1966	8 17 9 29 11	2909.6	132.81	38.70	58.45	297.13	3173.7*	20 48.6	41.73	56.8	2.972	3.376
		0.0	-0.4039	127.3866									
B	1966	8 17 9 29 20	2909.4	132.82	38.97	58.26	298.18	3176.9*	20 47.9	42.29	57.3	3.014	3.420
		0.0	-0.4061	127.1151									
U	1966	8 17 9 29 25	2909.3	132.83	39.13	58.14	298.76	3178.8*	20 47.5	42.60	57.7	3.238	3.645
		0.0	-0.4074	126.9642									
V	1966	8 17 9 29 59	2908.6	132.88	40.16	57.30	302.59	3192.9*	20 44.5	44.72	59.8	2.012	2.429
		0.0	-0.4170	125.9383									
U	1966	8 17 9 29 53	2908.7	132.87	39.99	57.44	301.98	3190.5*	20 45.0	44.38	59.5	2.957	3.373
		0.0	-0.4154	126.1045									
B	1966	8 17 9 30 6	2908.5	132.89	40.37	57.11	303.35	3196.1*	20 43.9	45.15	60.3	2.255	2.674
		0.0	-0.4192	125.7272									
U	1966	8 17 9 30 11	2908.3	132.90	40.53	56.97	303.92	3198.6*	20 43.4	45.48	60.6	2.429	2.850
		0.0	-0.4209	125.5664									
V	1966	8 17 9 30 40	2907.6	132.94	41.41	56.14	306.95	3213.3*	20 40.5	47.25	62.5	2.064	2.495
		0.0	-0.4308	124.6907									
U	1966	8 17 9 30 34	2907.8	132.93	41.22	56.32	306.30	3210.0*	20 41.2	46.87	62.1	3.059	3.485
		0.0	-0.4286	124.8819									
B	1966	8 17 9 30 48	2907.4	132.95	41.65	55.89	307.75	3217.6*	20 39.7	47.74	63.0	2.808	3.242
		0.0	-0.4338	124.4489									
U	1966	8 17 9 30 52	2907.3	132.95	41.80	55.75	308.22	3220.2*	20 39.2	48.02	63.3	3.214	3.650
		0.0	-0.4355	124.3082									
V	1966	8 17 9 31 17	2906.6	132.98	42.54	54.97	310.61	3234.7*	20 36.5	49.51	64.8	1.991	2.436
		0.0	-0.4452	123.5630									
U	1966	8 17 9 31 12	2906.7	132.98	42.40	55.12	310.15	3231.7*	20 37.1	49.22	64.5	2.736	3.180
		0.0	-0.4433	123.7089									
B	1966	8 17 9 31 24	2906.4	132.99	42.75	54.74	311.25	3238.9*	20 35.8	49.91	65.2	2.841	3.289
		0.0	-0.4481	123.3566									
U	1966	8 17 9 31 28	2906.3	133.00	42.89	54.59	311.67	3241.7*	20 35.3	50.18	65.5	3.041	3.491
		0.0	-0.4500	123.2207									
V	1966	8 17 9 31 57	2905.3	133.03	43.77	53.59	314.30	3261.0*	20 31.7	51.91	67.3	2.270	2.732
		0.0	-0.4628	122.3392									

APPENDIX D

TABLE D3. - CONTINUED

PAGEOS REDUCTION OF SATELLITE OBSERVATIONS 8-17-66 E1213

	UT	HT	LONG	LAT	ALT	AZ	SR	RA	DEC	PHASE	MAGO	EA MAG
U 1966 8 17	9 31 52	2905.5	133.02	43.62	53.76	313.86	3257.5*	20 32.4	51.61	67.0	3.158	3.619
	0.0	-0.4605	122.4903									
B 1966 8 17	9 32 5	2905.1	133.04	44.00	53.32	314.96	3266.3*	20 30.8	52.36	67.8	2.679	3.146
	0.0	-0.4664	122.1073									
U 1966 8 17	9 32 10	2904.9	133.04	44.16	53.13	315.41	3269.9*	20 30.1	52.66	68.1	2.667	3.136
	0.0	-0.4688	121.9510									
V 1966 8 17	9 32 35	2904.1	133.07	44.92	52.21	317.49	3288.5*	20 26.7	54.12	69.7	2.047	2.528
	0.0	-0.4811	121.1899									
U 1966 8 17	9 32 30	2904.2	133.06	44.76	52.41	317.06	3284.4*	20 27.5	53.81	69.3	2.933	3.412
	0.0	-0.4784	121.3513									
B 1966 8 17	9 32 41	2903.9	133.07	45.10	52.00	317.95	3292.8*	20 25.9	54.44	70.0	2.731	3.215
	0.0	-0.4839	121.0186									
U 1966 8 17	9 32 46	2903.7	133.08	45.24	51.83	318.32	3296.4*	20 25.3	54.71	70.3	2.881	3.367
	0.0	-0.4863	120.8772									
V 1966 8 17	9 33 24	2902.2	133.11	46.40	50.36	321.24	3327.6*	20 19.4	56.87	72.6	2.446	2.952
	0.0006	-0.5068	119.7174									
U 1966 8 17	9 33 20	2902.4	133.11	46.27	50.52	320.93	3324.1*	20 20.1	56.64	72.4	3.086	3.589
	0.0007	-0.5045	119.8434									
B 1966 8 17	9 33 29	2902.0	133.12	46.58	50.13	321.66	3332.6*	20 18.5	57.20	73.0	3.106	3.615
	0.0008	-0.5100	119.5409									
U 1966 8 17	9 33 36	2901.8	133.12	46.76	49.89	322.10	3337.9*	20 17.5	57.54	73.3	3.089	3.602
	0.0008	-0.5135	119.3541									
V 1966 8 17	9 33 58	2900.8	133.14	47.44	49.00	323.66	3357.8*	20 13.6	58.77	74.7	1.979	2.505
	0.0010	-0.5264	118.6776									
U 1966 8 17	9 33 54	2901.0	133.13	47.33	49.15	323.40	3354.3*	20 14.3	58.56	74.4	2.750	3.273
	0.0010	-0.5241	118.7937									
B 1966 8 17	9 34 2	2900.7	133.14	47.57	48.83	323.94	3361.6*	20 12.8	58.99	74.9	2.605	3.132
	0.0011	-0.5288	118.5515									
U 1966 8 17	9 34 6	2900.5	133.14	47.69	48.67	324.21	3365.3*	20 12.1	59.21	75.1	2.846	3.376
	0.0012	-0.5312	118.4304									
V 1966 8 17	9 34 34	2899.3	133.16	48.53	47.55	326.02	3391.4*	20 6.8	60.69	76.8	2.057	2.603
	0.0014	-0.5480	117.5921									
U 1966 8 17	9 34 29	2899.5	133.15	48.40	47.72	325.75	3387.4*	20 7.6	60.47	76.5	2.849	3.393
	0.0015	-0.5454	117.7184									
B 1966 8 17	9 34 40	2899.0	133.16	48.72	47.30	326.40	3397.4*	20 5.5	61.01	77.1	2.868	3.418
	0.0016	-0.5518	117.4051									
U 1966 8 17	9 34 46	2898.7	133.16	48.89	47.06	326.77	3403.2*	20 4.3	61.32	77.5	3.134	3.688
	0.0017	-0.5555	117.2282									
V 1966 8 17	9 35 14	2897.4	133.17	49.77	45.86	328.51	3432.5*	19 58.0	62.82	79.1	2.085	2.657
	0.0019	-0.5742	116.3487									
U 1966 8 17	9 35 8	2897.7	133.17	49.59	46.11	328.15	3426.1*	19 59.4	62.50	78.8	3.021	3.589
	0.0019	-0.5701	116.5358									
B 1966 8 17	9 35 20	2897.1	133.17	49.95	45.61	328.85	3438.6*	19 56.6	63.11	79.5	2.687	3.263
	0.0021	-0.5780	116.1716									
U 1966 8 17	9 35 25	2896.8	133.18	50.10	45.41	329.12	3443.6*	19 55.5	63.36	79.7	2.870	3.449
	0.0022	-0.5812	116.0251									
V 1966 8 17	9 35 51	2895.5	133.18	50.90	44.31	330.59	3471.9*	19 48.9	64.67	81.2	2.201	2.798
	0.0023	-0.5989	115.2261									
U 1966 8 17	9 35 46	2895.8	133.18	50.74	44.53	330.31	3466.2*	19 50.3	64.41	80.9	3.042	3.635
	0.0025	-0.5954	115.3828									
B 1966 8 17	9 35 57	2895.2	133.18	51.08	44.06	330.92	3478.5*	19 47.4	64.96	81.6	2.750	3.350
	0.0026	-0.6030	115.0438									
U 1966 8 17	9 36 3	2894.9	133.18	51.24	43.83	331.20	3484.3*	19 45.9	65.22	81.9	2.770	3.374
	0.0027	-0.6067	114.8820									
V 1966 8 17	9 36 31	2893.4	133.18	52.12	42.62	332.69	3516.9*	19 37.7	66.59	83.5	2.071	2.695
	0.0029	-0.6269	114.0064									
U 1966 8 17	9 36 27	2893.6	133.18	51.99	42.80	332.47	3512.0*	19 39.0	66.38	83.2	2.934	3.554
	0.0031	-0.6239	114.1379									
B 1966 8 17	9 36 37	2893.1	133.18	52.30	42.36	332.99	3523.9*	19 35.9	66.86	83.8	2.584	3.212
	0.0032	-0.6312	113.8241									
U 1966 8 17	9 36 42	2892.8	133.18	52.46	42.14	333.25	3529.9*	19 34.3	67.10	84.1	2.625	3.257
	0.0033	-0.6349	113.6671									
V 1966 8 17	9 37 2	2891.6	133.17	53.06	41.30	334.21	3553.6*	19 27.8	68.01	85.2	2.222	2.869
	0.0033	-0.6494	113.0592									
U 1966 8 17	9 36 57	2892.0	133.18	52.90	41.53	333.95	3547.0*	19 29.7	67.76	84.9	3.063	3.705
	0.0035	-0.6454	113.2264									
B 1966 8 17	9 37 9	2891.3	133.17	53.26	41.03	334.51	3561.2*	19 25.7	68.29	85.5	2.770	3.420
	0.0037	-0.6540	112.8668									
U 1966 8 17	9 37 15	2890.9	133.17	53.44	40.77	334.80	3568.6*	19 23.6	68.56	85.9	3.004	3.659
	0.0038	-0.6586	112.6792									
V 1966 8 17	9 37 40	2889.4	133.16	54.21	39.70	335.94	3599.6*	19 14.3	69.63	87.2	2.421	3.094
	0.0039	-0.6774	111.9139									
U 1966 8 17	9 37 35	2889.7	133.16	54.08	39.88	335.75	3594.2*	19 16.0	69.45	87.0	3.021	3.691
	0.0042	-0.6741	112.0458									
B 1966 8 17	9 37 45	2889.1	133.15	54.37	39.47	336.18	3606.3*	19 12.3	69.85	87.5	3.405	4.082
	0.0043	-0.6814	111.7516									
U 1966 8 17	9 37 50	2888.8	133.15	54.51	39.28	336.38	3612.1*	19 10.4	70.04	87.7	3.413	4.093
	0.0044	-0.6849	111.6097									
V 1966 8 17	9 38 15	2887.3	133.13	55.28	38.21	337.46	3644.5*	18 59.8	71.05	89.1	1.849	2.548
	0.0045	-0.7043	110.8385									
U 1966 8 17	9 38 10	2887.6	133.14	55.14	38.40	337.27	3638.4*	19 1.9	70.87	88.8	2.515	3.211
	0.0048	-0.7007	110.9806									

TABLE D3. - CONCLUDED

PAGEOS REDUCTION OF SATELLITE OBSERVATIONS 8-17-66 E1213

PAGEOS	UT	HT	LONG	LAT	ALT	AZ	SR	RA	DEC	PHASE	MAGO	EA MAG
B 1966 8 17	9 38 21	2886.9	133.13	55.45	37.97	337.70	3651.8*	18 57.3	71.27	89.4	2.538	3.241
	0.0050	-0.7086	110.6660									
U 1966 8 17	9 38 28	2886.5	133.12	55.68	37.66	338.00	3661.4*	18 54.0	71.55	89.8	2.972	3.681
	0.0051	-0.7143	110.4426									
V 1966 8 17	9 38 55	2884.7	133.09	56.51	36.50	339.10	3697.8*	18 40.8	72.55	91.2	1.887	2.618
	0.0052	-0.7358	109.6050									
U 1966 8 17	9 38 52	2884.9	133.10	56.39	36.66	338.95	3692.7*	18 42.7	72.41	91.0	2.835	3.562
	0.0056	-0.7328	109.7219									
B 1966 8 17	9 39 1	2884.3	133.09	56.68	36.27	339.31	3705.2*	18 38.0	72.74	91.5	2.636	3.371
	0.0057	-0.7402	109.4375									
U 1966 8 17	9 39 5	2884.0	133.08	56.81	36.10	339.47	3710.9*	18 35.8	72.88	91.7	2.903	3.640
	0.0058	-0.7435	109.3103									
V 1966 8 17	9 39 29	2882.4	133.05	57.53	35.09	340.37	3743.7*	18 22.8	73.66	92.9	2.078	2.834
	0.0058	-0.7626	108.5789									
U 1966 8 17	9 39 24	2882.7	133.06	57.39	35.29	340.20	3737.1*	18 25.5	73.51	92.7	3.223	3.975
	0.0062	-0.7587	108.7260									
B 1966 8 17	9 39 37	2881.9	133.04	57.78	34.76	340.67	3754.8*	18 18.2	73.91	93.3	2.487	3.250
	0.0064	-0.7690	108.3348									
U 1966 8 17	9 39 41	2881.6	133.03	57.90	34.59	340.82	3760.6*	18 15.7	74.03	93.5	2.568	3.334
	0.0065	-0.7724	108.2076									
V 1966 8 17	9 40 28	2878.2	132.95	59.34	32.63	342.48	3827.9*	17 45.7	75.29	95.9	2.100	2.904
	0.0069	-0.8109	106.7628									
U 1966 8 17	9 40 20	2878.8	132.96	59.09	32.98	342.19	3815.6*	17 51.4	75.09	95.5	2.581	3.378
	0.0073	-0.8039	107.0224									
B 1966 8 17	9 40 36	2877.6	132.93	59.58	32.31	342.73	3839.0*	17 40.4	75.47	96.2	3.404	4.213
	0.0077	-0.8172	106.5288									
U 1966 8 17	9 40 41	2877.2	132.92	59.73	32.11	342.90	3846.3*	17 36.9	75.58	96.5	3.507	4.320
	0.0078	-0.8213	106.3759									
V 1966 8 17	9 41 3	2875.6	132.87	60.40	31.20	343.62	3878.9*	17 20.9	76.02	97.6	1.950	2.782
	0.0076	-0.8396	105.6985									
U 1966 8 17	9 40 59	2875.9	132.88	60.28	31.36	343.49	3873.0*	17 23.9	75.94	97.4	2.651	3.479
	0.0082	-0.8363	105.8208									
B 1966 8 17	9 41 9	2875.1	132.86	60.58	30.97	343.80	3887.3*	17 16.7	76.12	97.8	2.579	3.414
	0.0084	-0.8443	105.5255									
U 1966 8 17	9 41 14	2874.8	132.84	60.73	30.76	343.97	3895.0*	17 12.8	76.20	98.1	3.022	3.862
	0.0085	-0.8486	105.3676									
V 1966 8 17	9 41 41	2872.6	132.77	61.56	29.66	344.81	3935.9*	16 51.8	76.59	99.4	2.492	3.355
	0.0084	-0.8713	104.5365									
U 1966 8 17	9 41 34	2873.1	132.79	61.36	29.92	344.61	3926.0*	16 56.9	76.51	99.1	3.271	4.128
	0.0090	-0.8659	104.7355									
B 1966 8 17	9 41 47	2872.1	132.75	61.75	29.41	345.00	3945.2*	16 46.9	76.66	99.7	3.026	3.893
	0.0093	-0.8765	104.3478									
U 1966 8 17	9 41 55	2871.5	132.72	62.01	29.07	345.25	3958.2*	16 40.2	76.75	100.1	2.770	3.644
	0.0095	-0.8836	104.0877									
V 1966 8 17	9 42 28	2868.8	132.61	63.00	27.77	346.21	4008.7*	16 13.7	76.97	101.6	1.823	2.725
	0.0095	-0.9111	103.0874									
U 1966 8 17	9 42 21	2869.4	132.63	62.79	28.04	346.01	3998.1*	16 19.2	76.94	101.3	3.093	3.988
	0.0101	-0.9053	103.2967									
B 1966 8 17	9 42 33	2868.4	132.59	63.15	27.57	346.35	4016.5*	16 9.6	76.99	101.8	2.232	3.137
	0.0104	-0.9153	102.9342									
U 1966 8 17	9 42 38	2868.0	132.57	63.31	27.36	346.50	4024.9*	16 5.2	77.00	102.0	2.621	3.531
	0.0106	-0.9198	102.7707									
V 1966 8 17	9 43 2	2866.0	132.47	64.04	26.42	347.17	4062.5*	15 45.9	77.01	103.1	2.023	2.953
	0.0102	-0.9400	102.0401									
U 1966 8 17	9 42 57	2866.4	132.49	63.88	26.62	347.02	4054.3*	15 50.1	77.01	102.9	2.995	3.920
	0.0110	-0.9357	102.1983									
B 1966 8 17	9 43 8	2865.4	132.45	64.23	26.18	347.33	4072.3*	15 40.9	76.99	103.4	2.884	3.818
	0.0113	-0.9453	101.8510									
U 1966 8 17	9 43 13	2865.0	132.42	64.38	25.98	347.47	4080.2*	15 36.9	76.98	103.6	3.081	4.019
	0.0115	-0.9495	101.6976									
V 1966 8 17	9 43 38	2862.8	132.30	65.15	25.00	348.14	4120.7*	15 17.2	76.84	104.8	2.112	3.072
	0.0111	-0.9709	100.9253									
U 1966 8 17	9 43 34	2863.2	132.32	65.02	25.16	348.03	4114.2*	15 20.3	76.87	104.6	2.971	3.926
	0.0120	-0.9675	101.0484									
B 1966 8 17	9 43 45	2862.2	132.27	65.34	24.75	348.31	4131.2*	15 12.2	76.79	105.0	2.841	3.805
	0.0123	-0.9765	100.7258									
U 1966 8 17	9 43 50	2861.7	132.24	65.52	24.52	348.46	4140.6*	15 7.7	76.74	105.3	3.186	4.154
	0.0125	-0.9814	100.5468									
V 1966 8 17	9 44 15	2859.5	132.10	66.27	23.58	349.09	4180.7*	14 49.7	76.47	106.4	2.202	3.192
	0.0121	-1.0023	99.7941									
U 1966 8 17	9 44 11	2859.9	132.13	66.15	23.73	348.99	4174.4*	14 52.5	76.52	106.2	2.682	3.668
	0.0130	-0.9991	99.9121									
B 1966 8 17	9 44 21	2859.0	132.07	66.46	23.35	349.24	4190.8*	14 45.3	76.39	106.6	3.116	4.110
	0.0133	-1.0076	99.6047									
U 1966 8 17	9 44 27	2858.4	132.03	66.63	23.13	349.39	4200.4*	14 41.2	76.31	106.9	3.319	4.318
	0.0135	-1.0126	99.4254									
V 1966 8 17	9 44 59	2855.4	131.82	67.62	21.90	350.18	4254.4*	14 19.6	75.80	108.3	2.361	3.388
	0.0132	-1.0403	98.4259									
U 1966 8 17	9 44 53	2856.0	131.86	67.43	22.14	350.02	4243.6*	14 23.7	75.91	108.0	3.171	4.191
	0.0142	-1.0348	98.6260									
B 1966 8 17	9 45 5	2854.9	131.78	67.80	21.68	350.32	4263.9*	14 16.0	75.70	108.5	2.644	3.675
	0.0146	-1.0451	98.2516									
U 1966 8 17	9 45 12	2854.2	131.72	68.03	21.40	350.50	4276.8*	14 11.3	75.56	108.8	2.804	3.840
	0.0148	-1.0517	98.0156									

TABLE D4. - COMPUTER PROGRAM E-1214 PRINTOUT

E1214 PAGEOS V BAND 8/17 2ND PASS

39 POINTS

MEAN NORMALIZED MAGNITUDE = 2.08686

SIGMA OF THE MAGNITUDES = 0.19343

BEST FIT SPECULAR MAGNITUDE = 2.07026
ASSUMING B=0

ASSUMED COEF. OF REFLECTIVITY = 0.89600 (FOR RADIUS OF CURVATURE DETERMINATIONS)

REGRESSION A = 0.55445

REGRESSION B = 0.02821

SPECULARITY FROM REGRESSION = 95.16 PERCENT

MIN. MAGNITUDE = 1.76154

MAX. MAGNITUDE = 2.56601

I	MAGNITUDE	PHASE ANGLE	4*E/EO	(8/3)*F(PSI)	RESIDUALS	BEST FIT DIFFUSE MAG.	SPEC MAG.	RADIUS
1	2.11062	24.92557	0.57255	2.44114	-0.05075	1.47465	2.24973	48.65393
2	1.96952	27.68491	0.65201	2.39256	0.03008	1.49648	2.08814	52.41254
3	2.19859	29.58784	0.52799	2.35687	-0.09294	1.51280	2.34469	46.57207
4	2.05580	31.60381	0.60220	2.31723	-0.01761	1.53121	2.18053	50.22926
5	1.87125	33.67191	0.71377	2.27474	0.09517	1.55131	1.97351	55.25371
6	2.15818	35.67209	0.54801	2.23199	-0.06939	1.57191	2.29067	47.74518
7	2.33382	37.74776	0.46616	2.18602	-0.14995	1.59450	2.48785	43.60059
8	1.96632	40.44176	0.65393	2.12414	0.03957	1.62568	2.07065	52.83652
9	1.86469	42.43307	0.71810	2.07693	0.10507	1.65008	1.95708	55.67326
10	1.79191	44.93976	0.76789	2.01591	0.15658	1.68246	1.87543	57.80646
11	1.76154	47.19971	0.78967	1.95955	0.17995	1.71324	1.84032	58.74887
12	2.08305	49.74199	0.58727	1.89484	-0.02062	1.74970	2.18664	50.08804
13	2.56601	52.04163	0.37641	1.33527	-0.22981	1.78438	2.72664	39.06035
14	1.85507	54.38872	0.72449	1.77366	0.12001	1.82146	1.93275	56.30052
15	2.05941	57.01476	0.60020	1.70395	-0.00231	1.86500	2.15002	50.93994
16	2.01162	59.84560	0.62721	1.62814	0.02684	1.91440	2.09417	52.26714
17	2.06408	62.47060	0.59763	1.55750	-0.00075	1.96257	2.14697	51.01155
18	1.99103	64.81885	0.63922	1.49420	0.04262	2.00762	2.06508	52.97208
19	2.26964	67.33774	0.49454	1.42638	-0.10014	2.05805	2.36176	46.20726
20	2.04665	69.67229	0.60730	1.36376	0.01438	2.10678	2.11769	51.70409
21	2.44632	72.61655	0.42027	1.28535	-0.17043	2.17108	2.54426	42.48254
22	1.97946	74.66187	0.64607	1.23139	0.05688	2.21765	2.03945	53.60089
23	2.05659	76.76569	0.60176	1.17641	0.01413	2.26723	2.11817	51.69266
24	2.08509	79.13486	0.58617	1.11528	0.00026	2.32517	2.14498	51.05850
25	2.20100	81.23555	0.52682	1.06186	-0.05758	2.37846	2.26455	48.32297
26	2.07071	83.47629	0.59399	1.00580	0.01117	2.43736	2.12384	51.55785
27	2.22247	85.18567	0.51650	0.96372	-0.06513	2.48376	2.28116	47.95461
28	2.42085	87.21695	0.43025	0.91457	-0.15000	2.54060	2.48798	43.59808
29	1.84854	89.08838	0.72886	0.87015	0.14987	2.59465	1.88573	57.53307
30	1.88745	91.19228	0.70320	0.82127	0.12559	2.65742	1.92381	56.53268
31	2.07751	92.90790	0.59028	0.78228	0.01376	2.71023	2.11887	51.67595
32	2.10026	95.86826	0.57804	0.71695	0.00337	2.80492	2.13892	51.20099
33	1.94985	97.55916	0.66393	0.68078	0.09028	2.86111	1.98171	55.04538
34	2.49179	99.36794	0.40304	0.64307	-0.16955	2.92299	2.54178	42.53114
35	1.82320	101.57152	0.74607	0.59851	0.17474	3.00096	1.84805	58.54010
36	2.02336	103.12833	0.62046	0.56797	0.04999	3.05781	2.05176	53.29807
37	2.11215	104.75391	0.57174	0.53695	0.00215	3.11881	2.14129	51.14516
38	2.20209	106.37003	0.52629	0.50698	-0.04246	3.18115	2.23200	49.05278
39	2.36051	108.28223	0.45484	0.47268	-0.11294	3.25721	2.39281	45.55130

MIN. RADIUS = 39.06035 FT.

MAX. RADIUS = 58.74887 FT.

MEAN RADIUS = 50.60999 FT.
USING :
TRUE MEAN SPECULAR MAG = 2.16413

AVERAGE RADIUS = 50.83214

SIGMA OF RADIUS = 4.67080

COEFF. OF VARIATION OF RADIUS = 0.09189

AVERAGE 4E/EO = 0.59423

STD ERROR OF RESIDUALS = 0.10191

COEFFICIENT OF VARIATION = 0.17150

SIGMA OF 4E/EO = 0.10086

AVERAGE F(PSI) = 0.52891

SUM OF SQUARES OF F(PSI) = 2.17770

FIGURE OF MERIT FOR SPECULARITY = 16.06003

PARAMETRIC SOLUTION

ASSUMED RADIUS	INDICATED REFLECTIVITY
40	1.4343853
45	1.1333408
50	0.9180067
55	0.7586831
60	0.6375046

CORRELATION COEFFICIENT = 0.17622

STUDENTS T = 1.10047

TABLE D4. - CONTINUED

E1214 PAGEOS U BAND 8/17 2ND PASS

78 POINTS

MEAN NORMALIZED MAGNITUDE = 2.93670

SIGMA OF THE MAGNITUDES = 0.23365

BEST FIT SPECULAR MAGNITUDE = 2.91168
ASSUMING B=0

ASSUMED COEF. OF REFLECTIVITY = 0.88400
(FOR RADIUS OF CURVATURE DETERMINATIONS)

REGRESSION A = 0.26617

REGRESSION B = 0.00541

SPECULARITY FROM REGRESSION = 98.01 PERCENT

MIN. MAGNITUDE = 2.42883

MAX. MAGNITUDE = 3.50663

I	MAGNITUDE	PHASE ANGLE	4*E/EO	(8/3)*F(PSI)	RESIDUALS	BEST FIT DIFFUSE MAG.	SPEC MAG.	RADIUS
1	3.04809	24.65363	0.24145	2.44572	-0.03794	2.31074	3.10925	44.84695
2	2.74990	25.72455	0.31776	2.42747	0.03847	2.31887	2.79571	51.81346
3	2.87417	27.49062	0.28340	2.39610	0.00427	2.33299	2.92498	48.81886
4	3.00339	28.23105	0.25160	2.38249	-0.02745	2.33918	3.06046	45.86601
5	3.04878	29.33858	0.24130	2.36164	-0.03764	2.34872	3.10782	44.87648
6	2.85724	30.18073	0.28785	2.34540	0.00900	2.35621	2.90617	49.24361
7	2.95858	31.36255	0.26220	2.32207	-0.01693	2.36706	3.01186	46.90410
8	2.78057	32.21393	0.30891	2.30488	0.03028	2.37513	2.82529	51.11237
9	2.60829	33.37505	0.36203	2.28095	0.08353	2.38646	2.64593	55.51349
10	3.03630	34.28690	0.24408	2.26176	-0.03431	2.39564	3.09212	45.20227
11	3.07299	35.45760	0.23597	2.23665	-0.04229	2.40776	3.13012	44.41805
12	3.23307	36.22687	0.20363	2.21986	-0.07455	2.41594	3.29904	41.09364
13	3.40368	37.45801	0.17402	2.19253	-0.10401	2.42939	3.48030	37.80276
14	2.68372	38.52161	0.33773	2.16849	0.05984	2.44136	2.72209	53.60020
15	2.61865	40.06331	0.35859	2.13297	0.08089	2.45929	2.65415	55.30362
16	2.97377	41.04687	0.25855	2.10992	-0.01902	2.47109	3.02277	46.66914
17	2.74700	42.07497	0.31861	2.08550	0.04117	2.48373	2.78613	52.04245
18	3.30365	43.38698	0.19081	2.05391	-0.08646	2.50030	3.36877	39.79515
19	2.72453	44.55936	0.32527	2.02528	0.04816	2.51554	2.76172	52.63084
20	2.86885	45.56927	0.28479	2.00033	0.00780	2.52900	2.91089	49.13666
21	2.76314	46.79773	0.31391	1.96966	0.03709	2.54577	2.80062	51.69627
22	2.83886	47.92783	0.29276	1.94115	0.01610	2.56160	2.87850	49.87500
23	2.89476	49.48128	0.27807	1.90153	0.00162	2.58399	2.93567	48.57910
24	2.90186	50.50197	0.27626	1.87525	-0.00005	2.59910	2.94246	48.42744
25	3.29403	51.76012	0.19251	1.84261	-0.08362	2.61817	3.35173	40.10852
26	3.19232	52.75603	0.21141	1.81660	-0.06458	2.63361	3.24398	42.14903
27	2.44388	54.08716	0.42122	1.78162	0.14542	2.65472	2.46900	60.22595
28	2.59878	55.18697	0.36522	1.75254	0.08957	2.67258	2.62733	55.99095
29	2.97181	56.76758	0.25902	1.71054	-0.01639	2.69892	3.01129	46.91646
30	3.23766	57.66823	0.20277	1.68650	-0.07252	2.71429	3.28763	41.31035
31	2.95725	59.49379	0.26252	1.63759	-0.01250	2.74624	2.99451	47.28050
32	2.42883	60.63077	0.42710	1.60704	0.15224	2.76669	2.45115	60.72314
33	3.05922	62.06987	0.23899	1.56829	-0.03566	2.79318	3.09845	45.07065
34	3.21431	63.26978	0.20717	1.53595	-0.06730	2.81581	3.25874	41.86356
35	2.73634	64.51633	0.32176	1.50235	0.04746	2.83982	2.76410	52.57301
36	3.04079	65.52640	0.24308	1.47513	-0.03107	2.85968	3.07702	45.51764
37	3.15849	67.02831	0.21810	1.43470	-0.05582	2.88985	3.19781	43.05476
38	2.66697	68.12964	0.34298	1.40511	0.06922	2.91248	2.69129	54.36572
39	2.93349	69.34630	0.26833	1.37249	-0.00526	2.93798	2.96394	47.95073
40	2.88073	70.30176	0.28169	1.34694	0.00824	2.95838	2.90917	49.17552
41	3.08550	72.36667	0.23327	1.29198	-0.03988	3.00361	3.11852	44.65611
42	3.08912	73.33437	0.23249	1.26636	-0.04052	3.02536	3.12158	44.59306
43	2.75006	74.43465	0.31771	1.23736	0.04486	3.05051	2.77317	52.35396
44	2.84582	75.14362	0.29089	1.21875	0.01814	3.06697	2.87070	50.05450
45	2.84891	76.52260	0.29007	1.18273	0.01750	3.09953	2.87312	49.99883
46	3.13421	77.46335	0.22304	1.15832	-0.04939	3.12218	3.16514	43.70760
47	3.02117	78.78107	0.24751	1.12435	-0.02474	3.15449	3.04817	46.12627
48	2.86997	79.74390	0.28449	1.09971	0.01238	3.17855	2.89290	49.54533
49	3.04181	80.94446	0.24285	1.06922	-0.02910	3.20909	3.06797	45.70772
50	2.76979	81.87204	0.31199	1.04584	0.04017	3.23309	2.78965	51.95819
51	2.93369	83.23662	0.26828	1.01174	-0.00336	3.26907	2.95606	48.12511
52	2.62508	84.09195	0.35648	0.99057	0.08495	3.29204	2.64152	55.62637
53	3.06324	84.88593	0.23810	0.97105	-0.03331	3.31364	3.08745	45.29947
54	3.00416	85.86414	0.25142	0.94720	-0.01987	3.34065	3.02650	46.58896
55	3.02121	86.98499	0.24750	0.92013	-0.02364	3.37213	3.04326	46.23080
56	3.41279	87.74976	0.17256	0.90183	-0.09848	3.39394	3.44391	38.44156
57	2.51511	88.84314	0.39447	0.87592	0.12357	3.42559	2.52822	58.60559
58	2.97162	89.76842	0.25907	0.85422	-0.01172	3.45283	2.99115	47.35365
59	2.83456	90.99460	0.29393	0.82581	0.02329	3.48955	2.85118	50.50655
60	2.90267	91.68828	0.27605	0.80991	0.00551	3.51066	2.92003	48.93025
61	3.22279	92.66370	0.20556	0.78778	-0.06486	3.54074	3.24552	42.11905
62	2.56785	93.52100	0.37577	0.76854	0.10545	3.56758	2.57992	57.22676
63	2.58093	95.45093	0.37127	0.72600	0.10118	3.62941	2.59247	56.89697
64	3.50663	96.48656	0.15827	0.70362	-0.11170	3.66340	3.53305	36.89555
65	2.65073	97.36649	0.34815	0.68486	0.07828	3.69275	2.66234	55.09546
66	3.02161	98.07822	0.24741	0.66986	-0.02238	3.71680	3.03762	46.35106
67	3.27120	99.06075	0.19660	0.64940	-0.07308	3.75047	3.29077	41.25058
68	2.76986	100.05666	0.31197	0.62897	0.04241	3.78517	2.78176	52.14723
69	3.09318	101.25681	0.23163	0.60478	-0.03781	3.82777	3.10862	44.86005
70	2.62132	102.04549	0.35771	0.58913	0.08836	3.85623	2.63103	55.89551
71	2.99529	102.89496	0.25348	0.57250	-0.01578	3.88731	3.00863	46.97398
72	3.08099	103.63123	0.23424	0.55828	-0.03494	3.91462	3.09507	45.14076
73	2.97079	104.57590	0.25927	0.54030	-0.00982	3.95016	2.98309	47.52969
74	3.18553	105.29834	0.21274	0.52675	-0.05627	3.97773	3.20016	43.00818
75	2.68152	106.20311	0.33842	0.51004	0.06949	4.01275	2.69040	54.38808
76	3.31930	106.89005	0.18808	0.49753	-0.08078	4.03970	3.33494	40.41992
77	3.17080	108.00574	0.21565	0.47756	-0.05310	4.08418	3.18388	43.33189
78	2.80351	108.84697	0.30245	0.46279	0.03378	4.11829	2.81253	51.41351

APPENDIX D

TABLE D4. - CONTINUED

MIN. RADIUS = 36.89555 FT.

MAX. RADIUS = 60.72314 FT.

MEAN RADIUS = 47.84773 FT.
USING :
TRUE MEAN SPECULAR MAG = 2.96861

AVERAGE RADIUS = 48.13962

SIGMA OF RADIUS = 5.31110

COEFF. OF VARIATION OF RADIUS = 0.11033

AVERAGE 4E/EO = 0.27377

STD ERROR OF RESIDUALS = 0.05963

COEFFICIENT OF VARIATION = 0.21779

SIGMA OF 4E/EO = 0.05896

AVERAGE F(PSI) = 0.52730

SUM OF SQUARES OF F(PSI) = 4.35080

FIGURE OF MERIT FOR SPECULARITY = 18.90613

PARAMETRIC SOLUTION

ASSUMED RADIUS	INDICATED REFLECTIVITY
40	1.2649155
45	0.9994405
50	0.8095468
55	0.6690468
60	0.5621852

CORRELATION COEFFICIENT = 0.05777

STUDENTS T = 0.51019

TABLE D4. - CONCLUDED

E1214 PAGEOS B BAND 8/17 2ND PASS

39 POINTS

MEAN NORMALIZED MAGNITUDE = 2.76025

SIGMA OF THE MAGNITUDES = 0.26543

BEST FIT SPECULAR MAGNITUDE = 2.72925
ASSUMING B=0

ASSUMED COEF. OF REFLECTIVITY = 0.89600 (FOR RADIUS OF CURVATURE DETERMINATIONS)

REGRESSION A = 0.30989

REGRESSION B = 0.00996

SPECULARITY FROM REGRESSION = 96.89 PERCENT
MIN. MAGNITUDE = 2.23205

MAX. MAGNITUDE = 3.40452

I	MAGNITUDE	PHASE ANGLE	4*E/E0	(8/3)*F(PSI)	RESIDUALS	BEST FIT DIFFUSE MAG.	SPEC MAG.	RADIUS
1	2.80174	25.23856	0.30295	2.43583	-0.03121	2.12979	2.89237	48.15968
2	2.63791	27.96332	0.35229	2.38744	0.01861	2.15157	2.71379	52.28772
3	2.76537	29.91002	0.31327	2.35066	-0.02004	2.16843	2.84971	49.11522
4	2.67882	31.92969	0.33926	2.31066	0.00635	2.18706	2.75509	51.30255
5	2.73287	34.03249	0.32278	2.26715	-0.00969	2.20770	2.81161	49.98450
6	2.99823	36.00217	0.25280	2.22478	-0.07926	2.22818	3.09783	43.81178
7	2.71541	38.13495	0.32802	2.17728	-0.00356	2.25162	2.78967	50.49205
8	2.66934	40.77689	0.34224	2.11628	0.01126	2.28247	2.73836	51.69949
9	2.49322	42.74715	0.40251	2.06938	0.07200	2.30680	2.55029	56.37665
10	2.59527	45.28711	0.36640	2.00733	0.03651	2.33986	2.65619	53.69319
11	2.33394	47.63440	0.46611	1.94858	0.13680	2.37210	2.38012	60.97252
12	2.76688	50.17650	0.31283	1.88365	-0.01583	2.40890	2.83403	49.47113
13	3.32741	52.40012	0.18668	1.82591	-0.14140	2.44270	3.43870	37.44713
14	2.64474	54.84206	0.35008	1.76168	0.02264	2.48159	2.70057	52.60707
15	3.01392	57.34676	0.24917	1.69509	-0.07761	2.52342	3.09010	43.96811
16	2.25485	60.29152	0.50133	1.61616	0.17533	2.57519	2.29028	63.54776
17	2.80835	62.97609	0.30111	1.54387	-0.02417	2.62487	2.86526	48.76468
18	2.84087	65.24582	0.29222	1.48269	-0.03244	2.66877	2.89717	48.05321
19	2.67918	67.81099	0.33915	1.41366	0.01517	2.72053	2.72522	52.01324
20	2.73103	70.01764	0.32333	1.35453	-0.00005	2.76693	2.77730	50.78050
21	3.10606	72.96567	0.22890	1.27611	-0.09371	2.83168	3.16808	42.41704
22	2.60454	74.90775	0.36328	1.22493	0.04119	2.87612	2.64163	54.05447
23	2.86767	77.12462	0.28510	1.16710	-0.03642	2.92863	2.91286	47.70728
24	2.68674	79.46840	0.33679	1.10675	0.01588	2.98628	2.72287	52.06958
25	2.75008	81.57317	0.31771	1.05335	-0.00268	3.03997	2.78654	50.56506
26	2.58401	83.80739	0.37022	0.99760	0.05039	3.09901	2.61354	54.75815
27	2.76982	85.52974	0.31198	0.95533	-0.00743	3.14602	2.80345	50.17276
28	3.40452	87.50165	0.17388	0.90775	-0.14505	3.20148	3.46249	37.03896
29	2.53760	89.38541	0.38639	0.86318	0.06789	3.25615	2.56203	56.07268
30	2.63642	91.47449	0.35277	0.81480	0.03476	3.31877	2.66169	53.55740
31	2.48736	93.31119	0.40468	0.77323	0.08709	3.37563	2.50822	57.47960
32	3.40380	96.24283	0.17400	0.70886	-0.14296	3.47000	3.44877	37.27377
33	2.57855	97.83076	0.37208	0.67505	0.05547	3.52305	2.59834	55.14273
34	3.02557	99.65825	0.24651	0.63711	-0.06973	3.58587	3.05388	44.70755
35	2.23205	101.80098	0.51197	0.59396	0.19615	3.66201	2.24467	64.89693
36	2.88440	103.40627	0.28074	0.56261	-0.03476	3.72089	2.90629	47.85199
37	2.84131	105.04111	0.29210	0.53156	-0.02309	3.78253	2.86117	48.85674
38	3.11566	106.63791	0.22688	0.50210	-0.08802	3.84442	3.13986	42.97205
39	2.64449	108.52277	0.35016	0.46846	0.03560	3.91973	2.65905	53.62247

MIN. RADIUS = 37.03896 FT.

MAX. RADIUS = 64.89693 FT.

MEAN RADIUS = 50.01048 FT.
USING :
TRUE MEAN SPECULAR MAG = 2.81048

AVERAGE RADIUS = 50.40414

SIGMA OF RADIUS = 6.20594

COEFF. OF VARIATION OF RADIUS = 0.12312

AVERAGE 4E/E0 = 0.32386

STD ERROR OF RESIDUALS = 0.07704

COEFFICIENT OF VARIATION = 0.23788

SIGMA OF 4E/E0 = 0.07530

AVERAGE F(PSI) = 0.52589

SUM OF SQUARES OF F(PSI) = 2.17326

FIGURE OF MERIT FOR SPECULARITY = 11.97332

PARAMETRIC SOLUTION

ASSUMED RADIUS	INDICATED REFLECTIVITY
40	1.4006081
45	1.1066542
50	0.8963901
55	0.7408181
60	0.6224931

CORRELATION COEFFICIENT = 0.08327

STUDENTS T = 0.52001

REFERENCES

1. Hardie, Robert H.: Photoelectric Reductions. Ch. 8 of Astronomical Techniques, W. A. Hiltner, ed., University of Chicago Press, Chicago, Illinois, 1962, pp. 178-208.

2. Johnson, H. L.; and Harris, D. L. III: Three-Color Observations of 108 Stars Intended for Use as Photometric Standards. Astrophys. J., vol. 120, 1954, pp. 196-199.

3. Iriarte, B.; Johnson, H. L.; Mitchell, R. I.; and Wisniewski, W. K.: Five-Color Photometry of Bright Stars. (Includes the Arizona-Tonantzintla Catalog of 1325 Stars.) Sky and Telescope, July 1965, pp. 21-31.

4. Veis, George: Optical Tracking of Artificial Satellites. Space Science Reviews, vol. II, 1963, pp. 250-296.

5. Tousey, R.: Optical Problems of the Satellite. J. Opt. Soc. Am., vol. XLVII, 1957, p. 261.

6. Tousey, R.: The Visibility of an Earth Satellite. Astronautica Acta, vol. II, 1956, p. 101.

7. Russell, H. N.: On the Albedo of the Planets and Their Satellites, Astrophys. J., vol. XLIII, April 1916, p. 123.

8. Emmons, R. H., et al: Photometric Measurements of Surface Characteristics of Echo I Satellite. NASA CR-200, April 1965.

9. Hald, A.: Statistical Theory with Engineering Applications. J. Wiley and Sons, 1962.

10. Elterman, L.: Atmospheric Attenuation Model, 1964, in the Ultraviolet, Visible, and Infrared Regions for Altitudes to 50 km. AF-CRL 64-740, 1964.

11. Johnson, H. L.: Relative U B V Response Functions. Astrophys. J., vol. 141, 1965, p. 940.

12. Zadunaisky, P. E.; Shapiro, L. L.; and Jones, H. M.: Experimental and Theoretical Results on the Orbit of Echo I. Special rept no. 61, Smithsonian Institute Astrophysical Observatory, Cambridge, Mass., 20 March 1961.

13. Nordberg, et. al.: Preliminary Results of Radiation Measurements from the Tiros III Meteorological Satellite. NASA TND-1338, May 1962.

14. Bakos, G. A.: Measures of the Earthshine. Special rept no. 162, Smithsonian Institution Astrophysical Observatory, August 1964.

15. Giedt, W. H.: Principles of Engineering Heat Transfer. D. Van Nostrand Co., January 1957.

16. Johnson, F. S.: The Solar Constant. J. Meteorol., vol. II, no. 6, Dec. 1954, p. 436.

17. Anon.: Smithsonian Meteorological Tables. Sixth edition, 1951, pp. 442-3.

18. Rasoal, S. I.; and Prabhakara, C.: Radiation Studies From Meteorological Satellites. NYU Geophysical Sciences Laboratory Report 65-1, January 1965.

19. Band, H. E.; and Block, L. C.: Spectral Reflectance and Albedo Measurements of the Earth From High Altitudes. AF-CRL 65-674, September 1965.

20. Goody, R. M.: Atmospheric Radiation. Claredon Press, 1964.

21. Hord, et. al.: The Atmosphere as a Part of the Space Environment. NASA TND-1387, January 1963.

22. Novosel'tsev, Y. P.: Spectral Reflectivity of Clouds. NASA TT F-328, April 1965.

23. Johnson, H. L.; and Morgan, W. W.: Fundamental Stellar Photometry for Standards of Spectral Type on the Revised System of Yerkes Spectral Atlas. Astrophys. J., vol. 117, no. 3, May 1953.

NASA-Langley, 1967 —— 7 CR-791